Probing Axions and Millicharged Particles in Supernovae

Zuowei Liu (Nanjing University)

超越标准模型前沿交叉研讨会

Nov 21-23, 2025, Nanjing

Outline

- Supernova (SN) constraints: cooling & calorimetric limits
- SN constraints on millicharged particles (MCPs)
  - e^+e^- annihilation
  - pionic processes
  - low-energy SN (LESN) constraints

  [Changqian Li, ZL, Wenxi Lu, Zicheng Ye, 2408.04953, JHEP]
- SN constraints on lepton-flavor-violating (LFV) axion-like particles (ALPs)
  - $e\mu$ coalescence — [Yonglin Li, ZL, 2501.12075]
  - semi-Compton — [Zi-Miao Huang, ZL, 2506.16922, JHEP]
  - LESN constraints — [Zi-Miao Huang, Changqian Li, ZL, 2510.22523]

1 Supernova constraints

Core-collapse supernovae (type II)

massive star with $\gtrsim 8$ solar mass will form iron cores

core $>$ 1.4 solar mass (Chandrasekhar limit) $\rightarrow$ collapse

implosion & explosion $\rightarrow$ neutron star or black hole

$\rightarrow$ neutrino (SN1987A) & light & heavy elements

porto-neutron star: high temperature & high density

$\rightarrow$ ideal probes of light feebly interacting particles (FIPs)

One-zone model for the supernova core

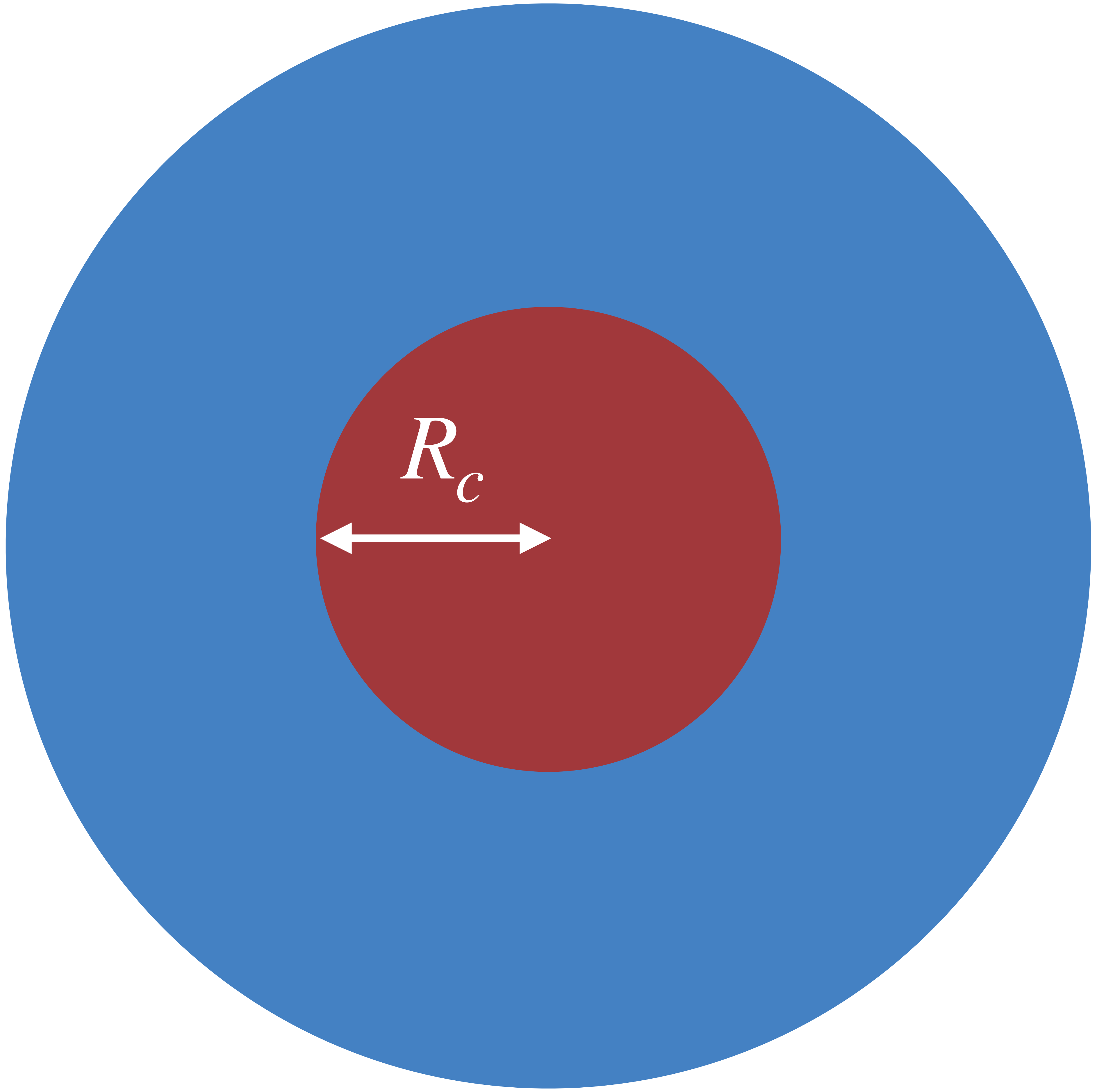

one zone model

Radius: $R_c = 12.9$ km

Temperature: $T_c = 30$ MeV

Nuclear Density: $\rho_c = 3 \times 10^{14}\,\mathrm{g/cm^3}$

Proton Abundance: $Y_p = 0.15$

[Caputo+, 2201.09890]

Two kinds of supernova constraints

- cooling limits
- calorimetric limits

Supernova cooling limit

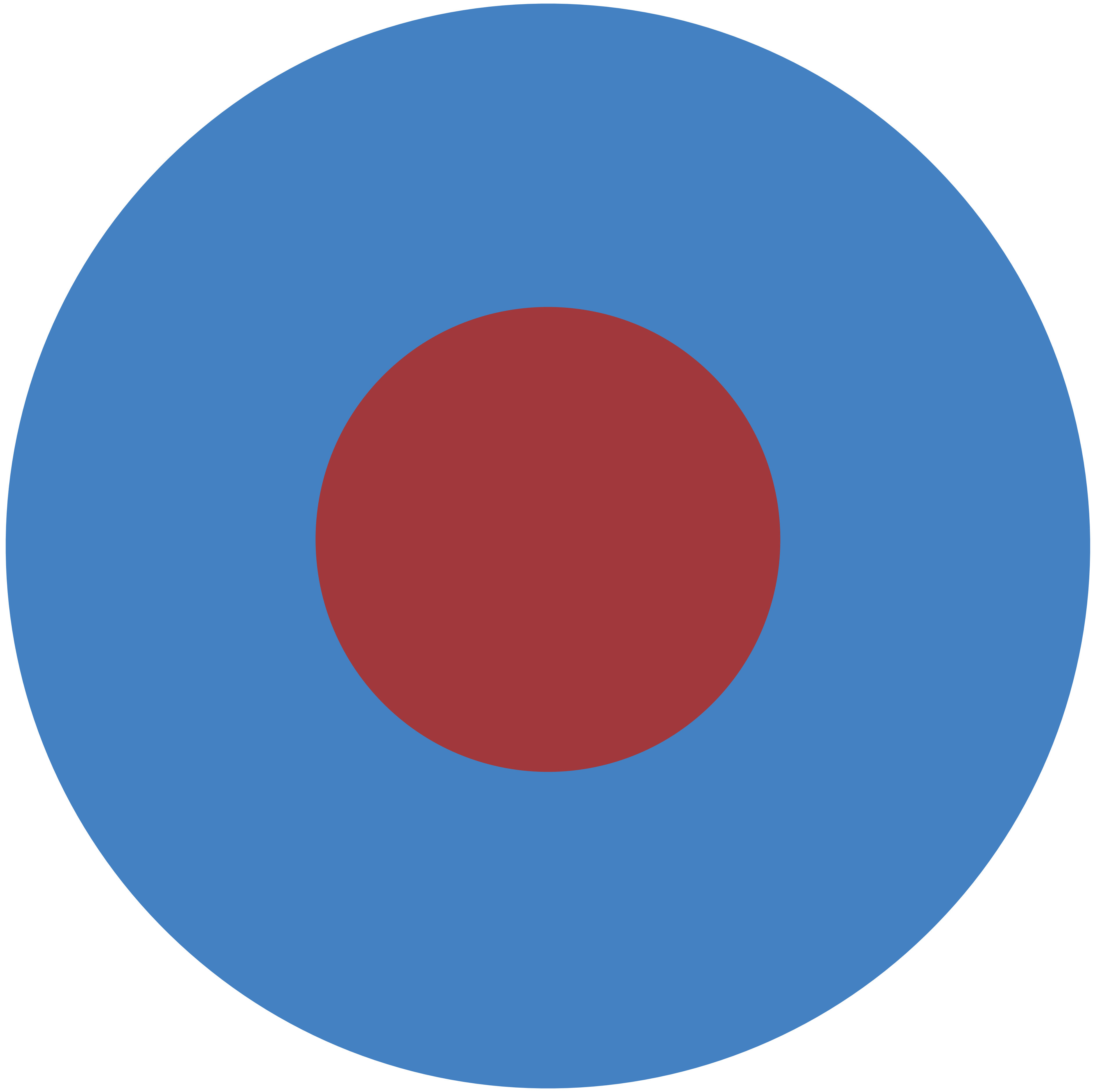

Supernova cooling limit

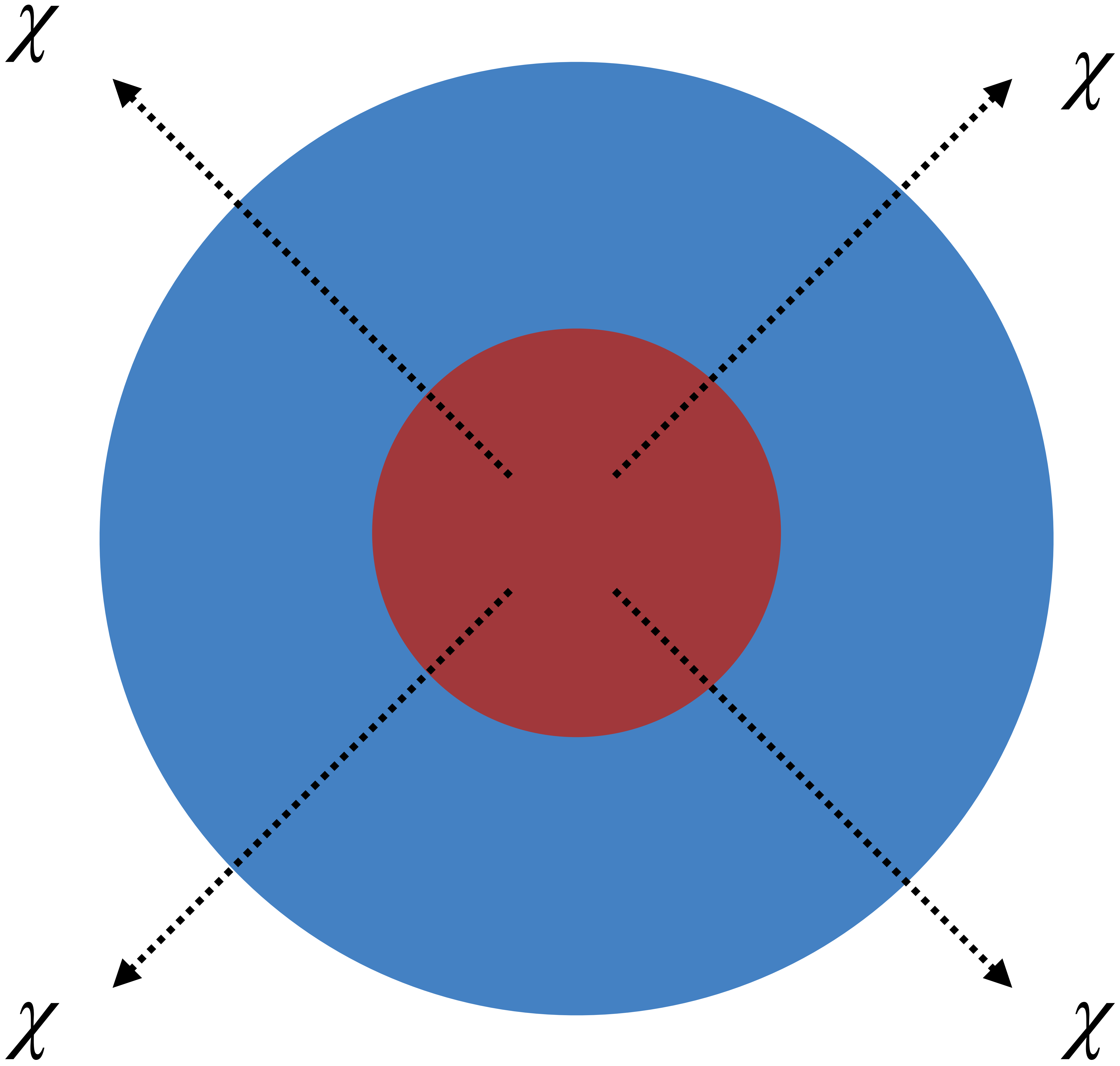

Supernova cooling limit

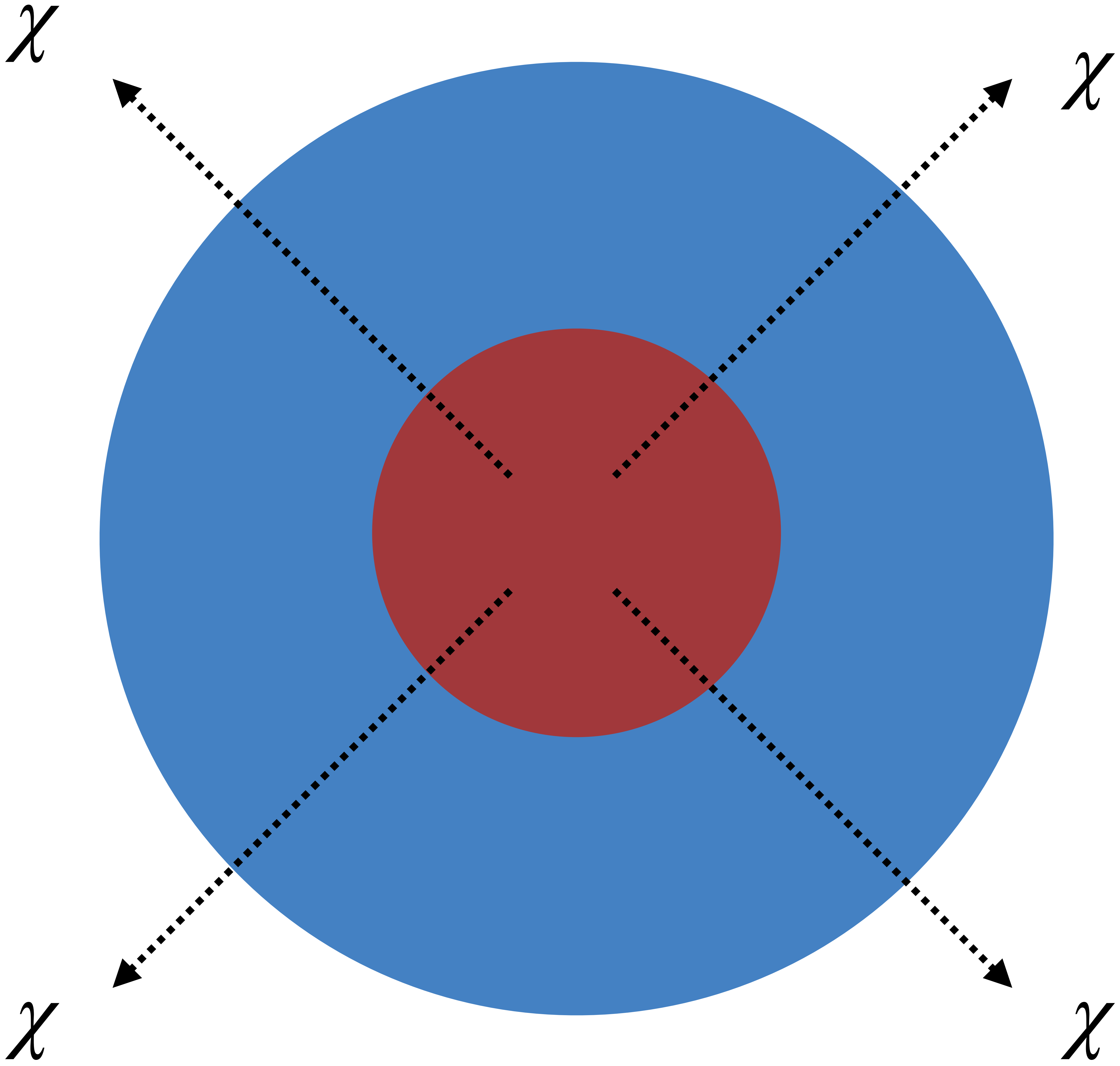

exotic energy loss $\Longrightarrow$ over-cooling

Supernova cooling limit

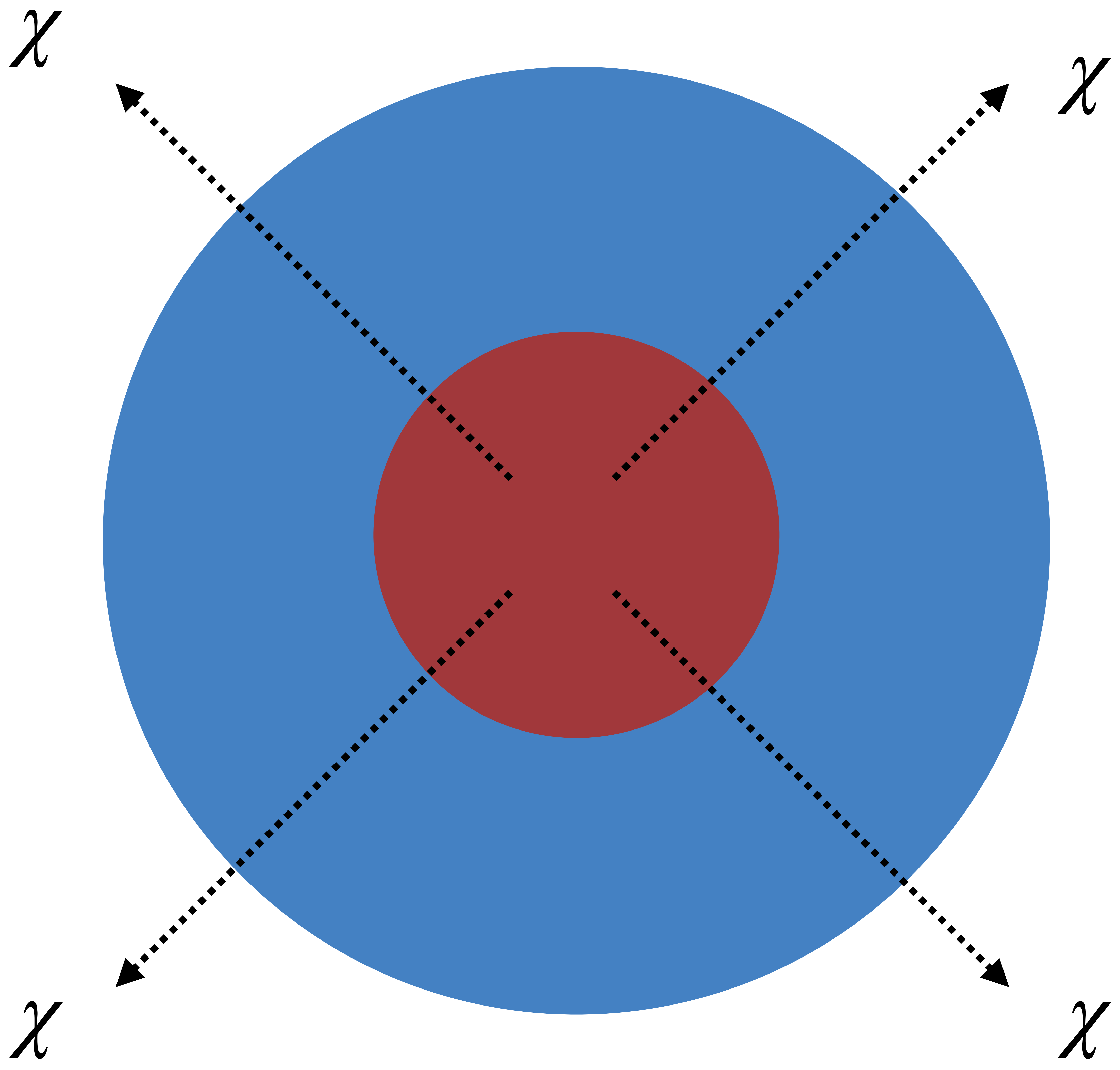

exotic energy loss $\Longrightarrow$ over-cooling

NP luminosity from the SN core should be smaller than that of neutrinos at about 1 second postbounce:

$$L_a \leq L_\nu = 3 \times 10^{52}\, \mathrm{erg}/s$$ **[Raffelt, 96']**

Supernova “calorimetric” limit

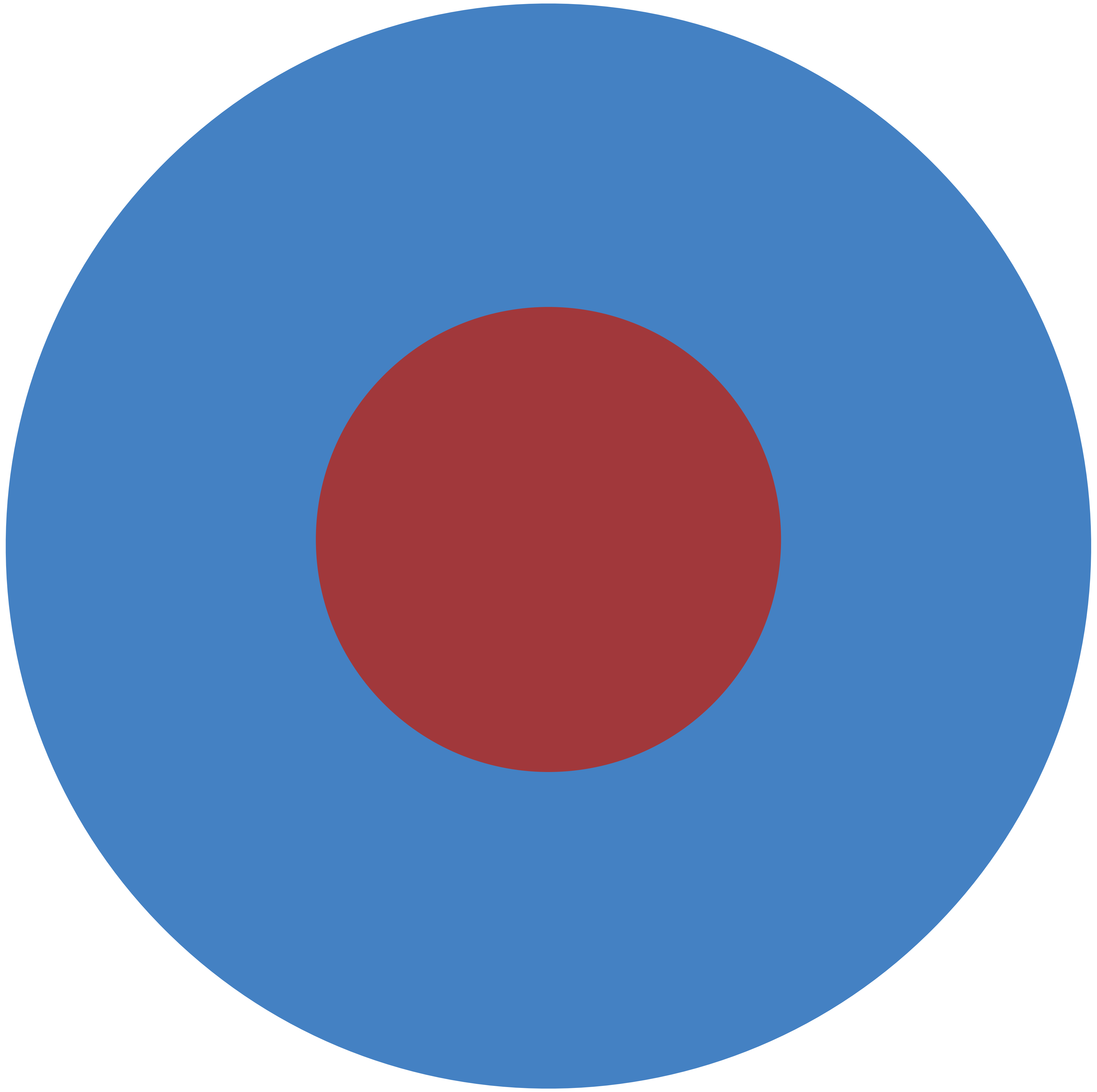

Supernova “calorimetric” limit

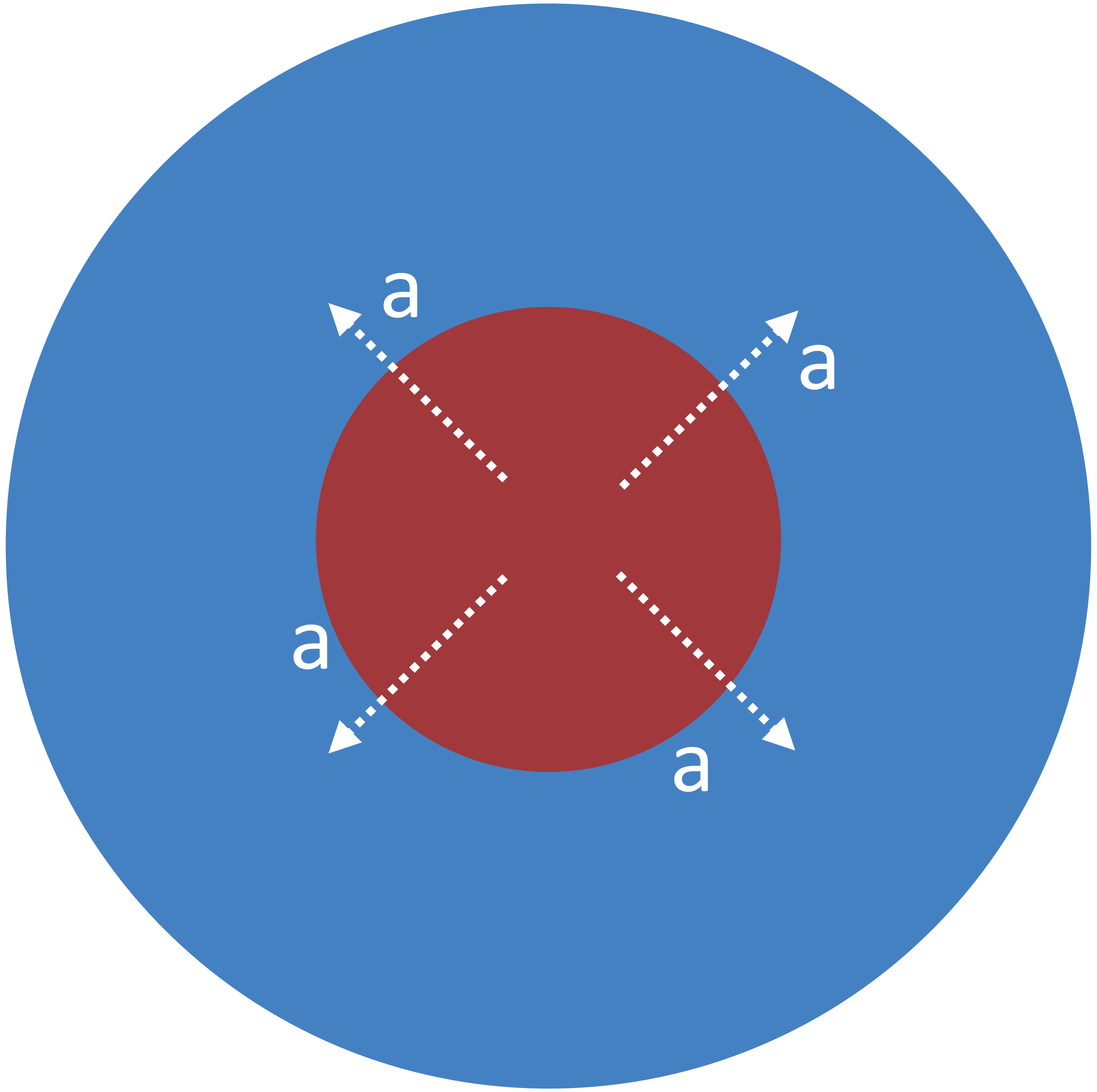

Supernova “calorimetric” limit

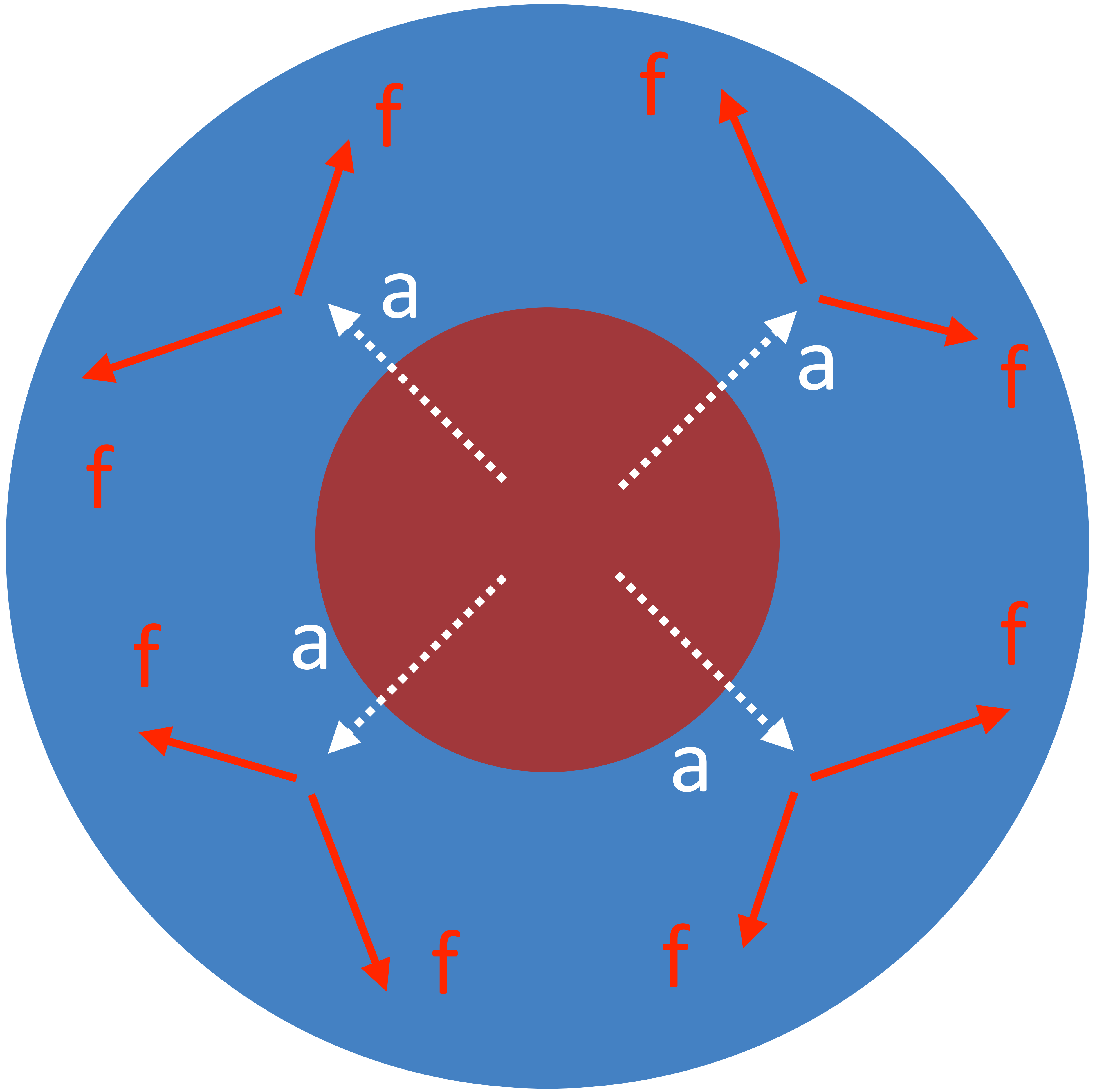

Supernova “calorimetric” limit

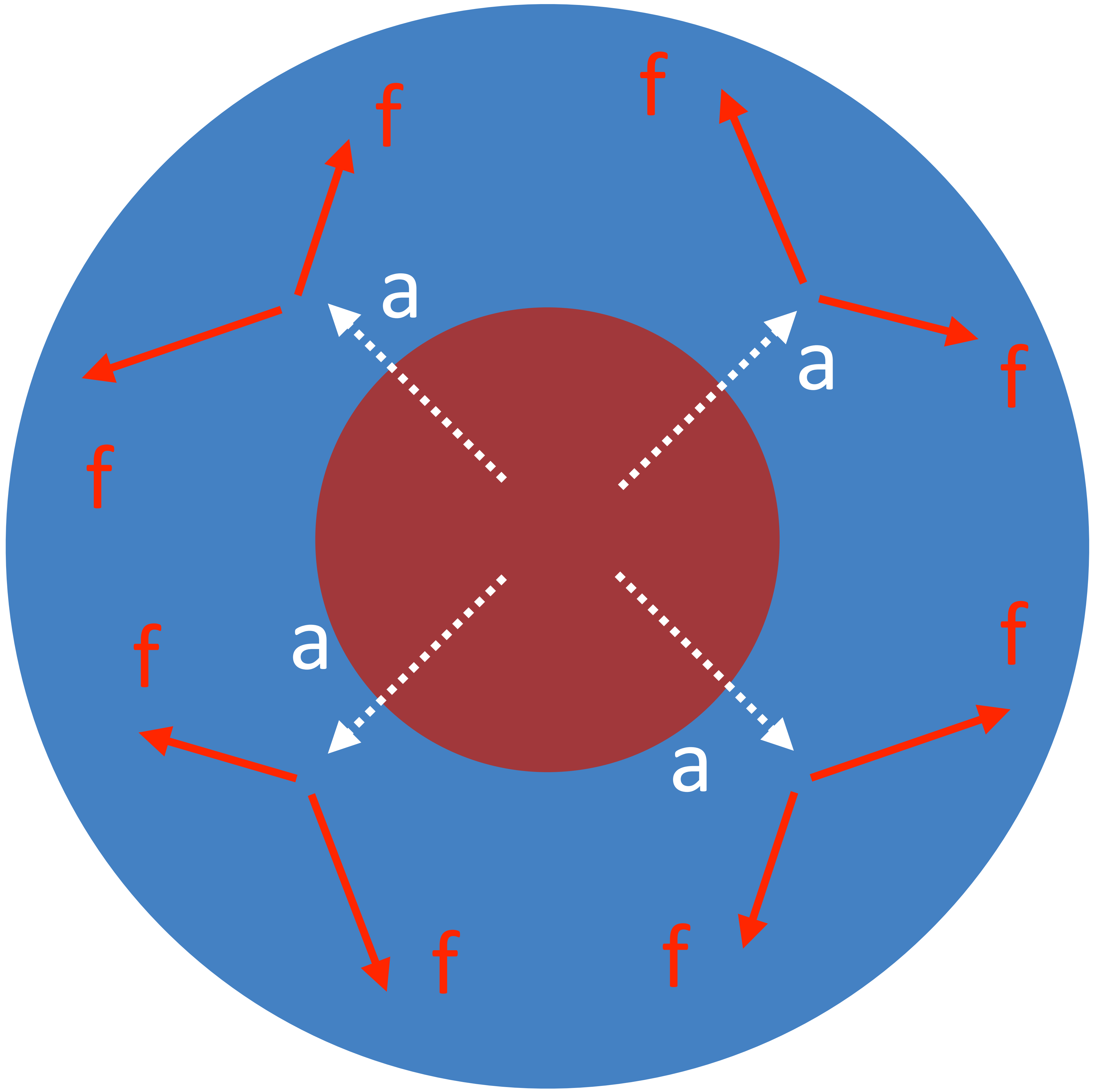

NP-induced energy deposition in the SN mantle

should be less than the explosion energy

[Falk & Schramm, 78’]

[Sung+, 1903.07923]

[Caputo+, 2201.09890]

Low-Energy Supernovae (LESNe)

underluminous Type-II P SN

core-collapse SN with a relatively small mass

10-100 times dimmer than typical CCSNe

explosion energy as low as 0.1 B

$B = 10^{51}$ erg

[Caputo+, 2201.09890]

[Burrows & Vartanyan, 2009.14157]

2

SN constraints on millicharged particles (MCPs)

Millicharged particles (MCPs)

Hidden sector particle χ with a millicharge ϵ under the SM photon A_μ

$$e\,\epsilon\,A_\mu\,\bar{\chi}\,\gamma^\mu\,\chi + m_\chi\,\bar{\chi}\chi$$

- charge quantization **[Dirac 1931; magnetic monopole?]**
- neutrino millicharge
- dark matter millicharge **[see e.g., PandaX, Nature 23]**

Kinetic mixing & Stueckelberg mass mixing & millicharge

[from https://inspirehep.net/]

The Stueckelberg Z-prime Extension with Kinetic Mixing and Milli-Charged Dark Matter From the Hidden Sector #1

Daniel Feldman (Northeastern U.), Zuowei Liu (Northeastern U.), Pran Nath (Northeastern U.) (Feb, 2007)

Published in: *Phys.Rev.D* 75 (2007) 115001 • e-Print: hep-ph/0702123 [hep-ph]

pdf DOI cite claim reference search 431 citations

$$-\frac{\tilde{\delta}}{2} B_{\mu\nu} X^{\mu\nu} - \frac{M_1^2}{2}(\partial_\mu \sigma + X_\mu + \tilde{\epsilon} B_\mu)^2 + g_D X_\mu \bar{\chi}\gamma^\mu \chi$$

χ can can have a millicharge either via the kinetic mixing $\tilde{\delta}$ or via the mass mixing $\tilde{\epsilon}$

millicharged χ is accompanied with a massless (massive) dark photon in the kinetic (mass) mixing case

Constraints on millicharged particles

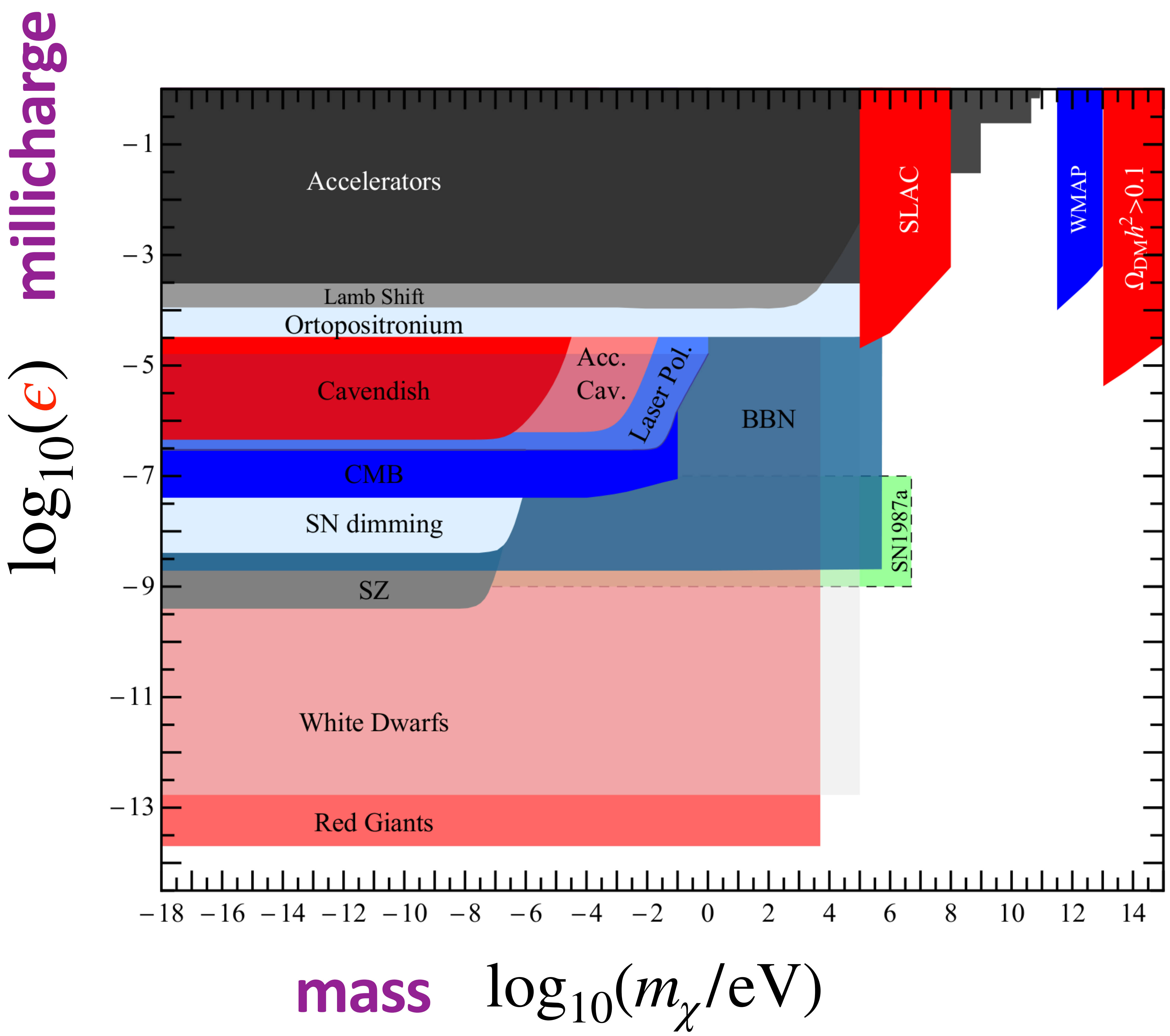

$$e\,\epsilon\,A_\mu\,\bar{\chi}\,\gamma^\mu\,\chi + m_\chi\,\bar{\chi}\,\chi$$

[Jaeckel & Ringwald, 1002.0329]

high-mass: accelerator

low-mass: stellar cooling

Constraints on millicharged particles

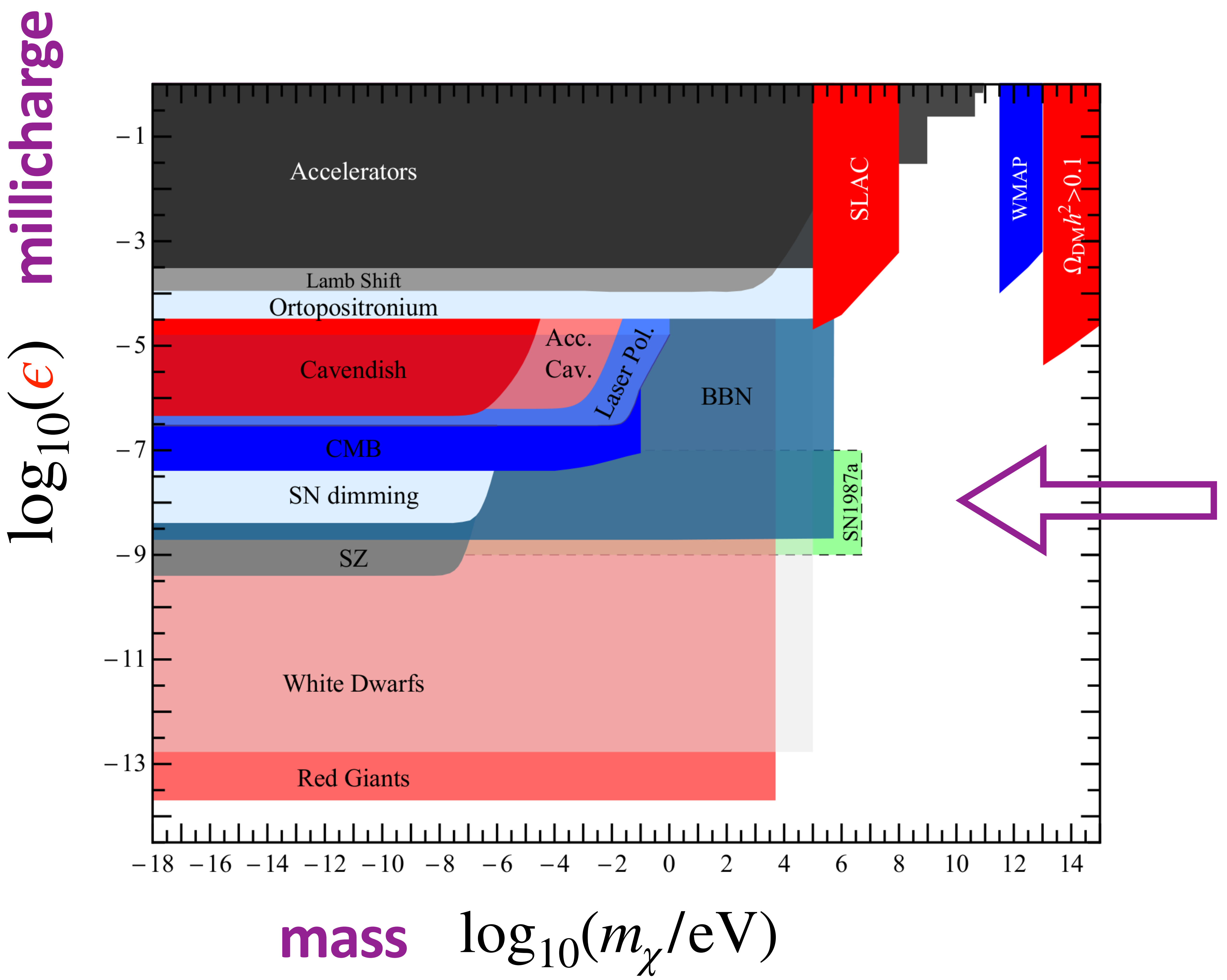

$$e\,\epsilon\,A_\mu\,\bar{\chi}\,\gamma^\mu\,\chi + m_\chi\,\bar{\chi}\,\chi$$

[Jaeckel & Ringwald, 1002.0329]

Supernova constraints

high-mass: accelerator

low-mass: stellar cooling

MCP production in the SN core

MCP production channels in the SN core (I)

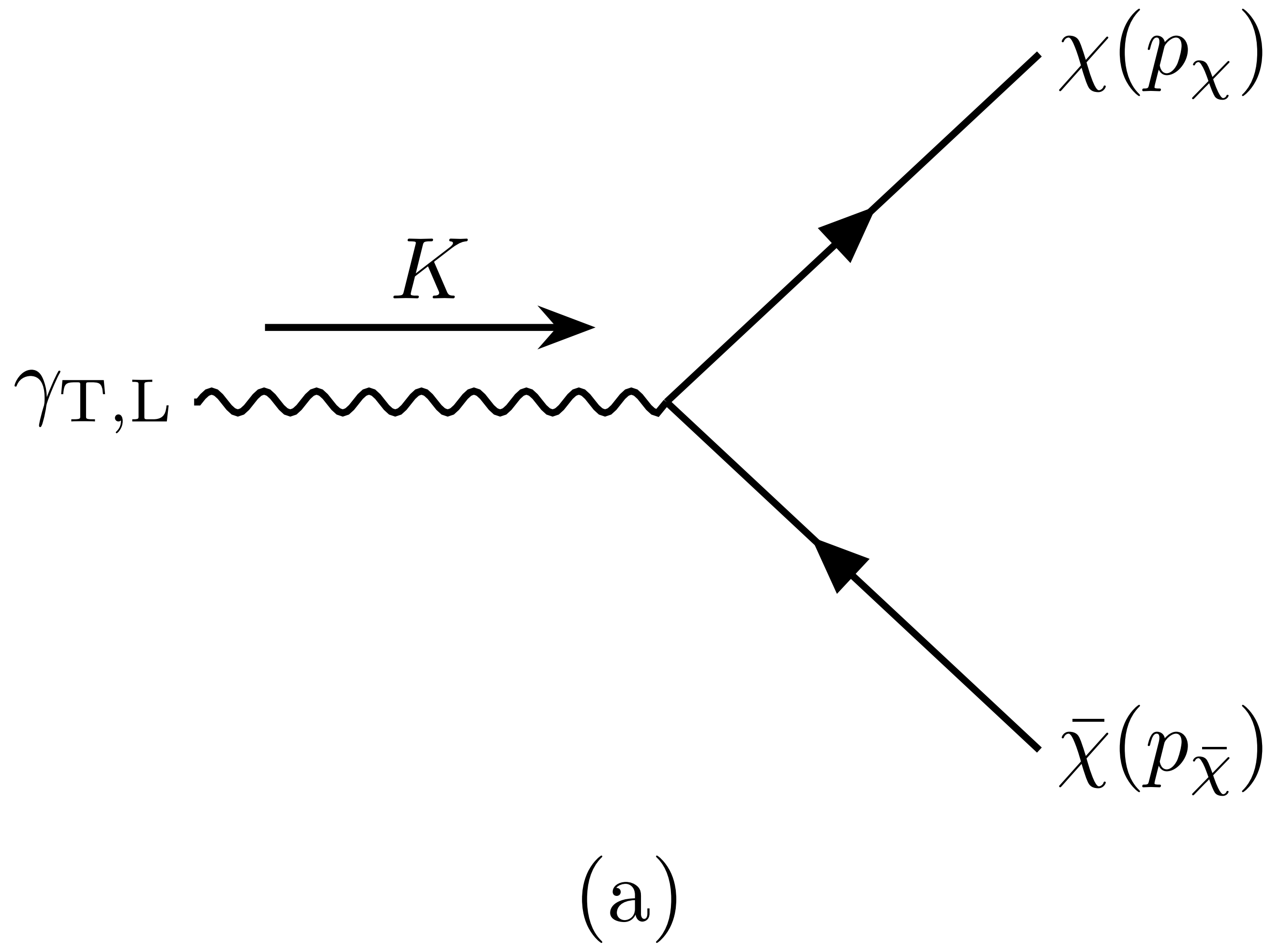

plasmon decay

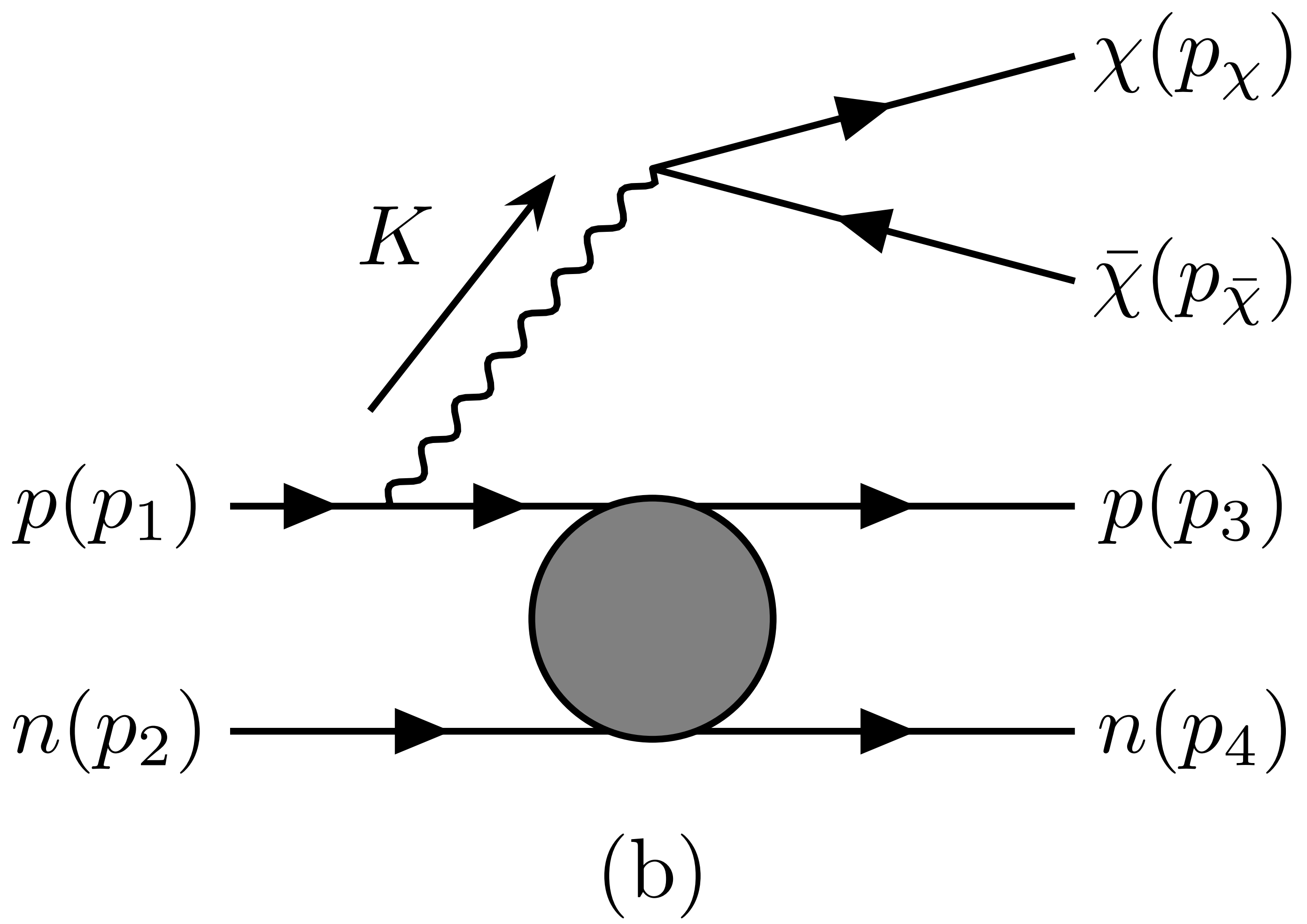

proton bremsstrahlung

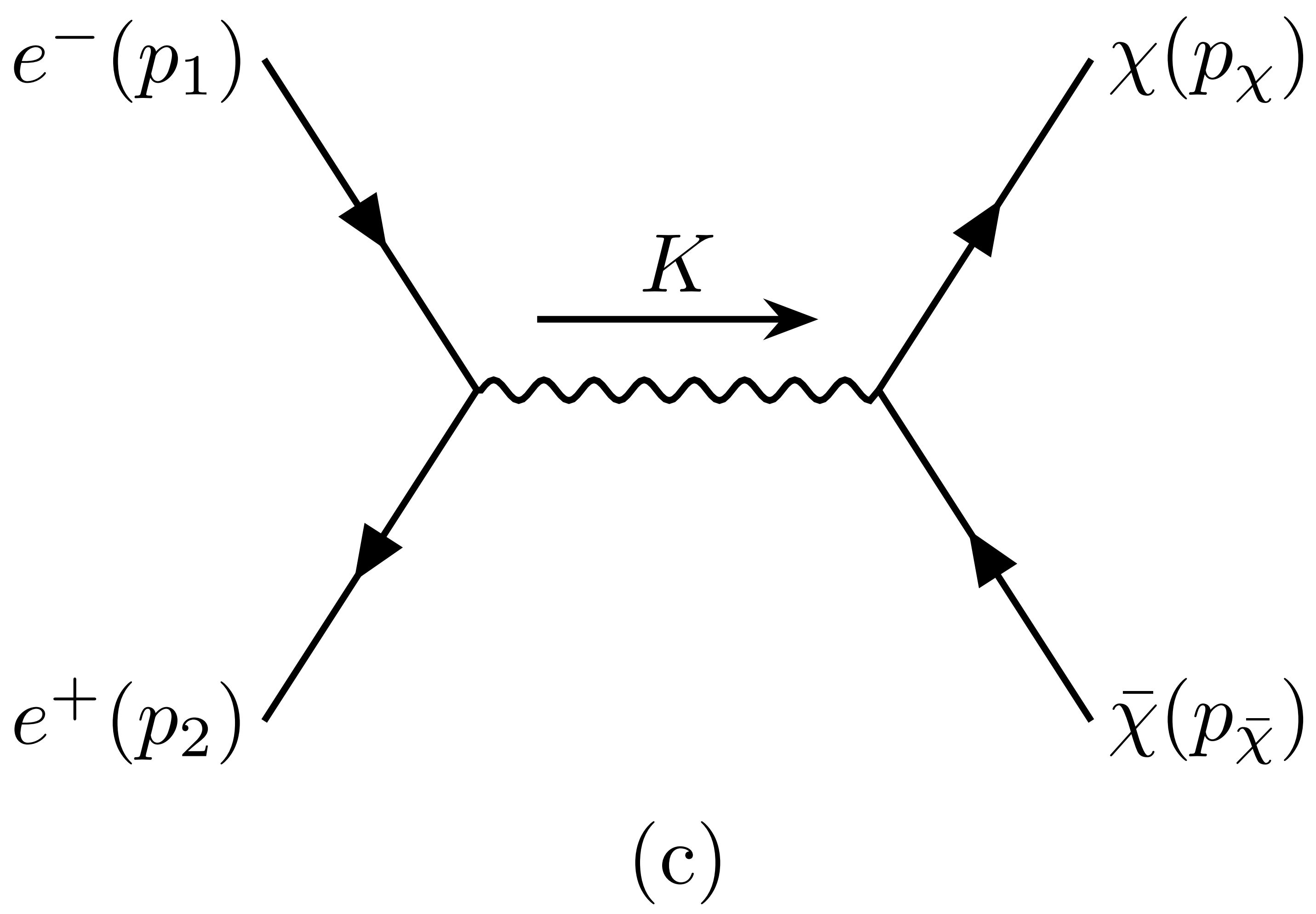

electron-positron annihilation

[Davidson+, hep-ph/0001179]

[Chang+, 1803.00993]

MCP production channels in the SN core (I)

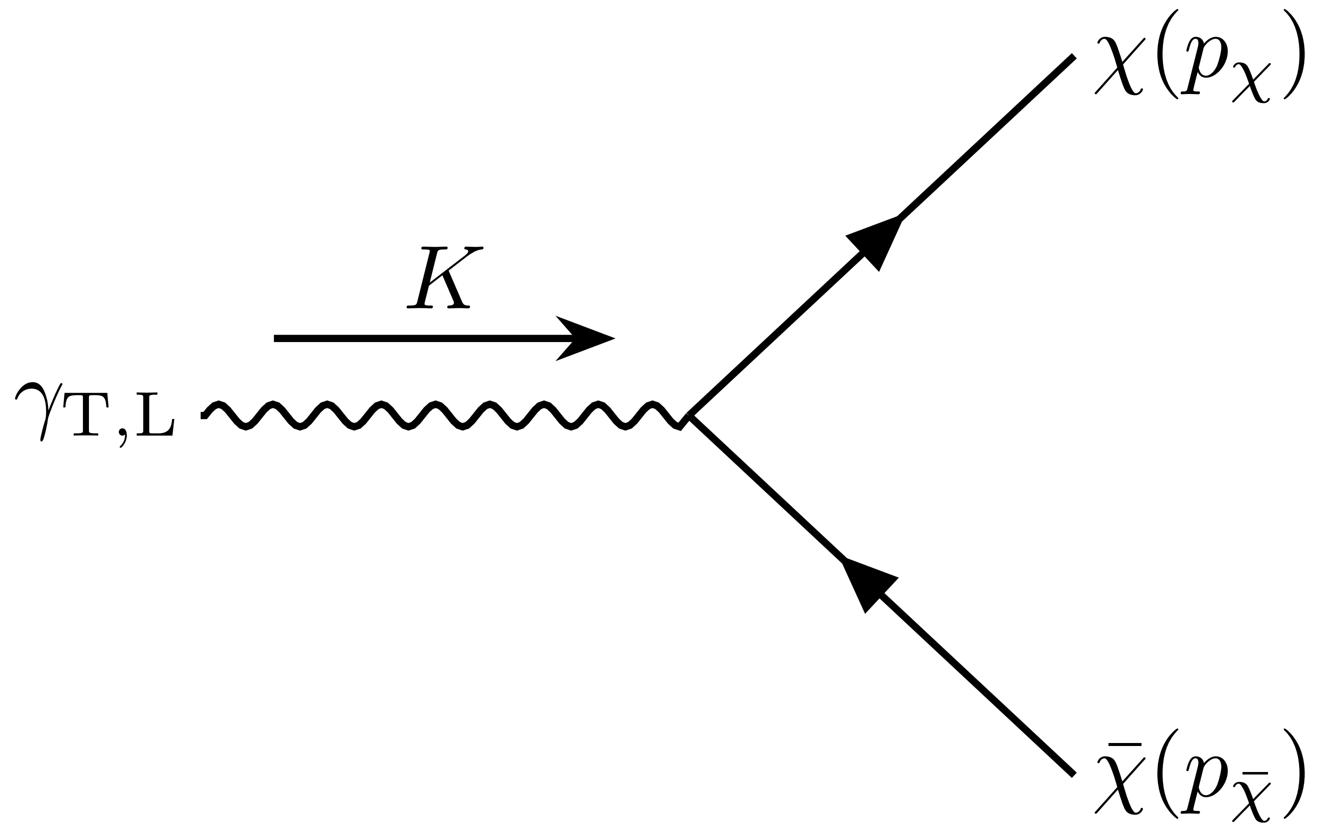

(a)

plasmon
decay

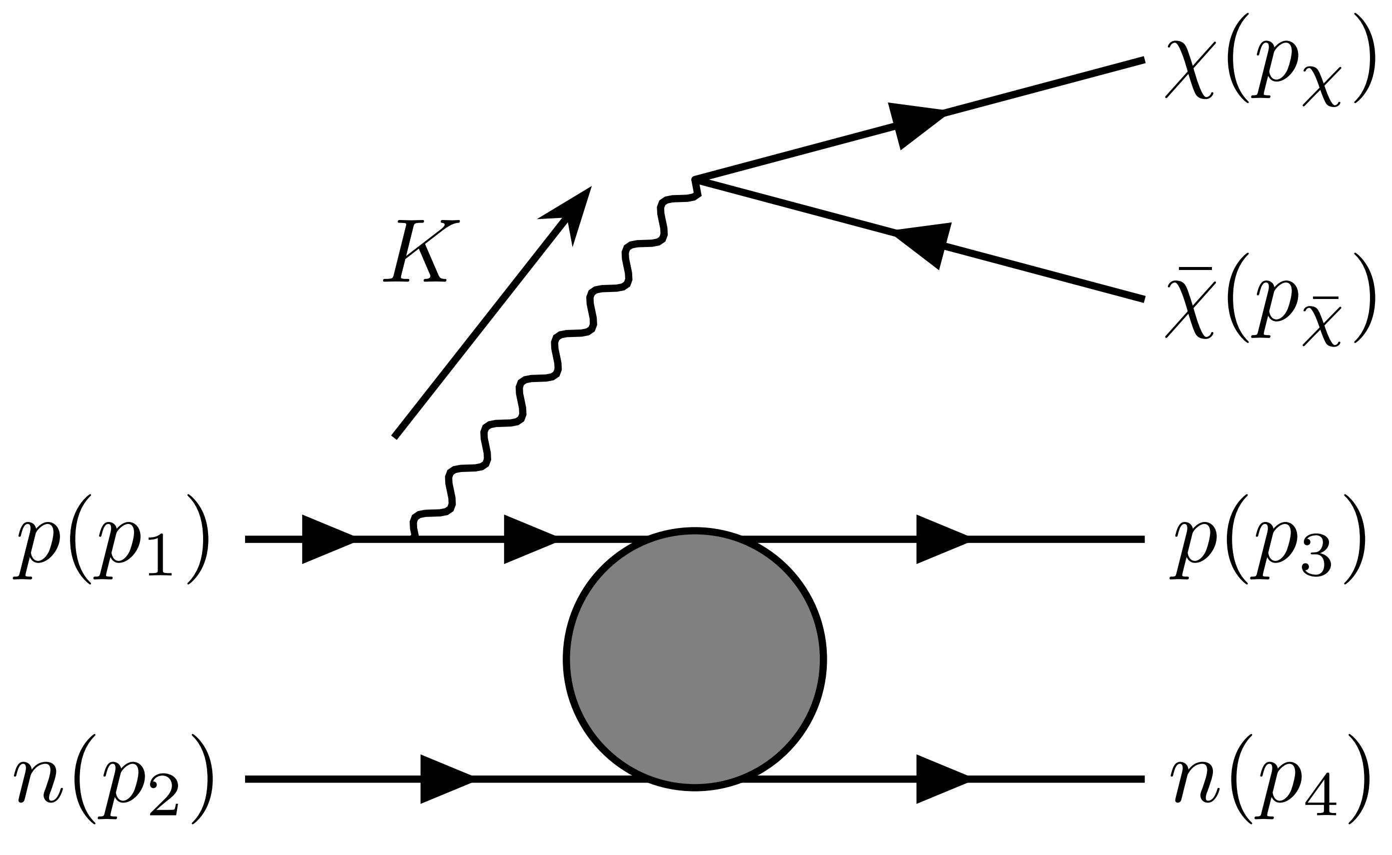

(b)

proton
bremsstrahlung

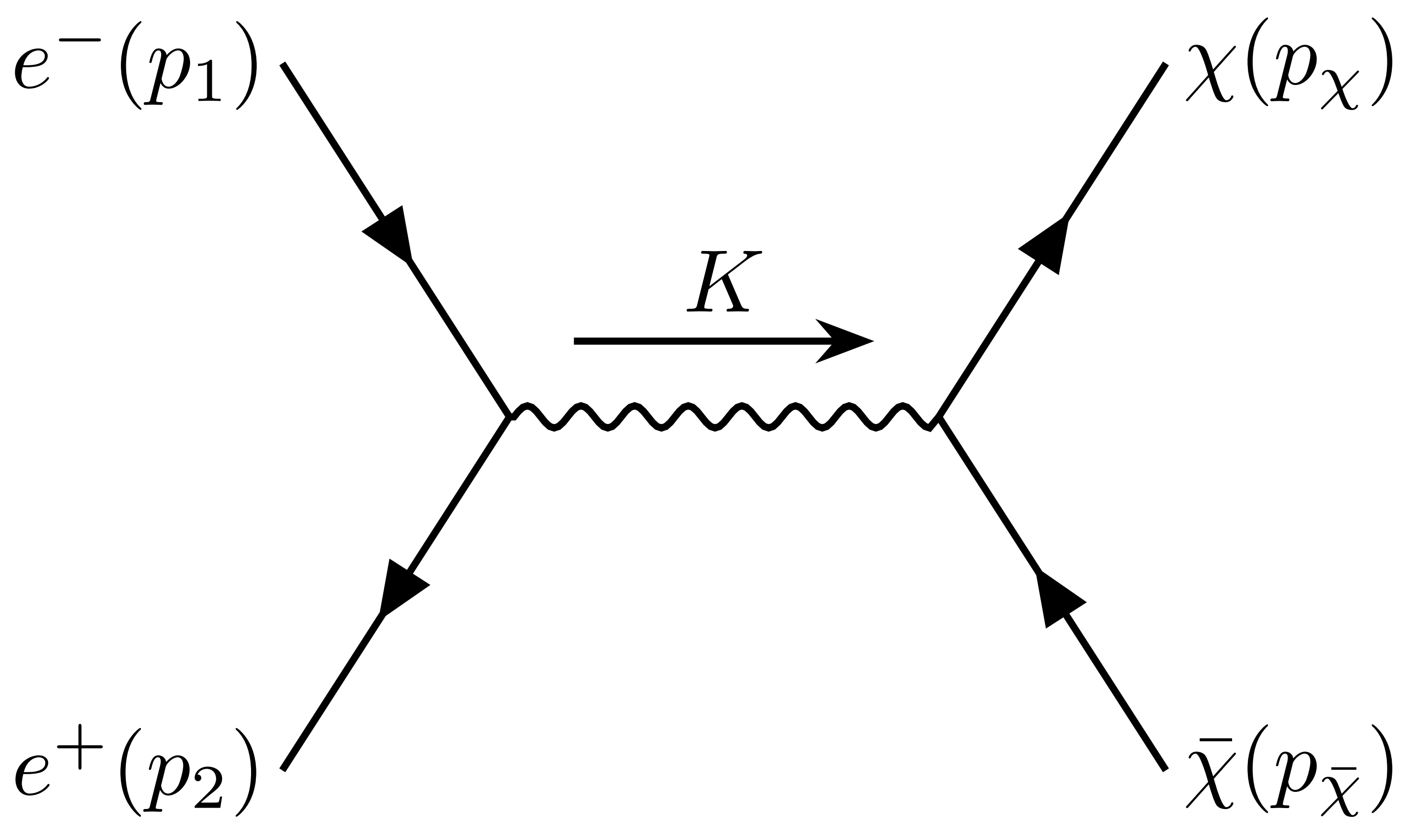

(c)

electron-positron
annihilation

[Davidson+, hep-ph/0001179]

[Chang+, 1803.00993]

(previously omitted for MCPs)

Particle mass/energy in the one-zone model

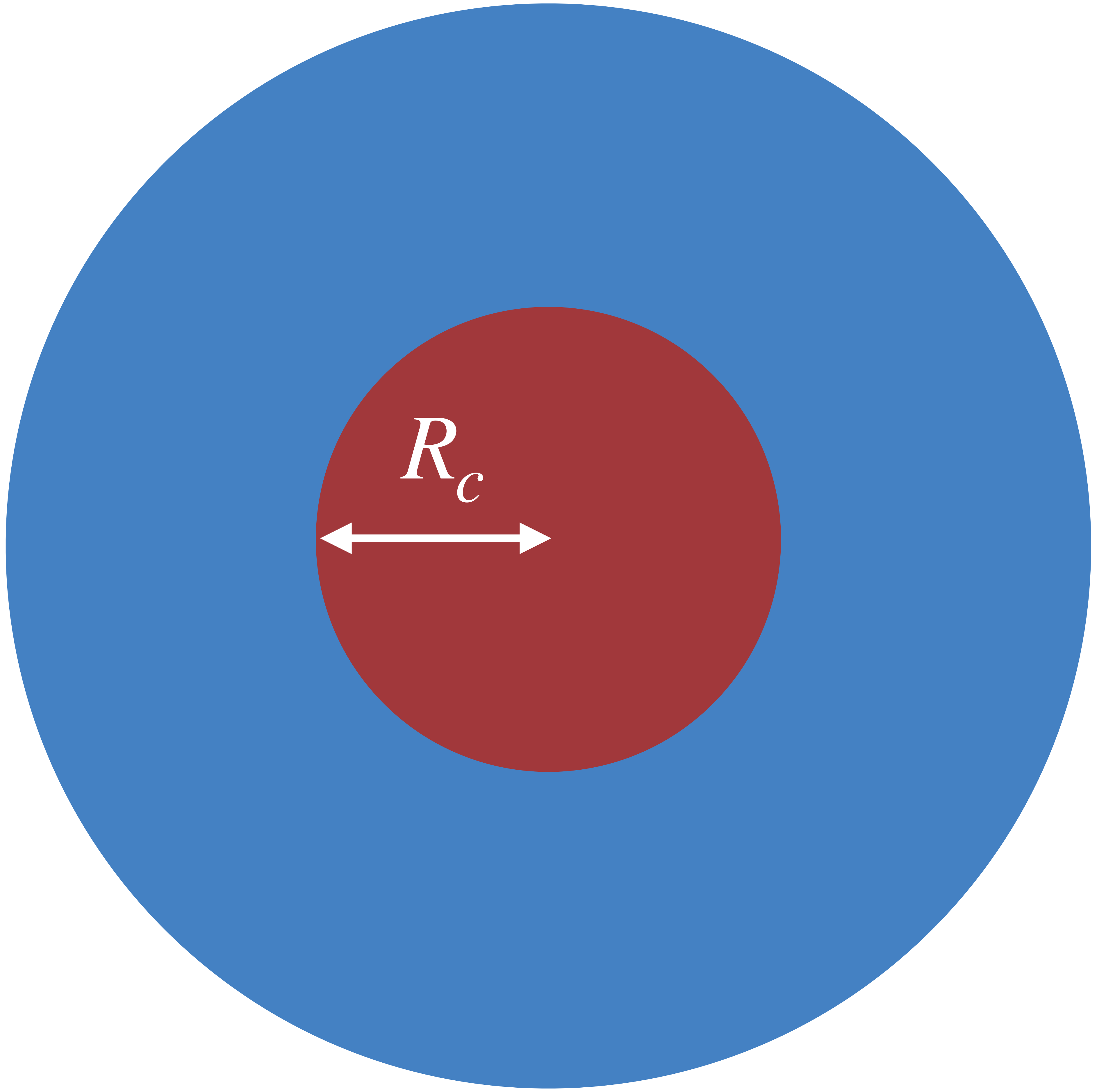

Photon mass < 12 MeV

(plasmon decay)

Nucleon: $\langle E_n \rangle \simeq 45$ MeV

(proton bremsstrahlung)

electron: $\langle E_{e^-} \rangle \simeq 160$ MeV

positron: $\langle E_{e^+} \rangle \simeq 90$ MeV

(electron-positron annihilation)

low-mass

high-mass

MCP production channels in the SN core (II)

pionic processes: processes w/ negatively charged pions in the initial state

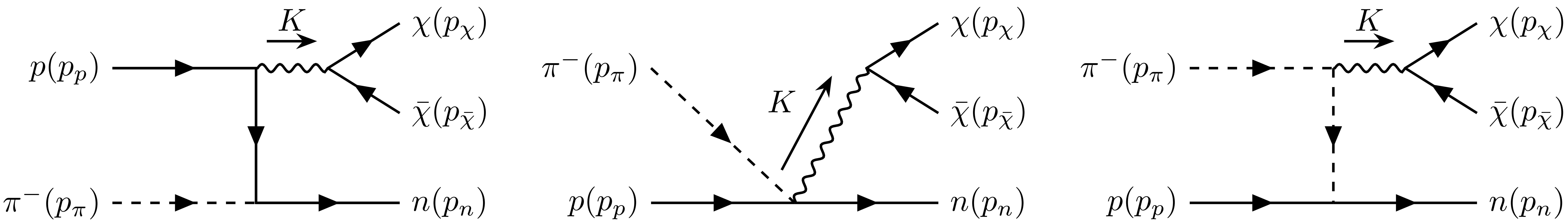

not consider previously for MCPs

Thermal pions can be as abundant as muons

[Fore & Reddy, 1911.02632]

T = 30 MeV in β-equilibrium

nuclear saturation density $n_0 = 0.16\,\mathrm{fm}^{-3}$

for the one-zone model: $n_b/n_0 \simeq 1.1$

solid curves: pions included

dashed curves: w/o pions

including pions increases p, but decreases e/μ

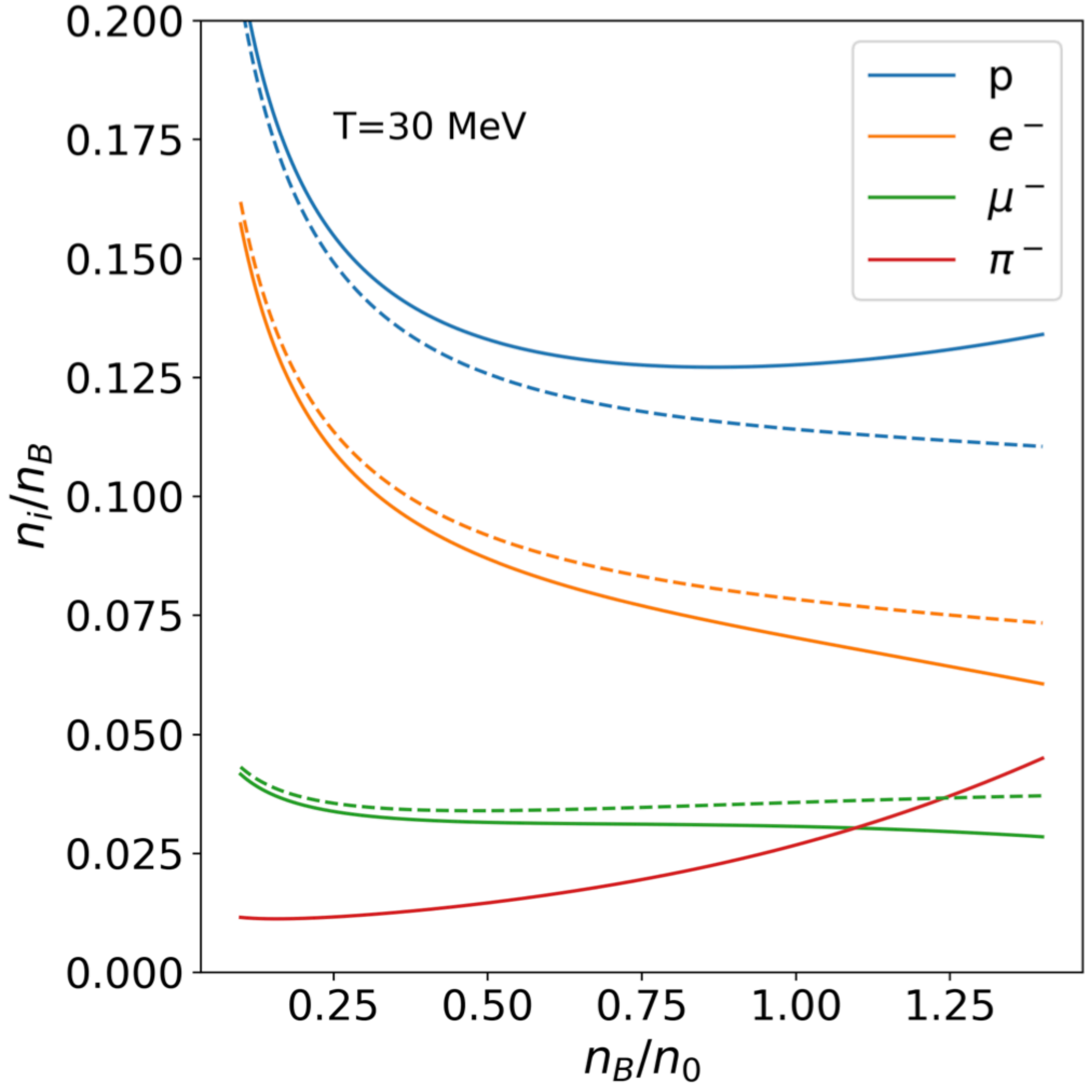

Energy deposition in the mantle

Total energy transfer from the core to the mantle

Total energy transfer from the core to the mantle

$$E_m = \text{lapse}^2 \times 4\pi\Delta t \int_0^{R_c} dr r^2 \int_{m'_\chi}^{\infty} dE_\chi \frac{d\Phi}{dE_\chi} \Delta E_\chi \leq 0.1\ B$$

ΔE_χ = energy deposited by a single χ in the mantle

$\Delta t = 3\ s$

$\dfrac{d\Phi}{dE_\chi}$ = total χ flux (3 production channels)

$\text{lapse} \equiv \sqrt{1 - \dfrac{2GM}{R_c}}$ = gravitational redshift & $m'_\chi = \dfrac{m_\chi}{\text{lapse}}$

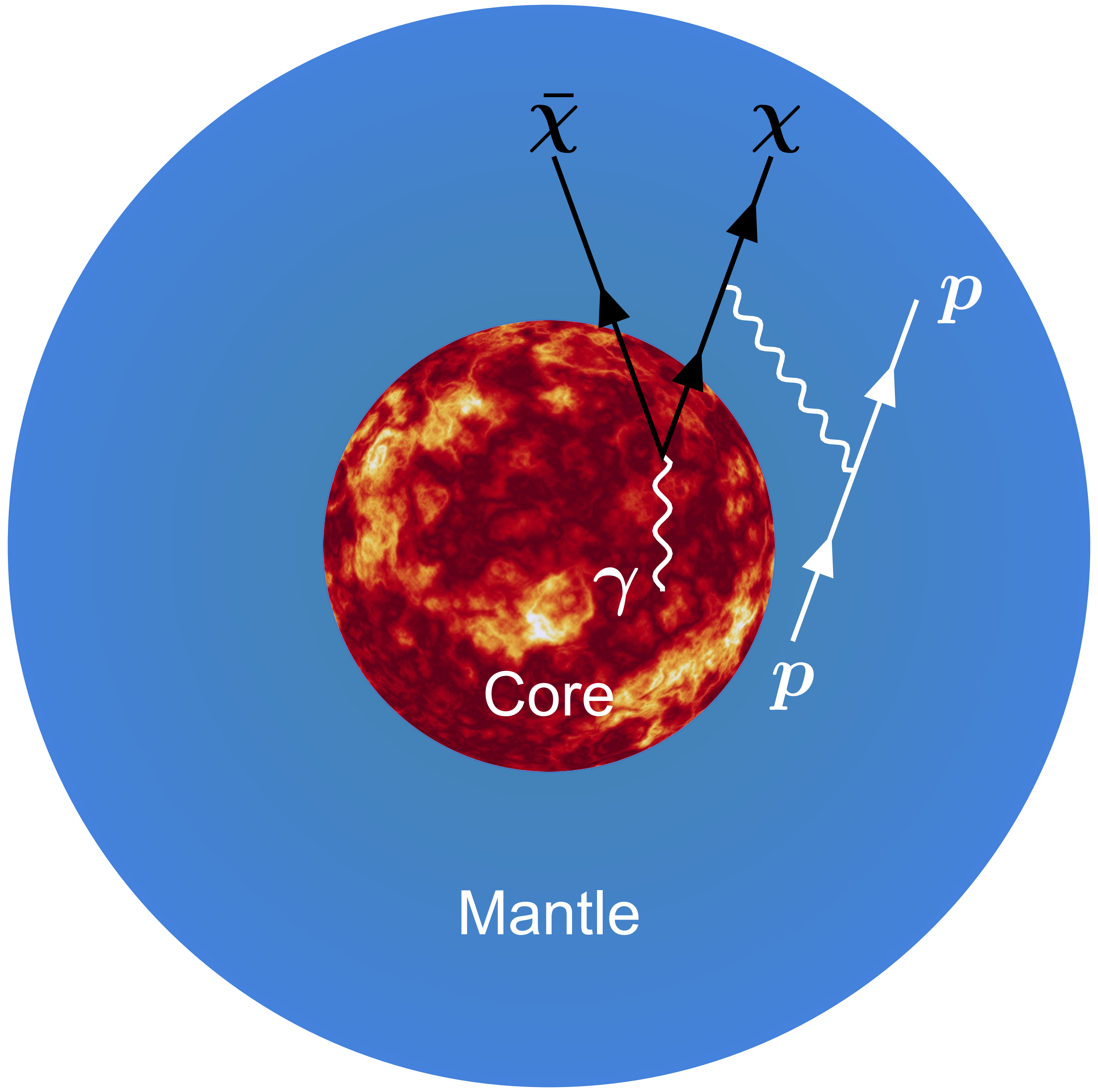

[Caputo+, 2201.09890]

LESN constraints on millicharged particles

Low-energy supernova limits on millicharged particles

[Li, ZL, Lu, Ye, 2408.04953]

$$e\,\epsilon\,A_\mu\,\bar{\chi}\,\gamma^\mu\,\chi$$

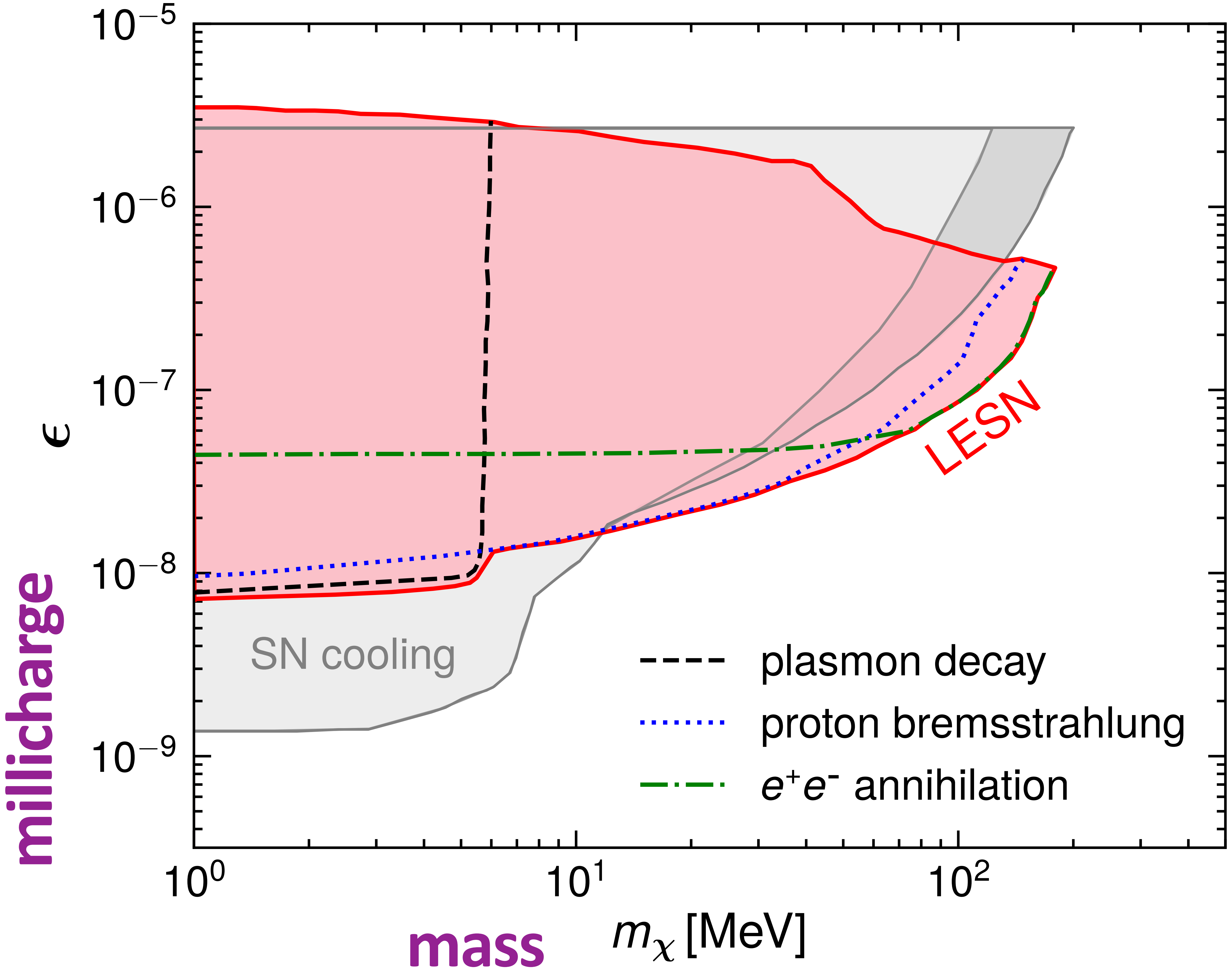

w/o pionic processes

probe new para space for $m \gtrsim$ 10 MeV

better than SN cooling in high-mass region

[Davidson+, hep-ph/0001179]

[Chang+, 1803.00993]

plasmon decay: $m \lesssim$ 6 MeV

proton bremsstrahlung: $6 \lesssim m \lesssim 30$ MeV

electron-positron annihilation: $m \gtrsim 30$ MeV

Low-energy supernova limits on millicharged particles

[Li, ZL, Lu, Ye, 2408.04953]

$e\,\epsilon\,A_\mu\,\bar{\chi}\,\gamma^\mu\,\chi$

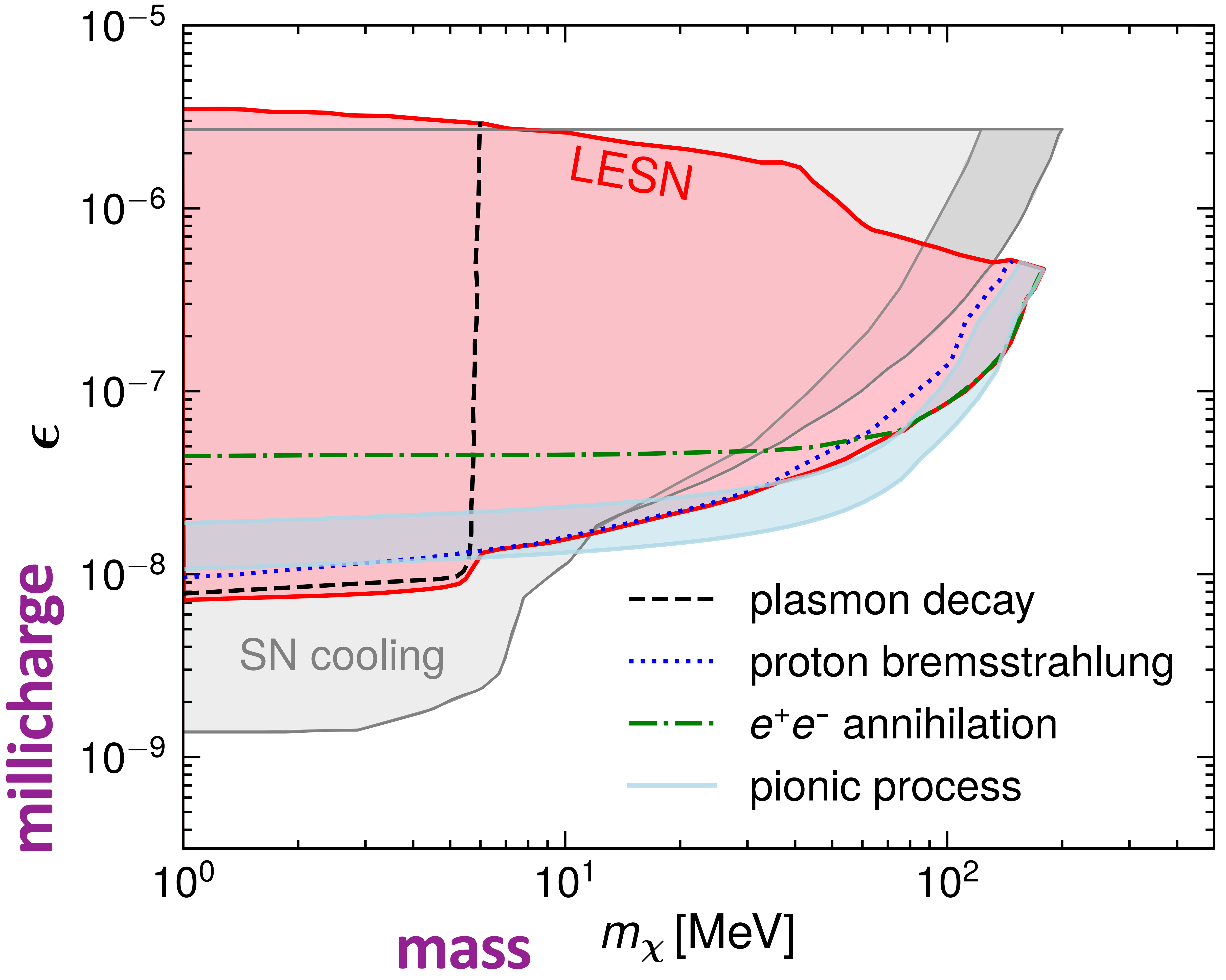

w/ pionic processes

pionic processes can probe new para space for $m \gtrsim$ 10 MeV

3

SN Constraints on Lepton Flavor Violating Axion-Like Particles

Lepton Flavor Violating Axion-Like Particles

Lepton flavor violating axions/ALPs

Lepton flavor violating (LFV) axions or axion-like particles (ALPs)

$$\mathscr{L}_{\rm int} = -\, i g_{ae\mu}\, a\, \bar{e}\, \gamma_5\, \mu + \mathrm{h.c.}$$

LFV couplings to electrons and muons

[F. Wilczek, 82]

[L. Calibbi, D. Redigolo, R. Ziegler, and J. Zupan, 2006.04795]

new muon decay channel $\Longrightarrow$ muon-decay constraints

Axion production in the SN core

Different axion production channels in the SN (1)

(1) muon decay

$$\mu^- \to e^- + a$$

axion mass < muon mass

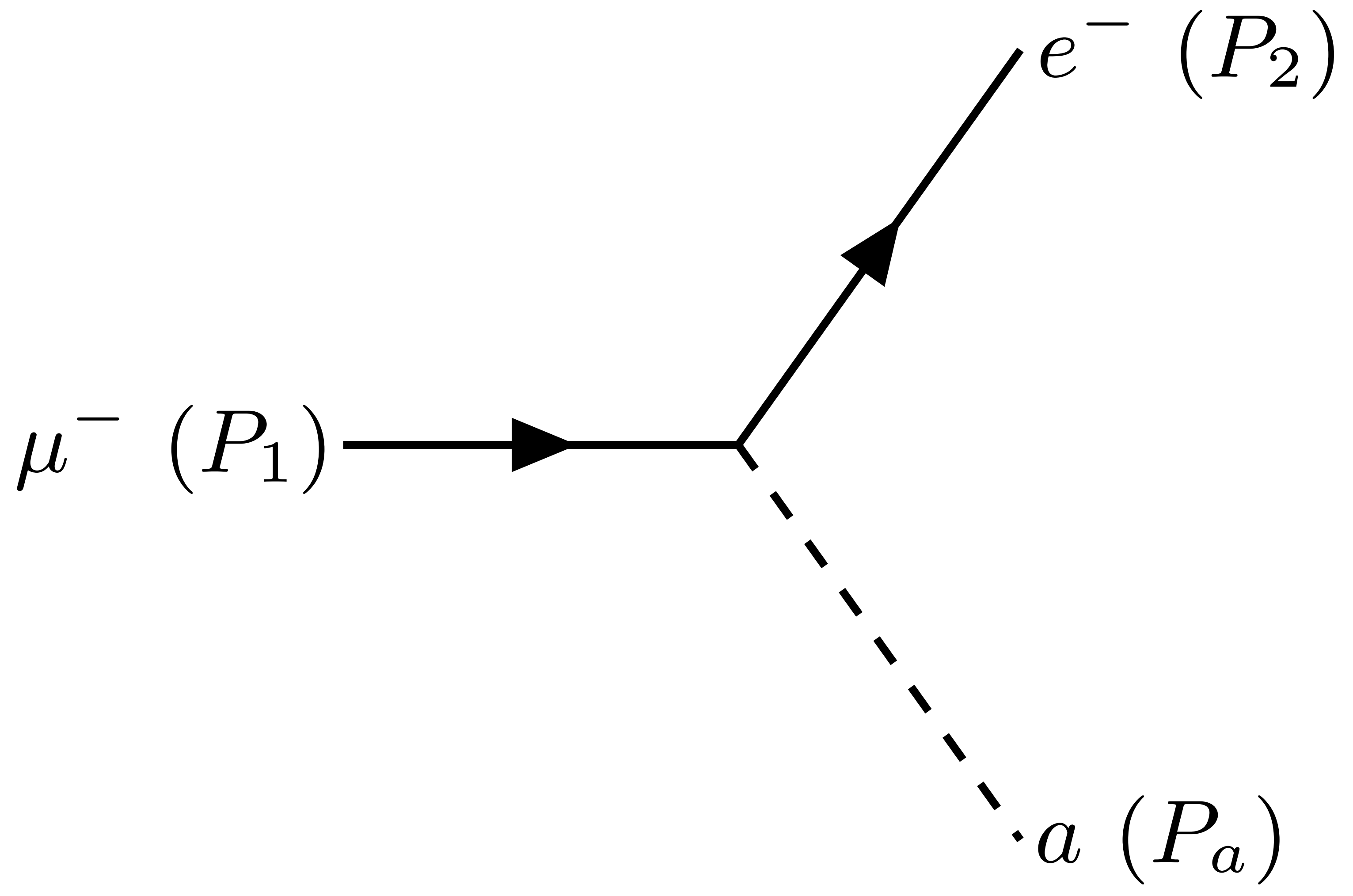

[L. Calibbi, D. Redigolo, R. Ziegler, and J. Zupan, 2006.04795]

Different axion production channels in the SN (2)

(2) bremsstrahlung

$$e/\mu + p \to \mu/e + p + a$$

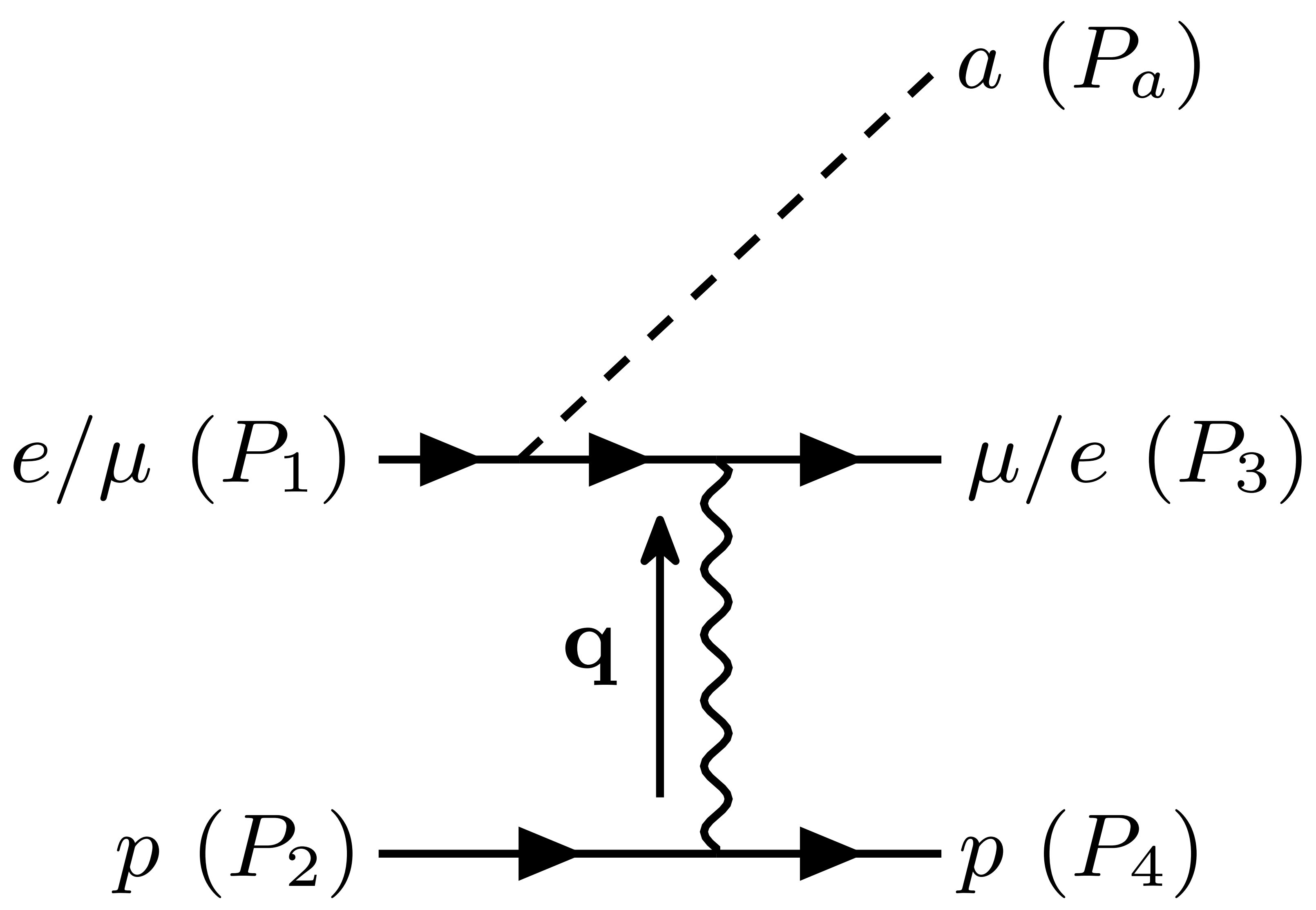

[H.-Y. Zhang, R. Hagimoto, and A. J. Long, 2309.03889]

Different axion production channels in the SN (3)

(3) electron-muon coalescence

$$e^-/\mu^- + \mu^+/e^+ \to a$$

axion mass > muon mass

[Li, ZL, 2501.12075]

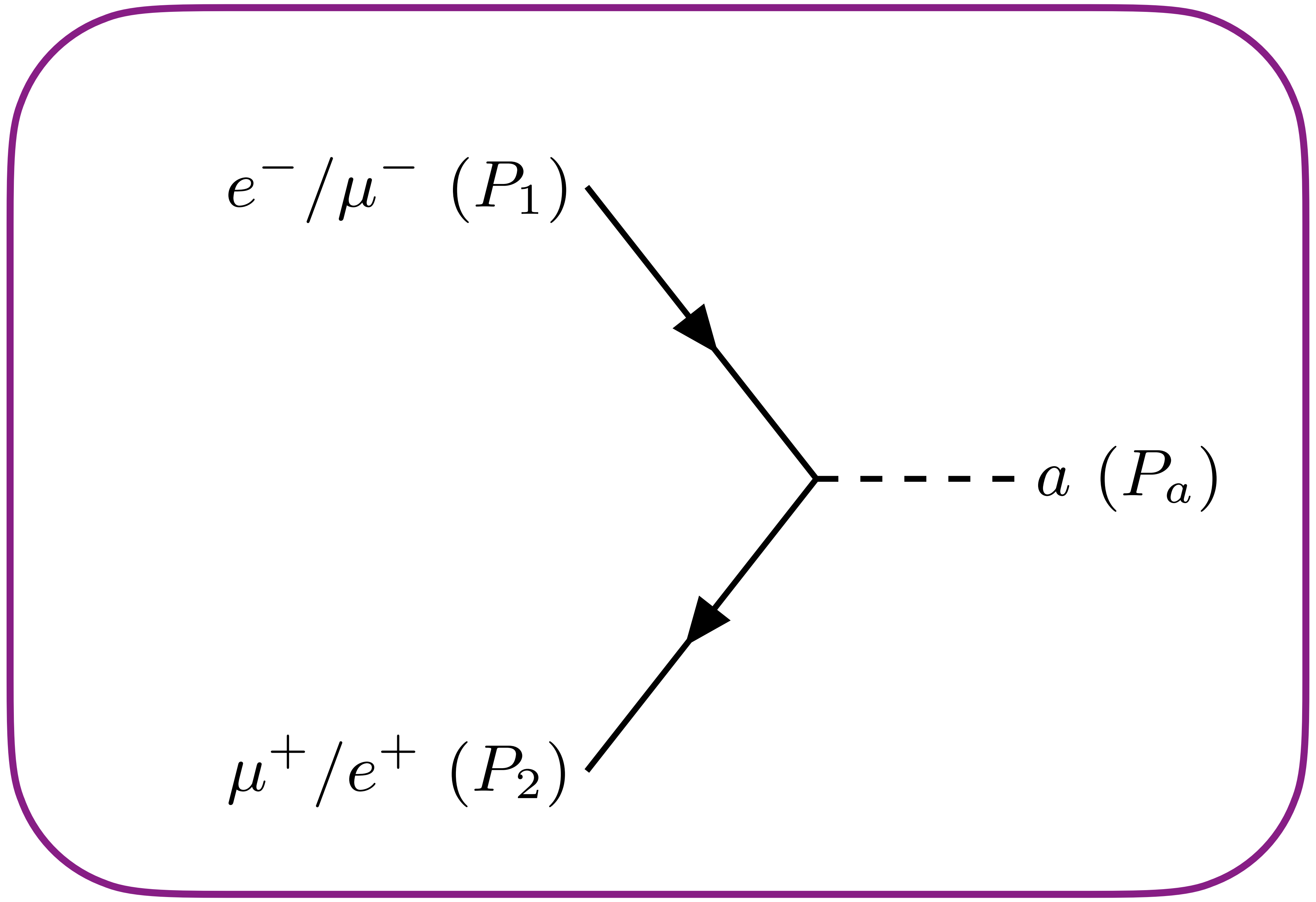

Different axion production channels in the SN (4)

(4) semi-Compton

$$\mu(e) + \gamma \rightarrow e(\mu) + a$$

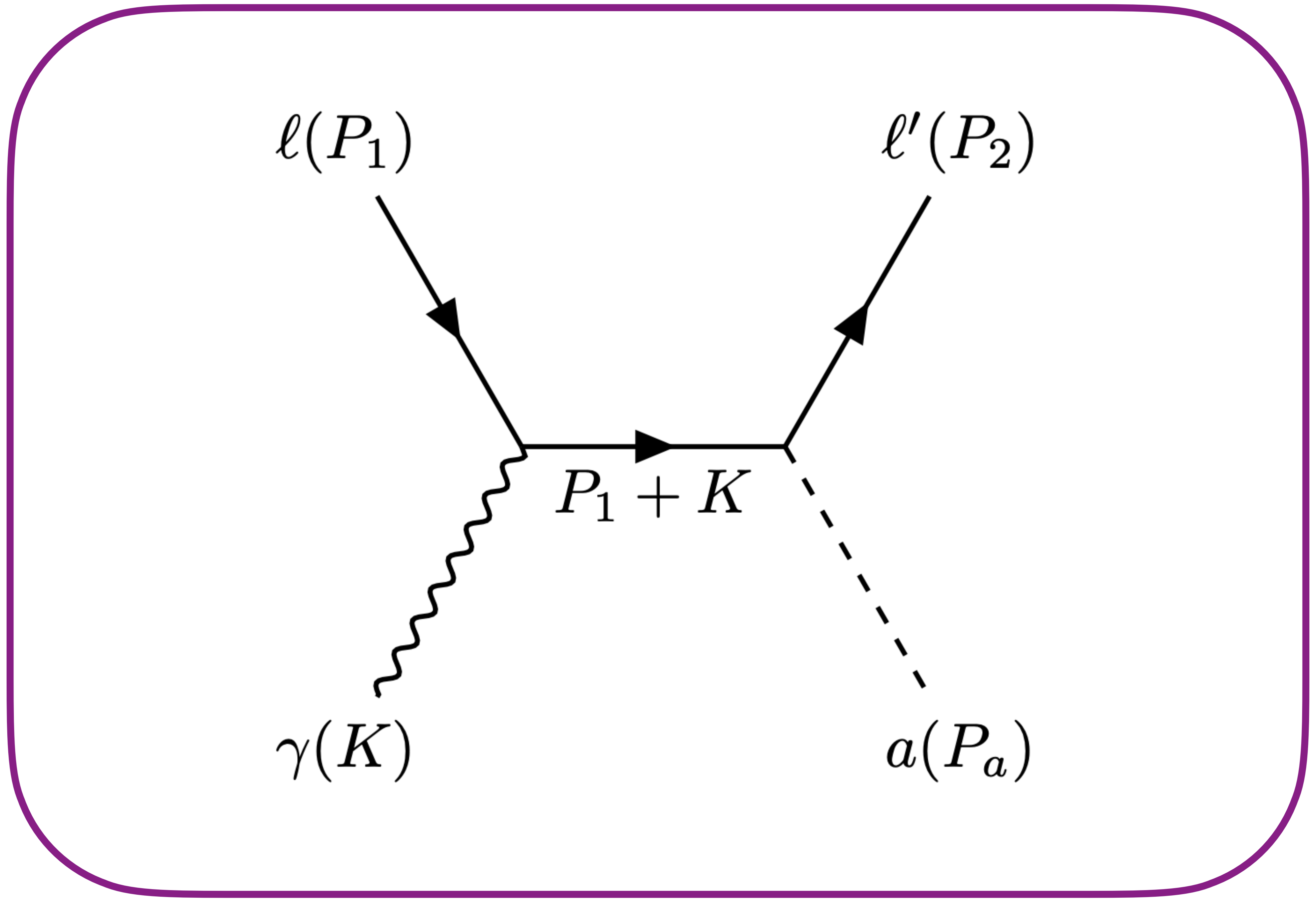

[Huang, Li, ZL, 2510.22523]

[see arXiv:2503.15630 for electron couplings only]

Four production channels in the SN

muon decay

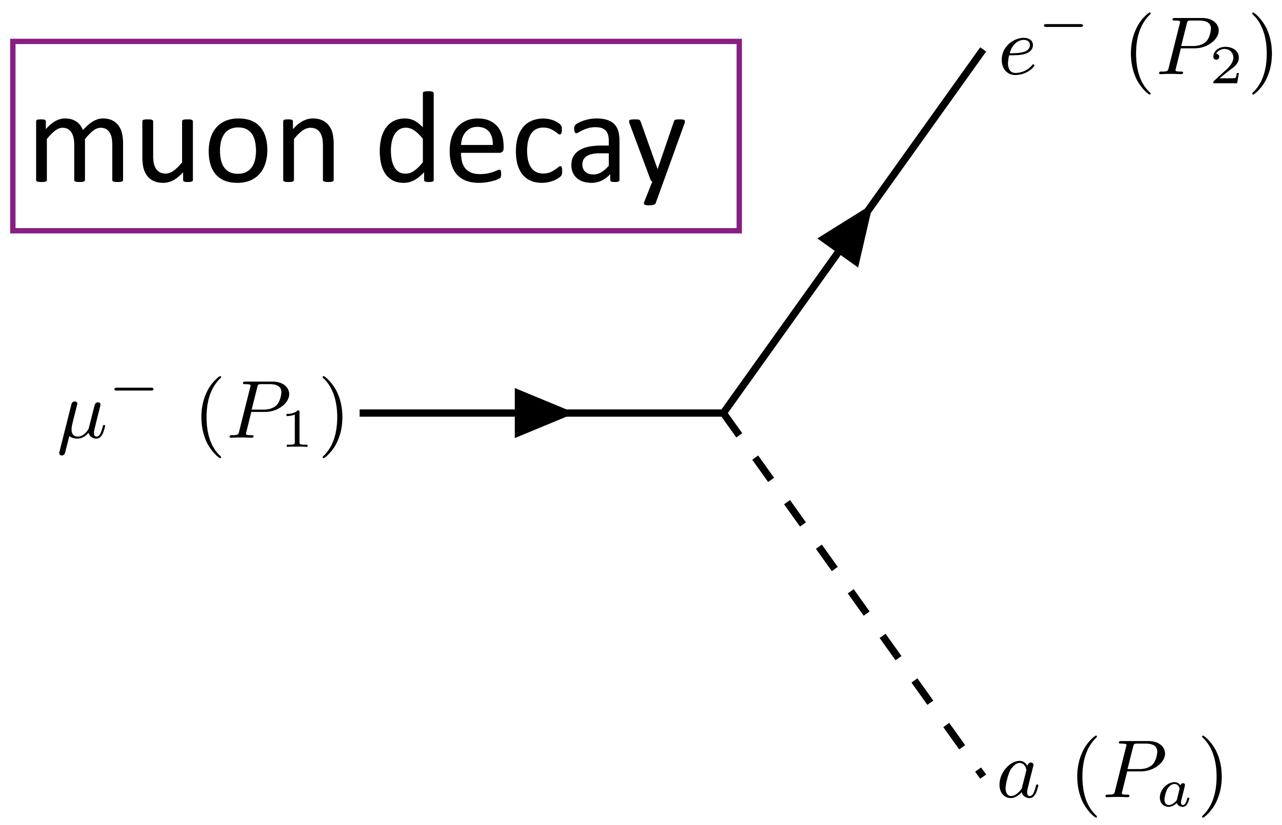

e-mu coalescence

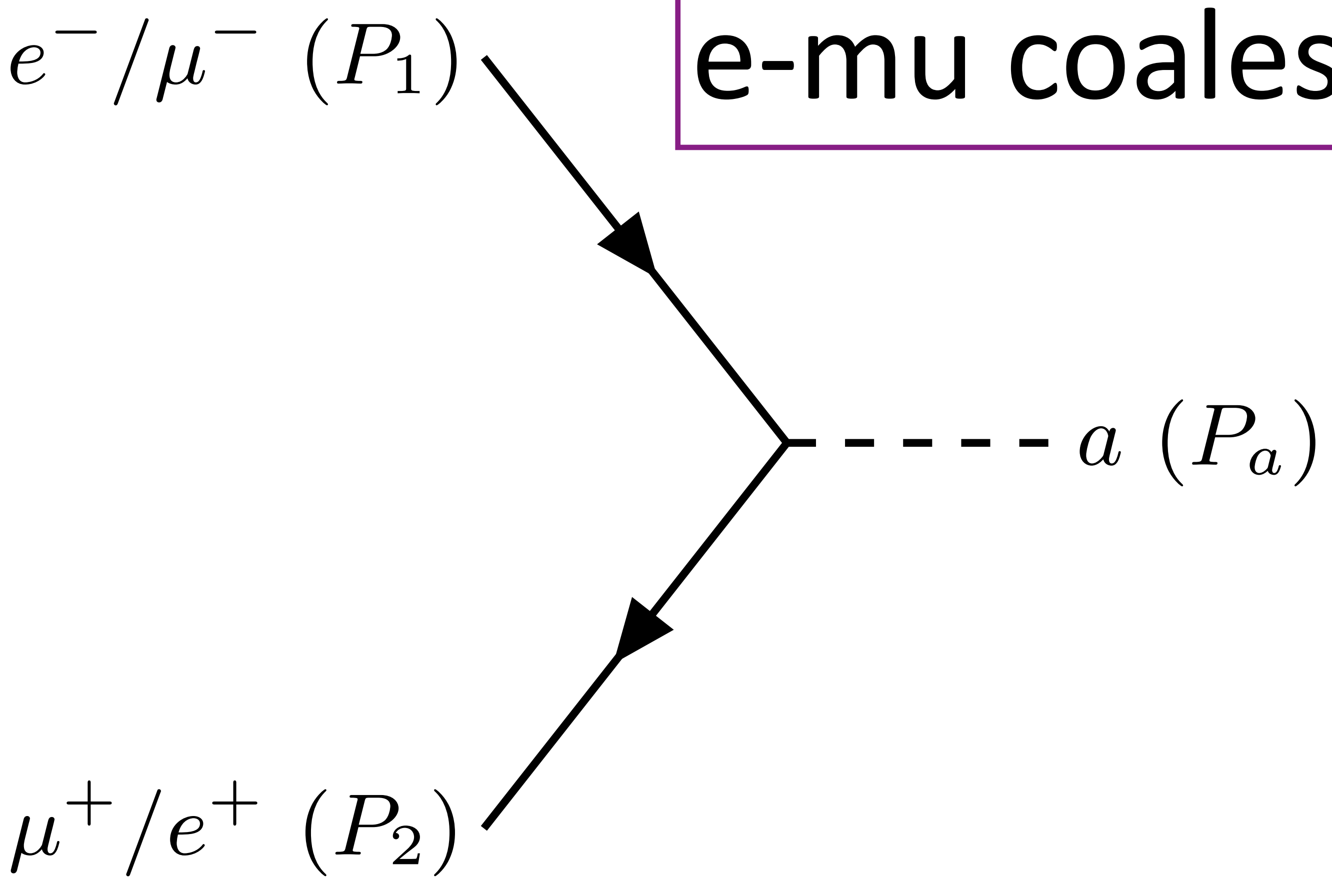

bremsstrahlung

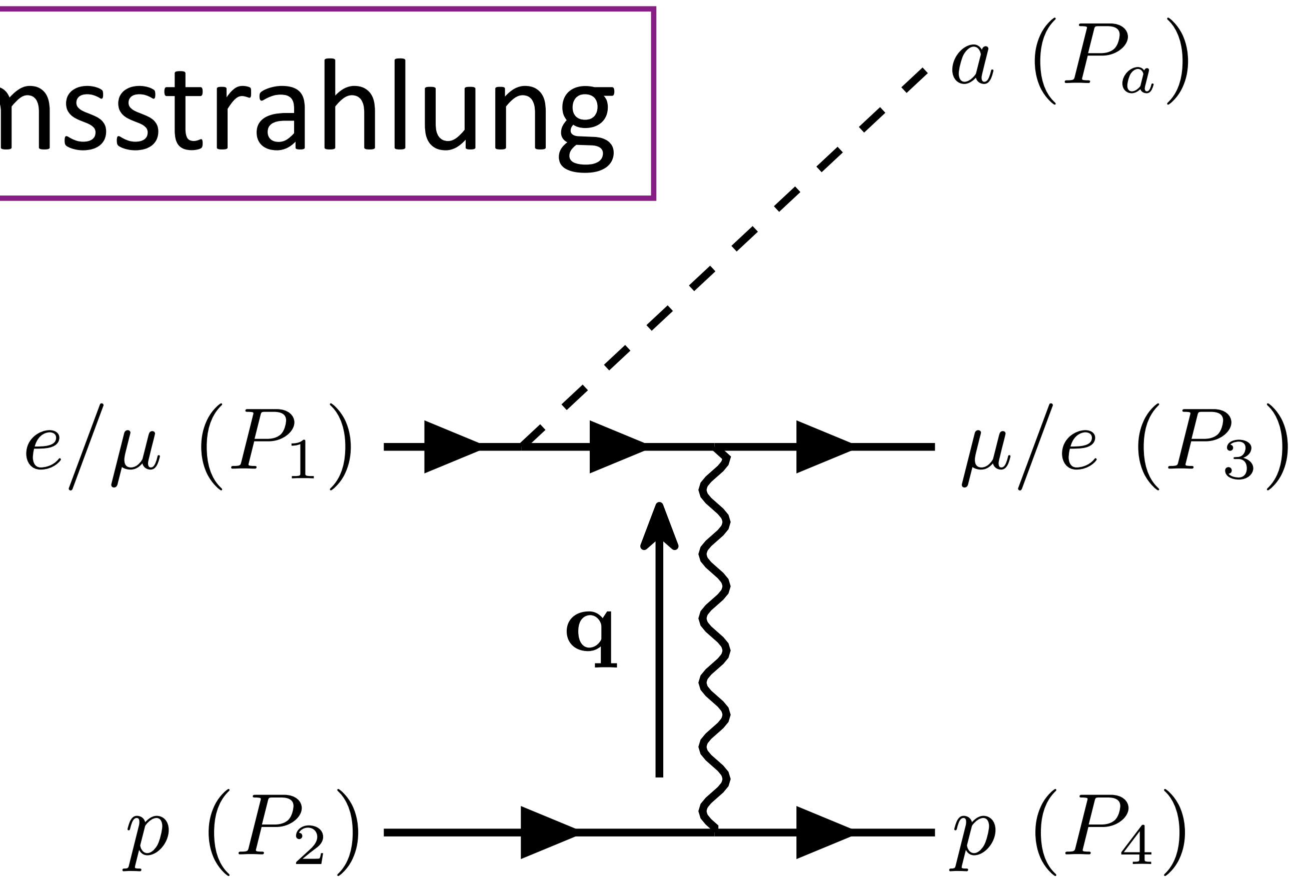

semi-Compton

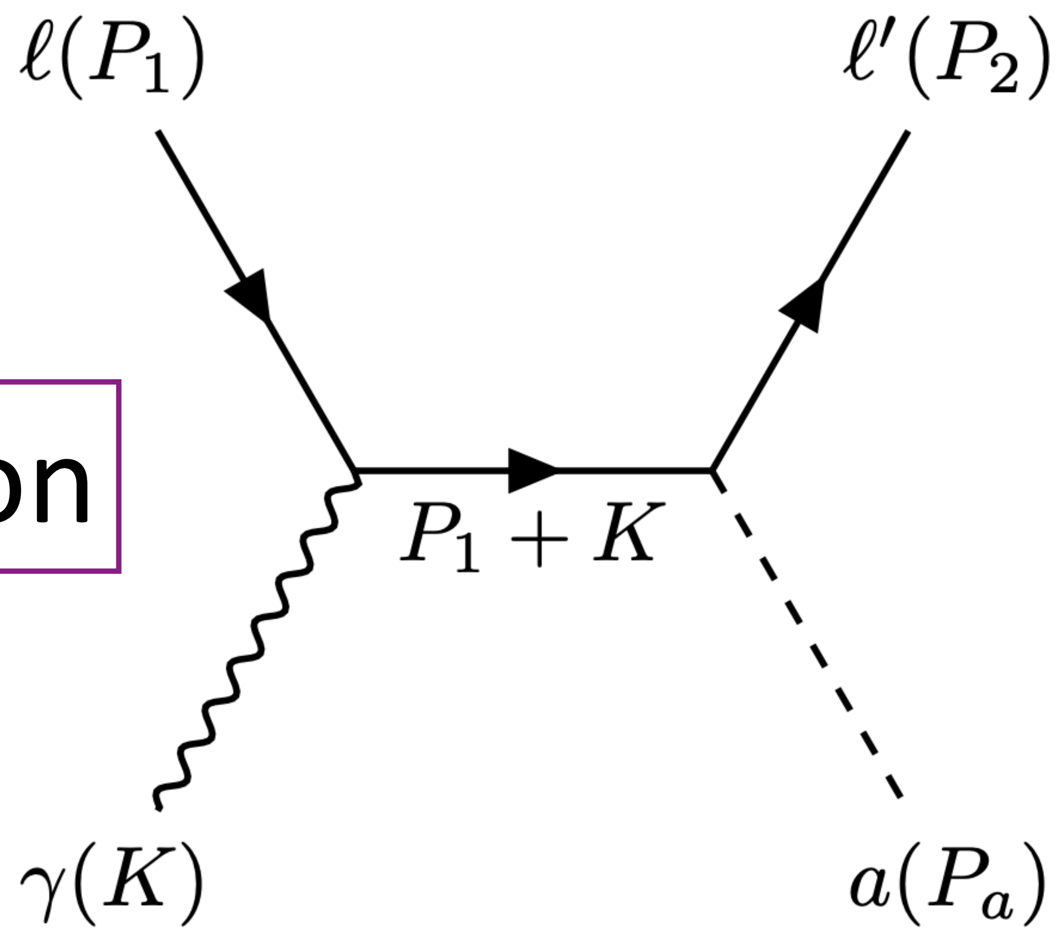

Four production channels in the SN

muon decay

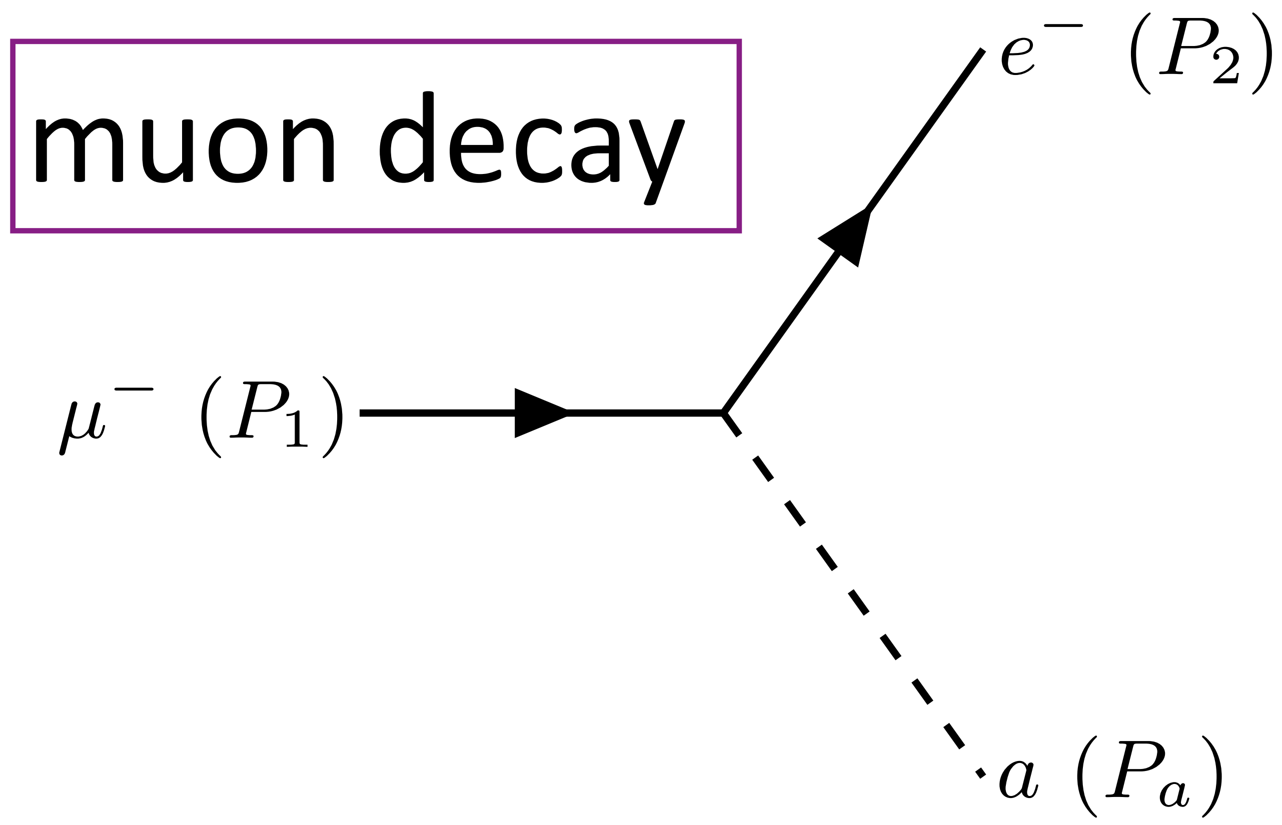

e-mu coalescence

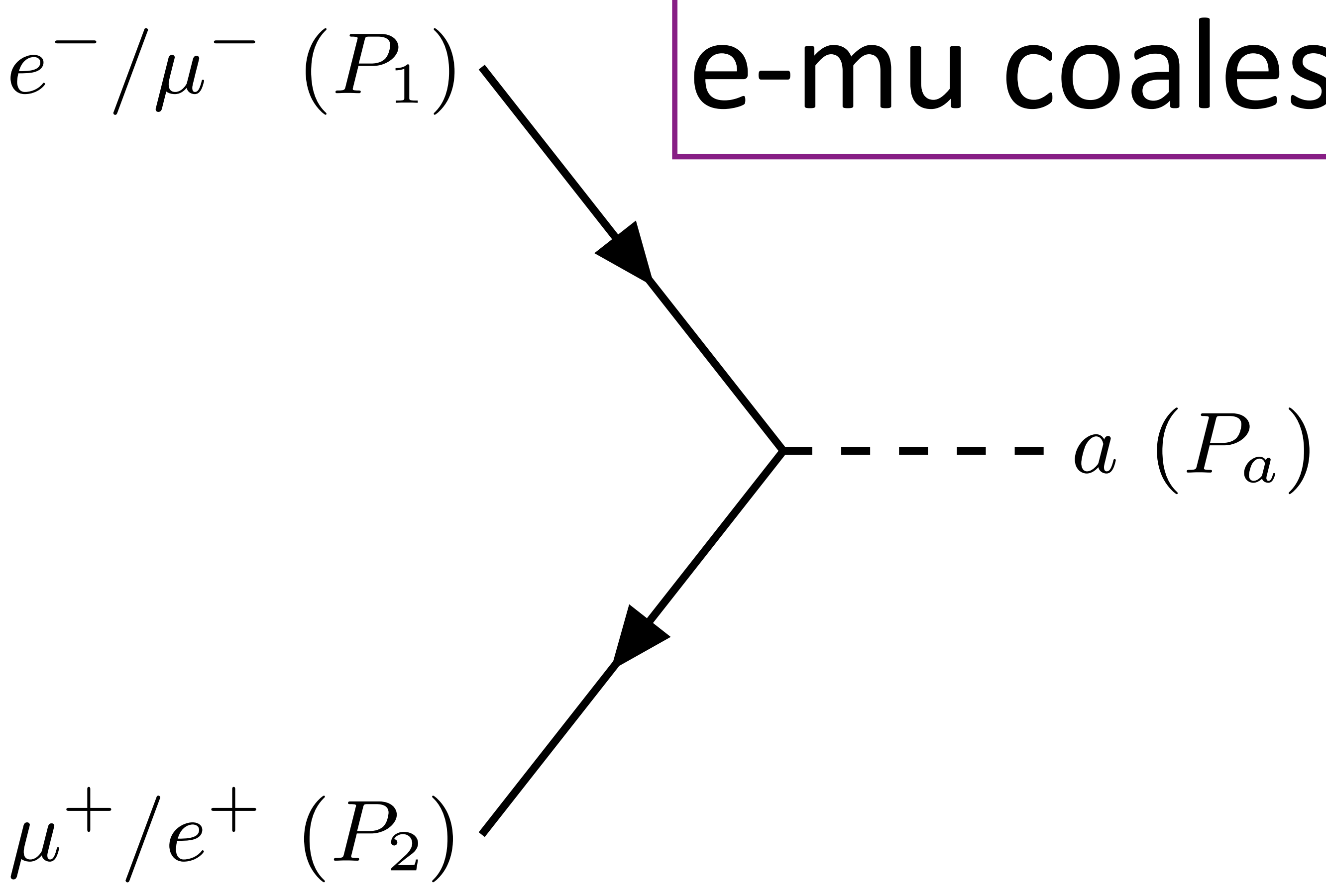

not studied previously for LFV-ALPs

bremsstrahlung

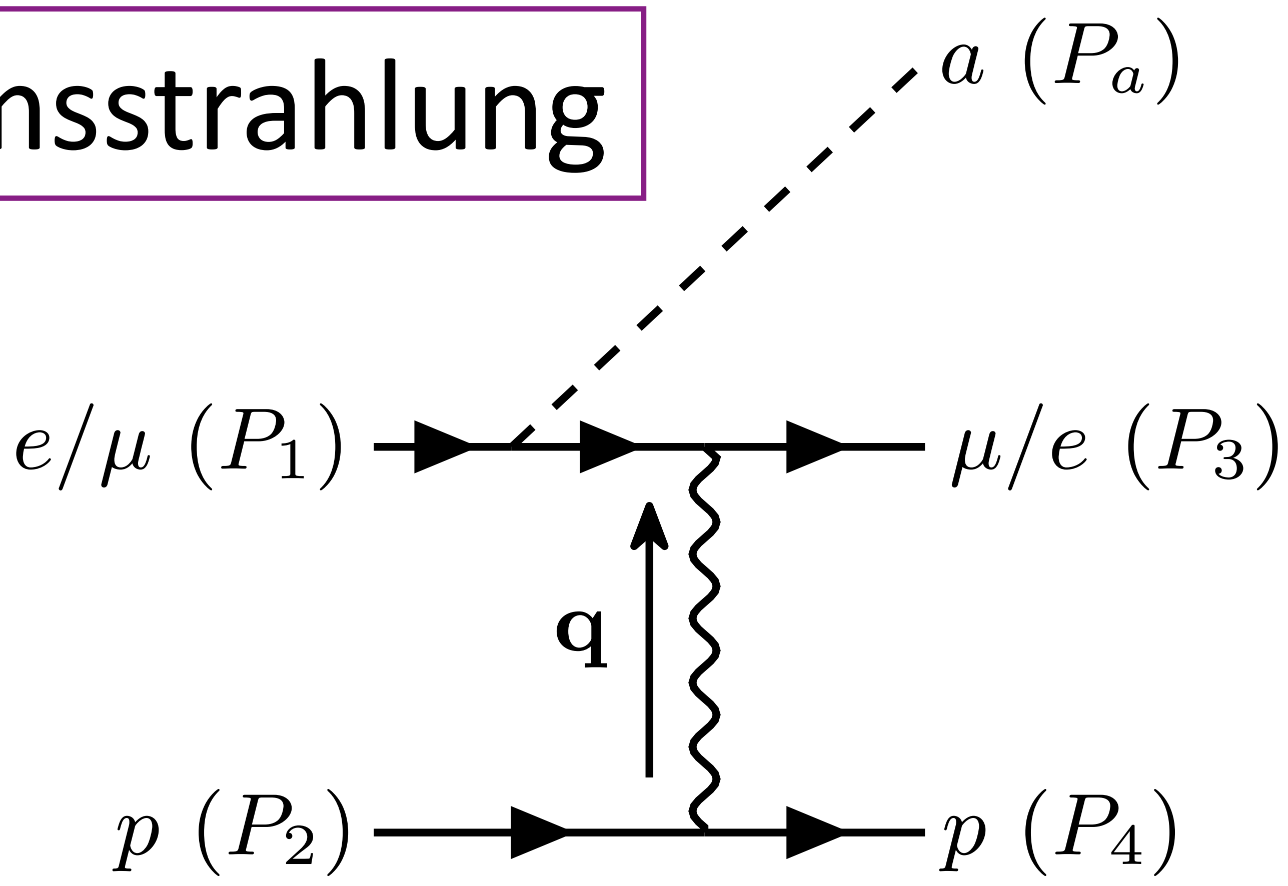

semi-Compton

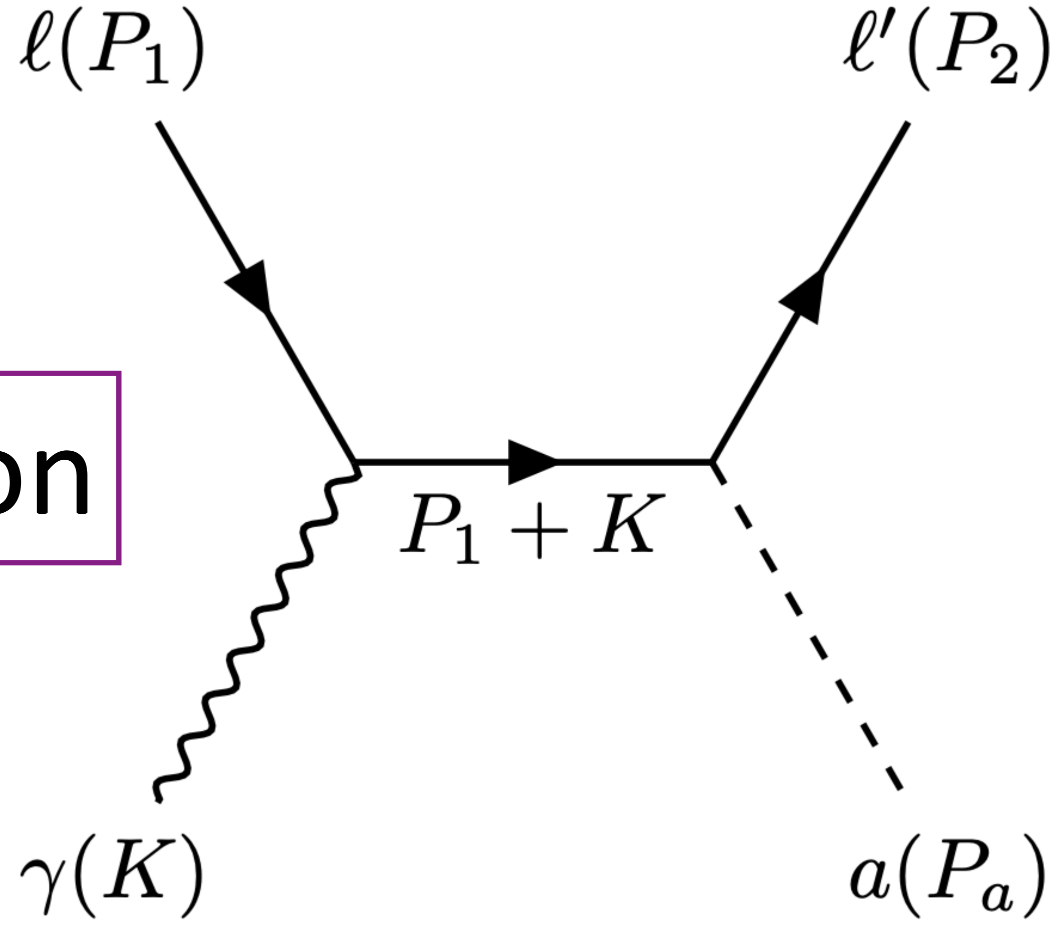

comparison between diff production channels

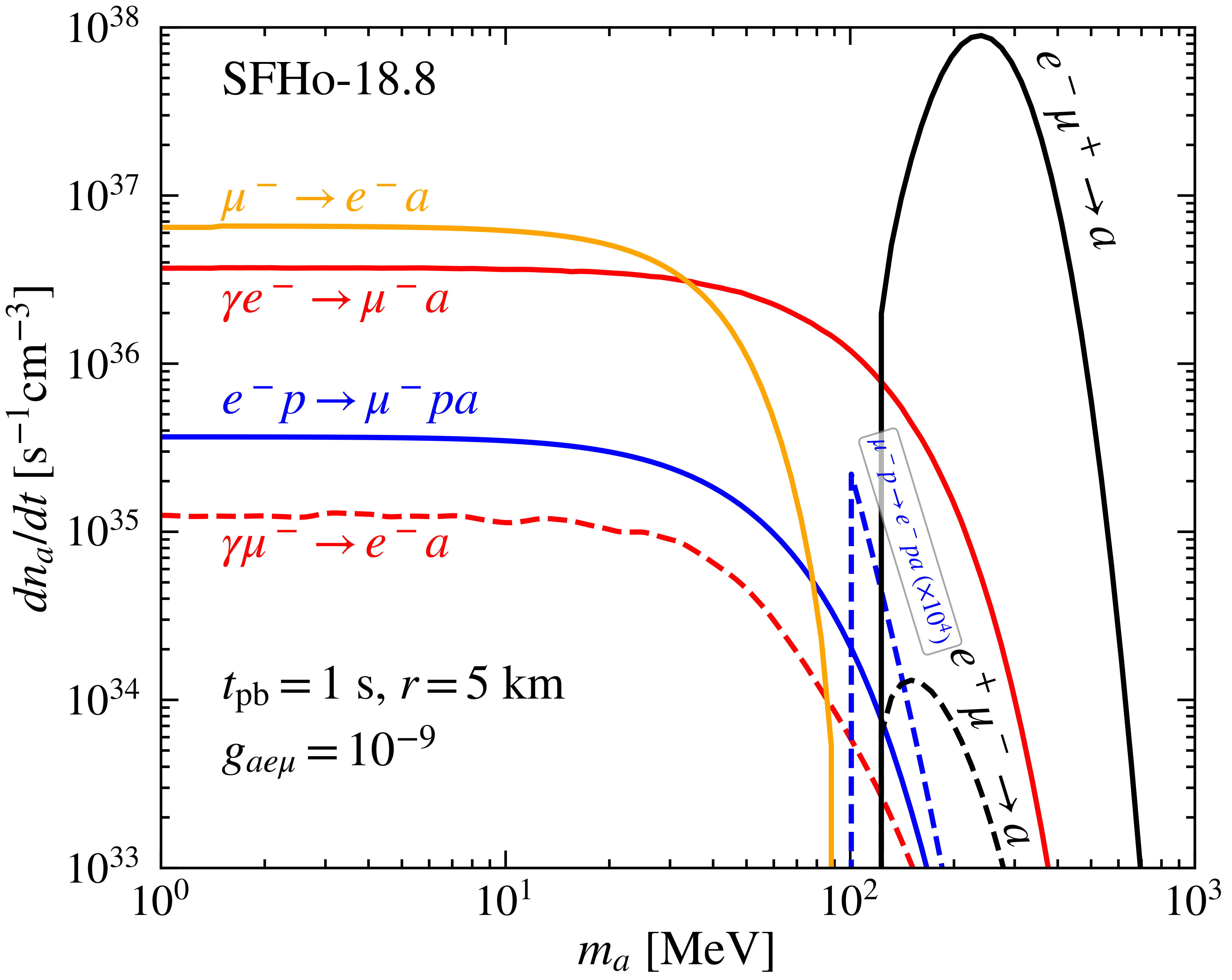

dominant production modes

$m_a \lesssim 30$ MeV: muon decay

$m_a \gtrsim 110$ MeV: e-mu coalescence

$30 \lesssim m_a \lesssim 110$ MeV: semi-Compton

bremsstrahlung is subdominant

[Huang, Li, ZL, 2510.22523]

Axion luminosity at the gain radius

Axion luminosity @ R_g is obtained via the volume integration of the production rate

$$L_a = \int_0^{R_g} dr\ 4\pi r^2\, \mathrm{lapse}(r)^2 (1+2v_r) \int_{m'_a}^{\infty} dE_a\ E_a \frac{d^2 n_a}{dt dE_a} \left\langle e^{-\tau_a(R_g, E_a, r)} \right\rangle$$

[A. Caputo, G. Raffelt, and E. Vitagliano, 2204.11862]

r = position of production

lapse(r) = gravitational effects

v_r = radial velocity of the emitting material: $v_r \ll 1$

$m'_a = m_a/\mathrm{lapse}$

Axion luminosity at the gain radius

Axion luminosity @ R_g is obtained via the volume integration of the production rate

$$L_a = \int_0^{R_g} dr\ 4\pi r^2 \,\mathrm{lapse}(r)^2 (1+2v_r) \int_{m'_a}^{\infty} dE_a\ E_a \frac{d^2 n_a}{dt dE_a} \langle e^{-\tau_a(R_g, E_a, r)} \rangle$$

[A. Caputo, G. Raffelt, and E. Vitagliano, 2204.11862]

↓ differential axion production rate

r = position of production

lapse(r) = gravitational effects

v_r = radial velocity of the emitting material: $v_r \ll 1$

$m'_a = m_a/\mathrm{lapse}$

Axion luminosity at the gain radius

Axion luminosity @ R_g is obtained via the volume integration of the production rate

$$L_a = \int_0^{R_g} dr\ 4\pi r^2\, \mathrm{lapse}(r)^2 (1 + 2v_r) \int_{m'_a}^{\infty} dE_a\ E_a \frac{d^2 n_a}{dt dE_a} \langle e^{-\tau_a(R_g, E_a, r)} \rangle$$

absorption term

differential axion production rate

[A. Caputo, G. Raffelt, and E. Vitagliano, 2204.11862]

r = position of production

lapse(r) = gravitational effects

v_r = radial velocity of the emitting material: $v_r \ll 1$

$m'_a = m_a/\mathrm{lapse}$

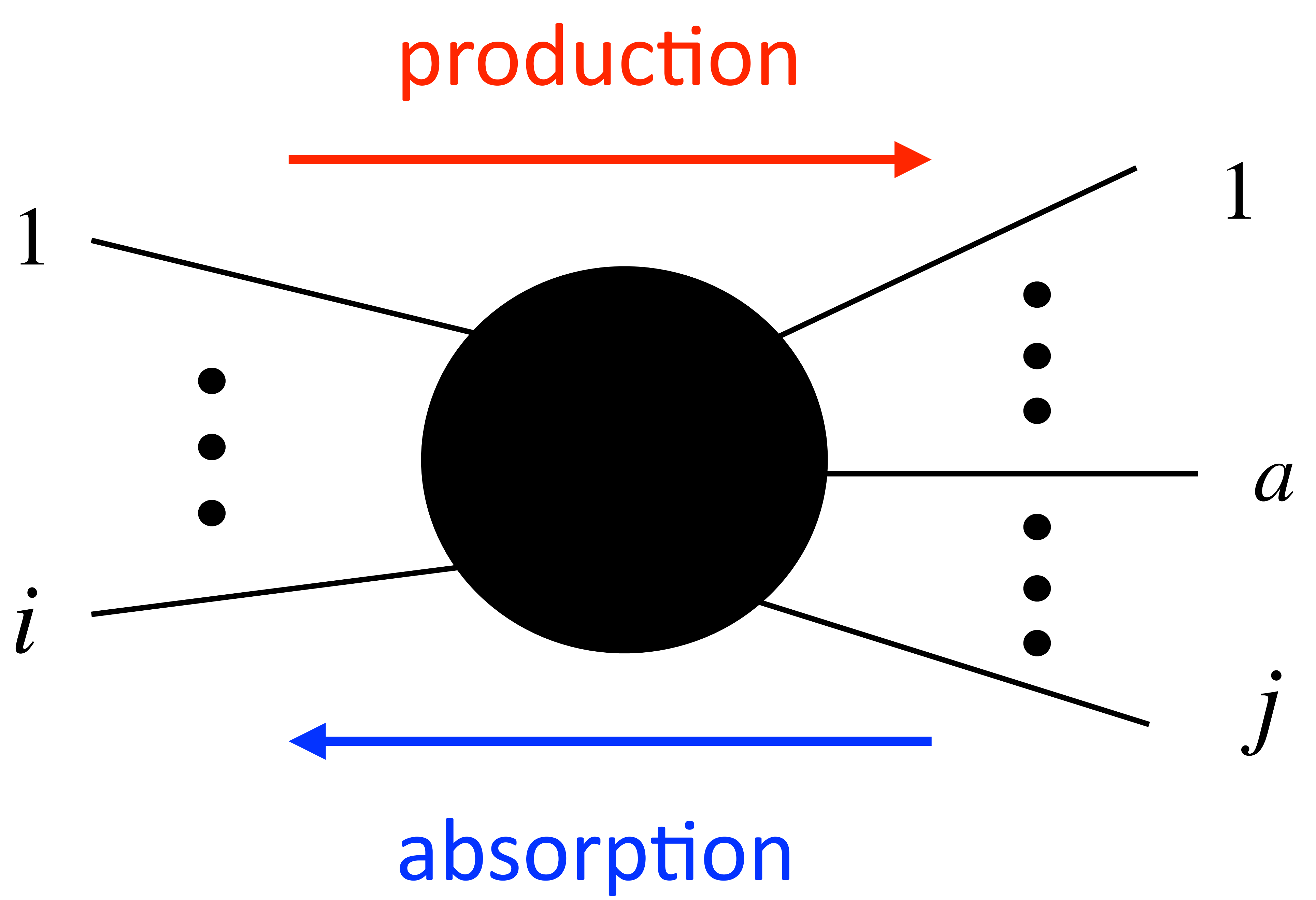

ALP production & absorption in SN

[see e.g., Weldon 83', Kolb & Turner 90']

Production rate (changing rate of # density per energy) (n_a = axion # density)

$$\frac{d^2 n_a}{dt dE_a} = \frac{|\mathbf{p_a}|}{4\pi^2} \int \prod_i d\Phi_i \, f_i \prod_{j \neq a} d\Phi_j \, (1 \pm f_j) \, (2\pi)^4 \delta^{(4)}(P_i - P_j) \left| \mathscr{M} \right|^2$$

Absorption rate (dimension df/dt w/ f = occupation function) (decay width for decay)

$$\Gamma_A(E_a, r) = \frac{1}{2E_a} \int \prod_{j \neq a} d\Phi_j \, f_j \prod_i d\Phi_i \, (1 \pm f_i) \, (2\pi)^4 \delta^{(4)}(P_j - P_i) \left| \mathscr{M} \right|^2$$

Particle distributions in the supernova

Production (absorption) rate depends on the particle distributions

lepton & anti-lepton

$$f_{\ell^\pm} = \frac{1}{e^{(E_\ell \pm \mu_\ell)/T} + 1}$$

leptonn chemical potential: $\mu_\ell = \mu_\ell(r)$

Temperature: $T = T(r)$

both μ & T are function of r:

SN profiles

The SFHo-18.8 SN profiles (SN core)

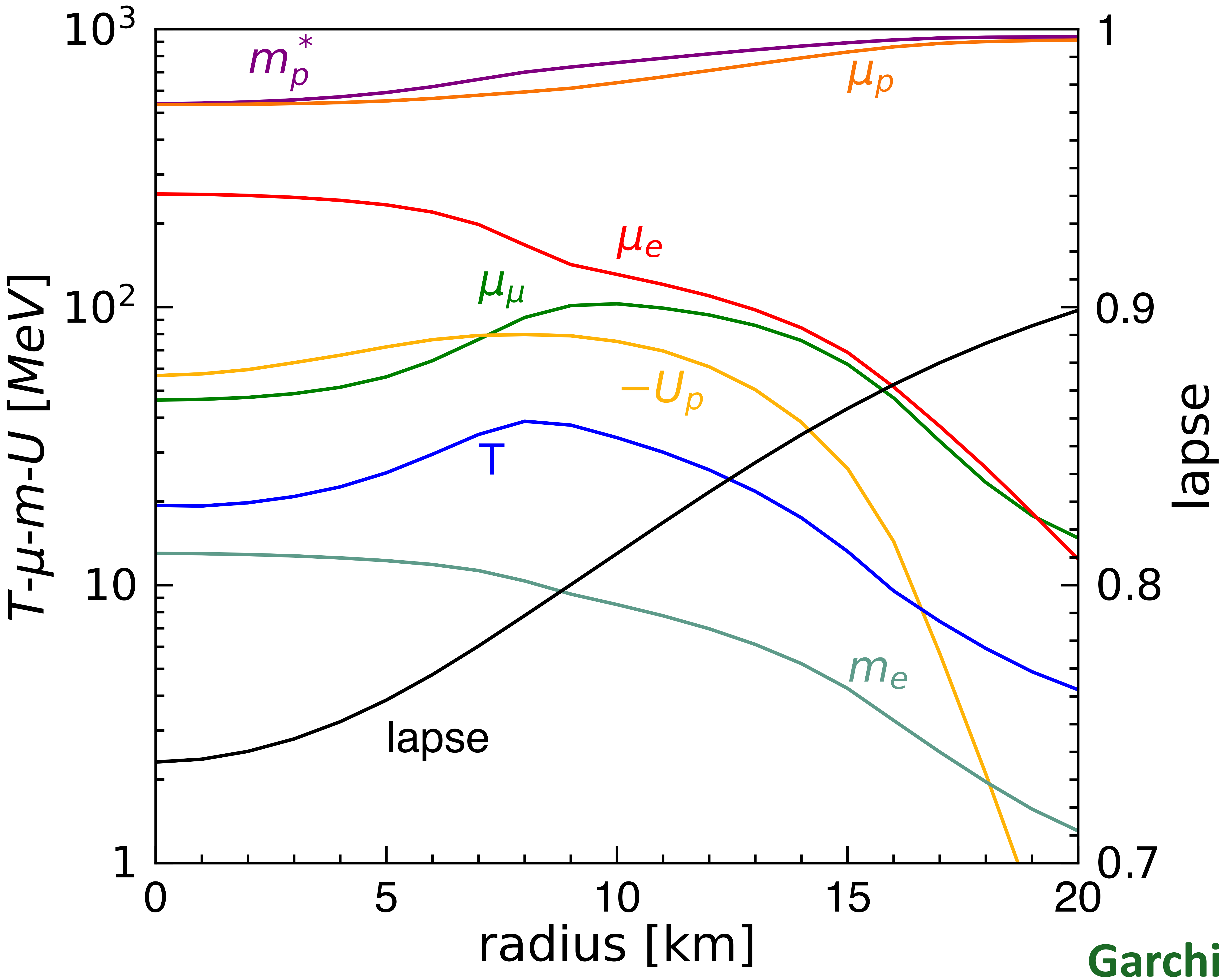

- chemical potentials of e, mu, & p
- temperature T
- proton effective mass m_p^*
- electron effective mass m_e
- proton self-energy U_p
- lapse factor

[R. Bollig et al., 2005.07141]

Garching core-collapse supernova research archive

Absorption term (survival probability)

$$\langle e^{-\tau_a(R_g,E_a,r)}\rangle = \int_{-1}^{1}\frac{d\mu}{2}\exp\left[-\int_0^{s_{\max}}\frac{ds}{v}\,\Gamma\left(E_a,\sqrt{r^2+s^2+2rs\mu}\right)\right]$$

$\mu = \cos\beta$

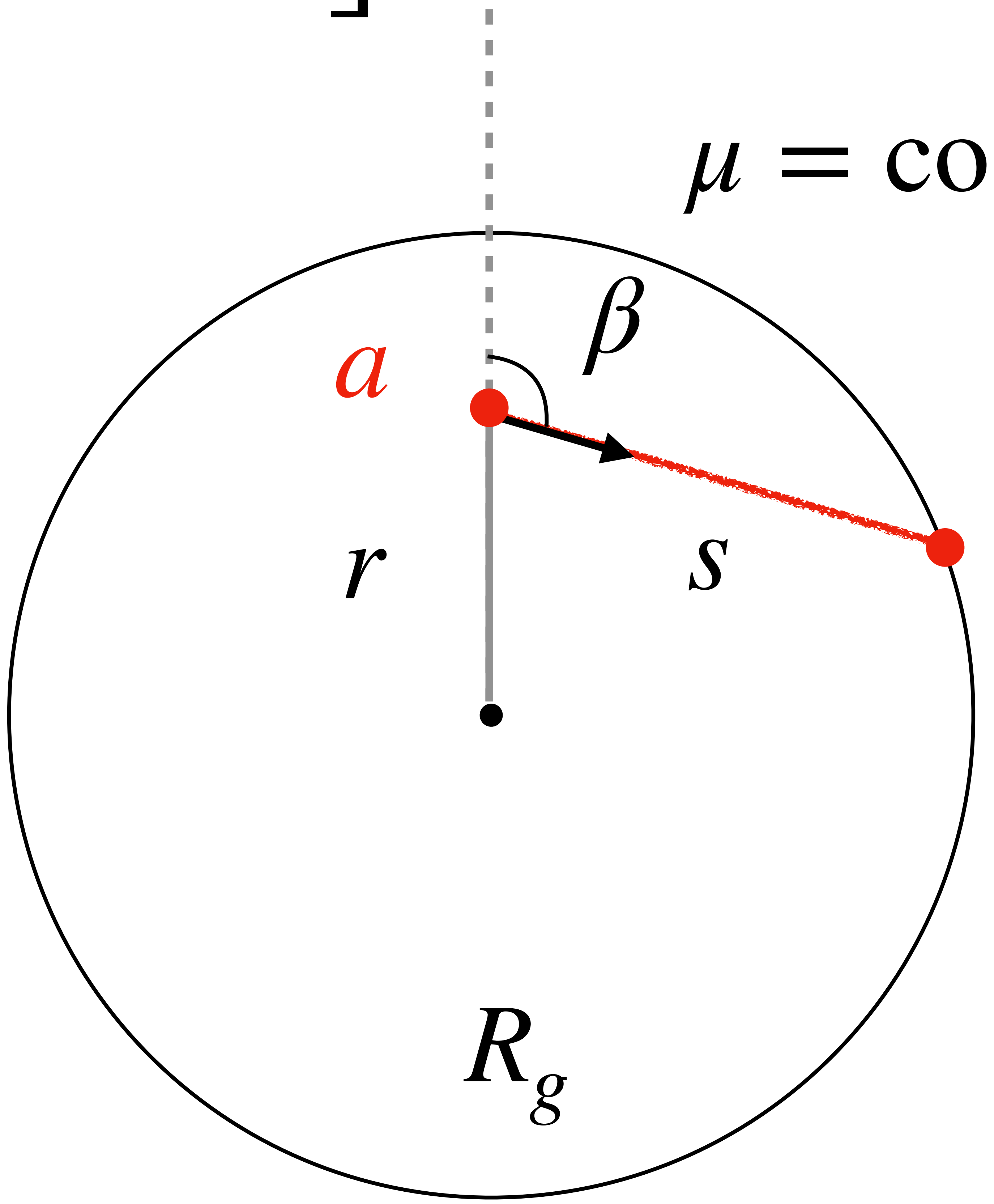

$\Gamma = \Gamma_A - \Gamma_E$ with Γ_A (Γ_E) = absorption (emission) rate

r = axion production point

s = axion propagation distance between r and R_g

β = angle between trajectory & radial direction

[A. Caputo, G. Raffelt, and E. Vitagliano, 2204.11862]

Absorption term (survival probability)

$$\langle e^{-\tau_a(R_g,E_a,r)}\rangle = \int_{-1}^{1}\frac{d\mu}{2}\exp\left[-\int_0^{s_{\max}}\frac{ds}{v}\,\Gamma\left(E_a,\sqrt{r^2+s^2+2rs\mu}\right)\right]$$

optical depth

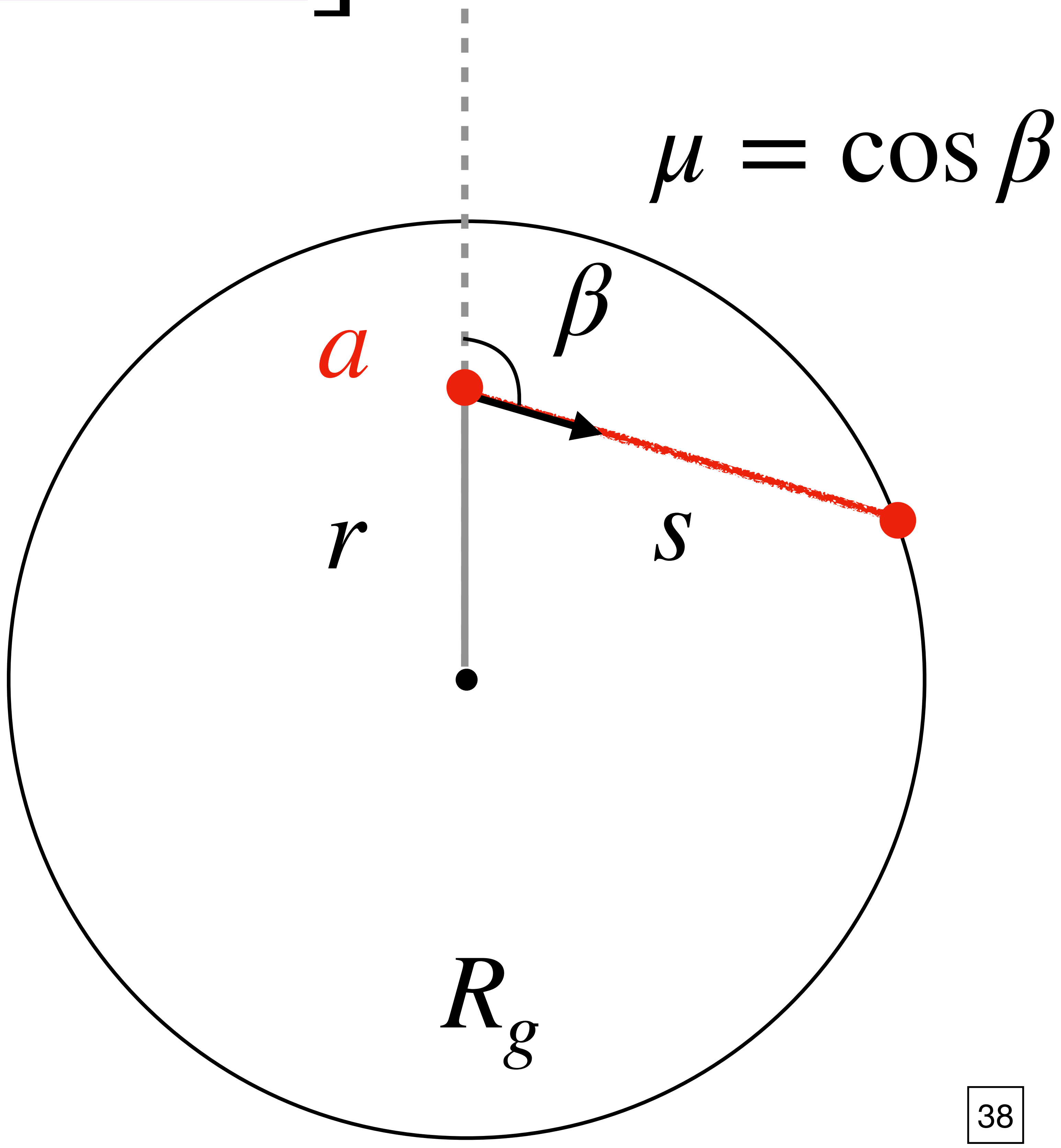

$\Gamma = \Gamma_A - \Gamma_E$ with Γ_A (Γ_E) = absorption (emission) rate

r = axion production point

s = axion propagation distance between r and R_g

β = angle between trajectory & radial direction

[A. Caputo, G. Raffelt, and E. Vitagliano, 2204.11862]

Absorption channels (inverse process of production)

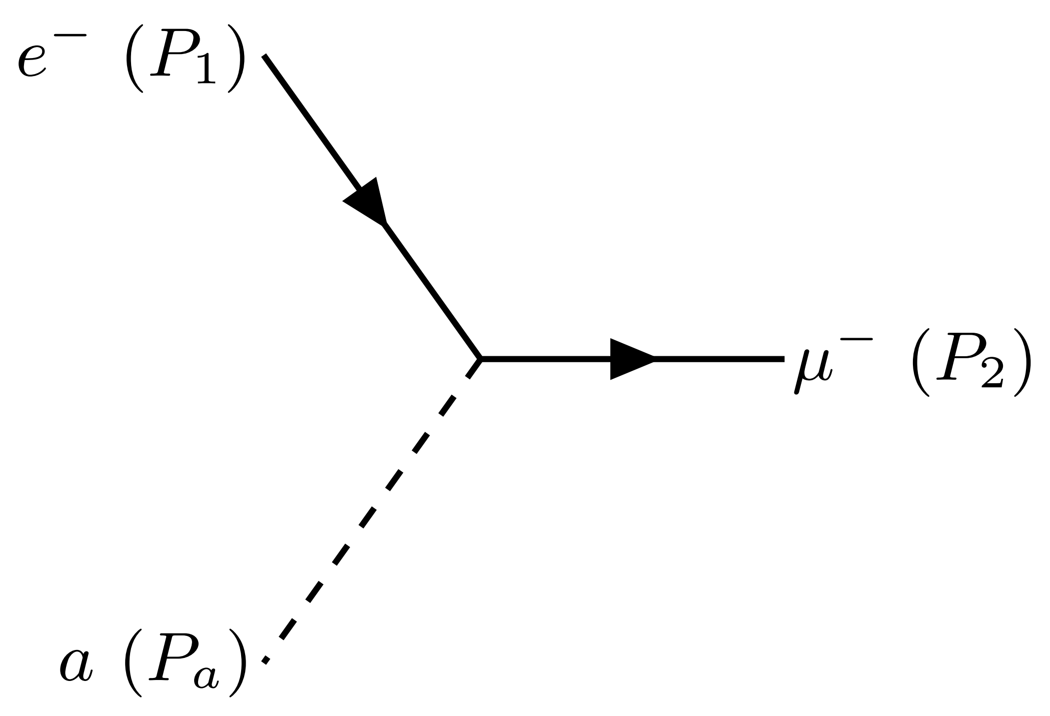

e-a coalescence

inverse bremsstrahlung

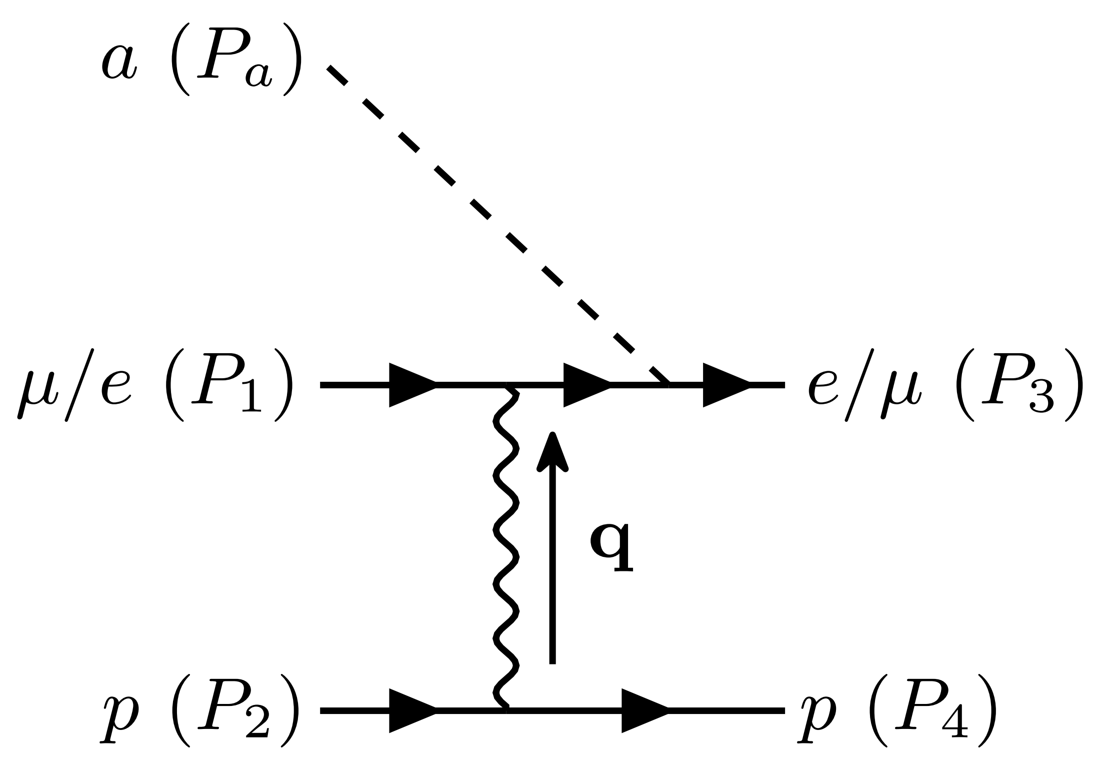

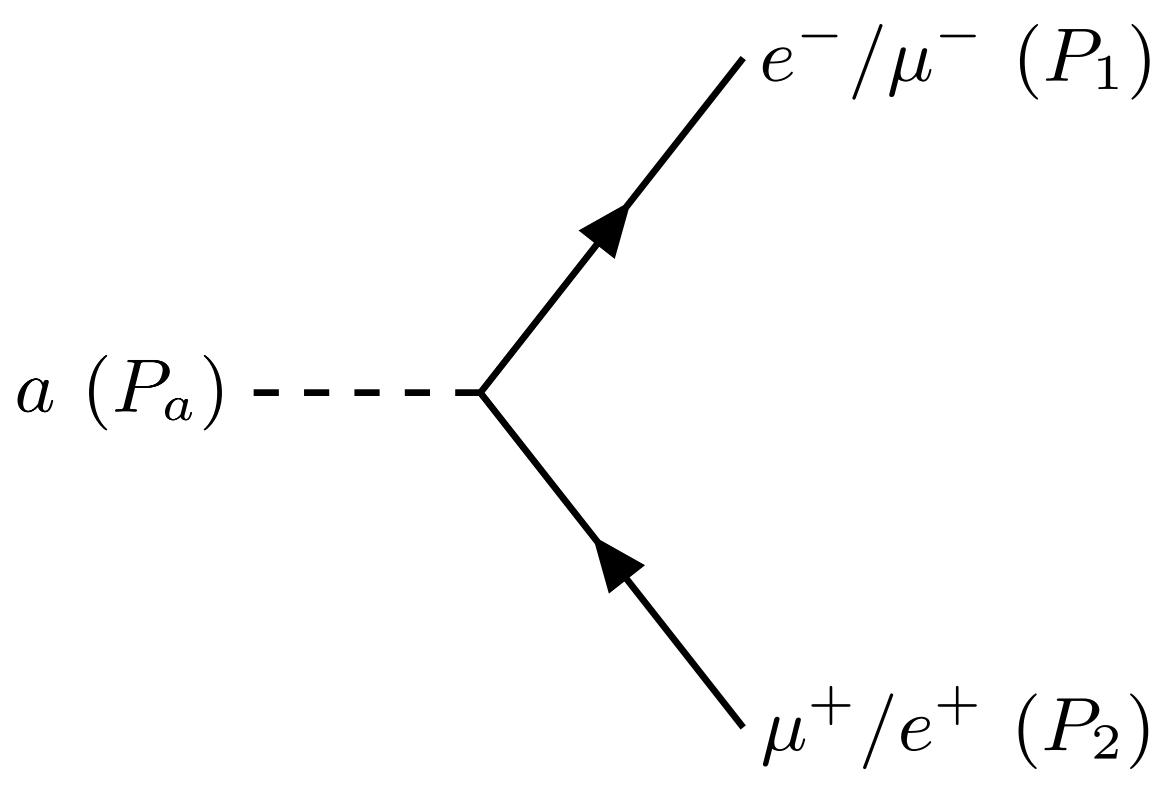

axion decay

inverse Compton

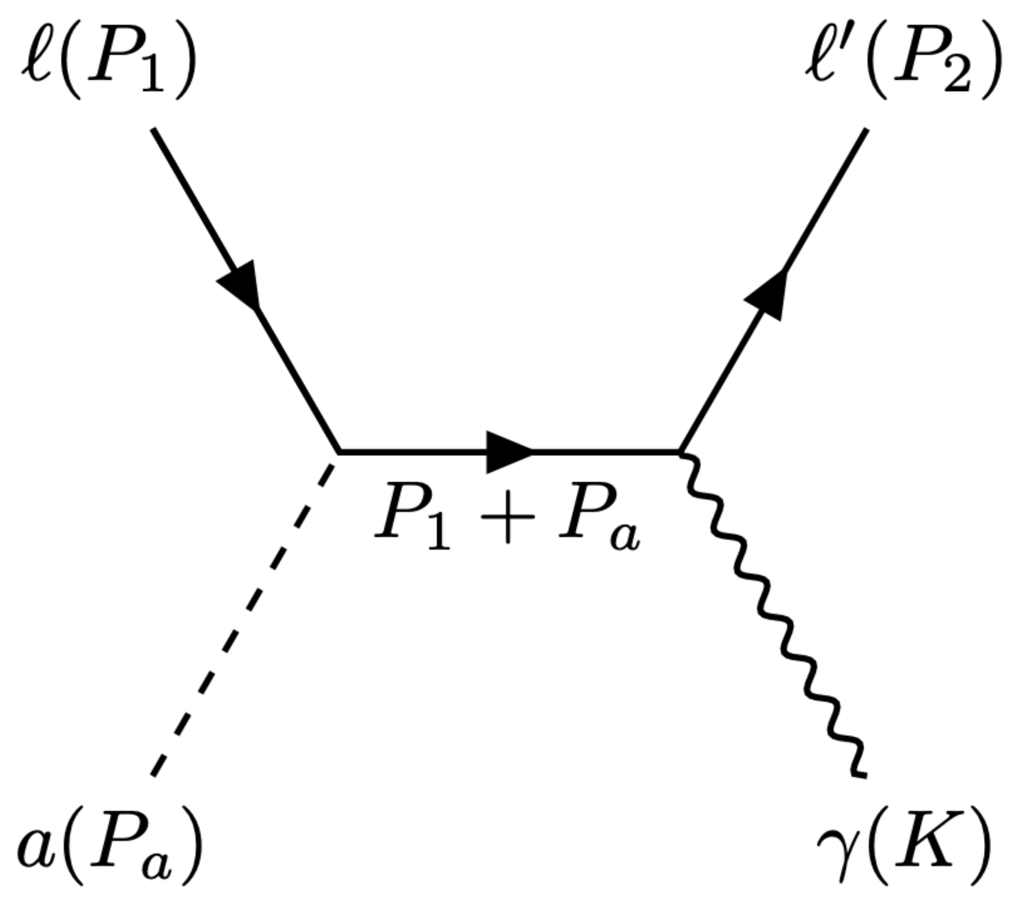

Absorption channels (inverse process of production)

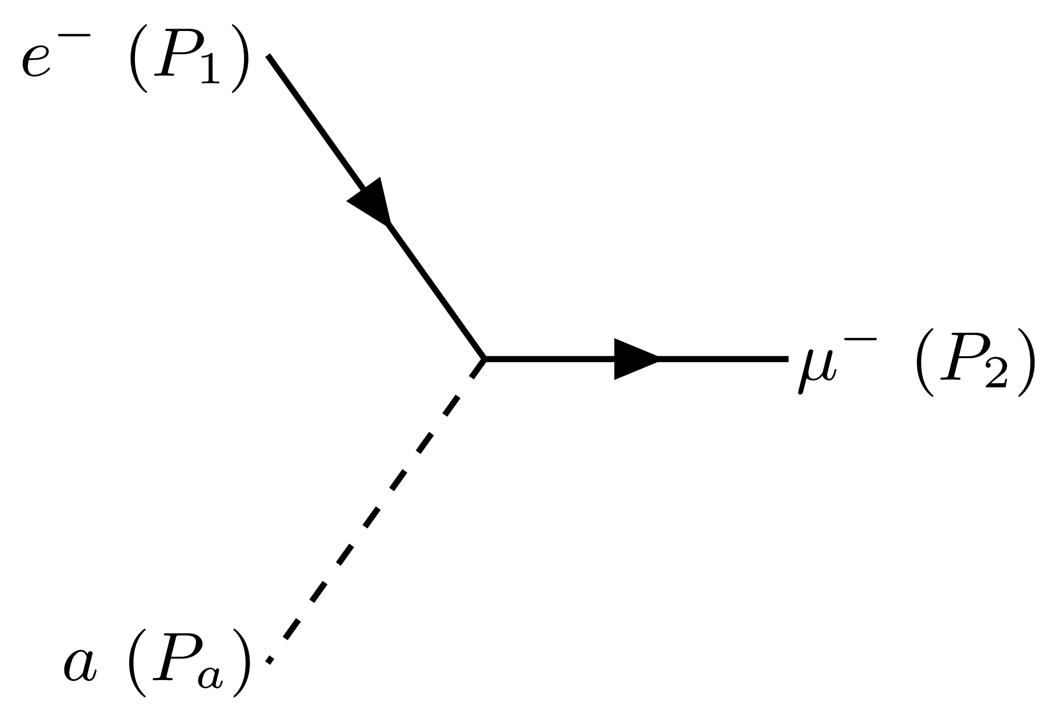

e-a coalescence

inverse bremsstrahlung

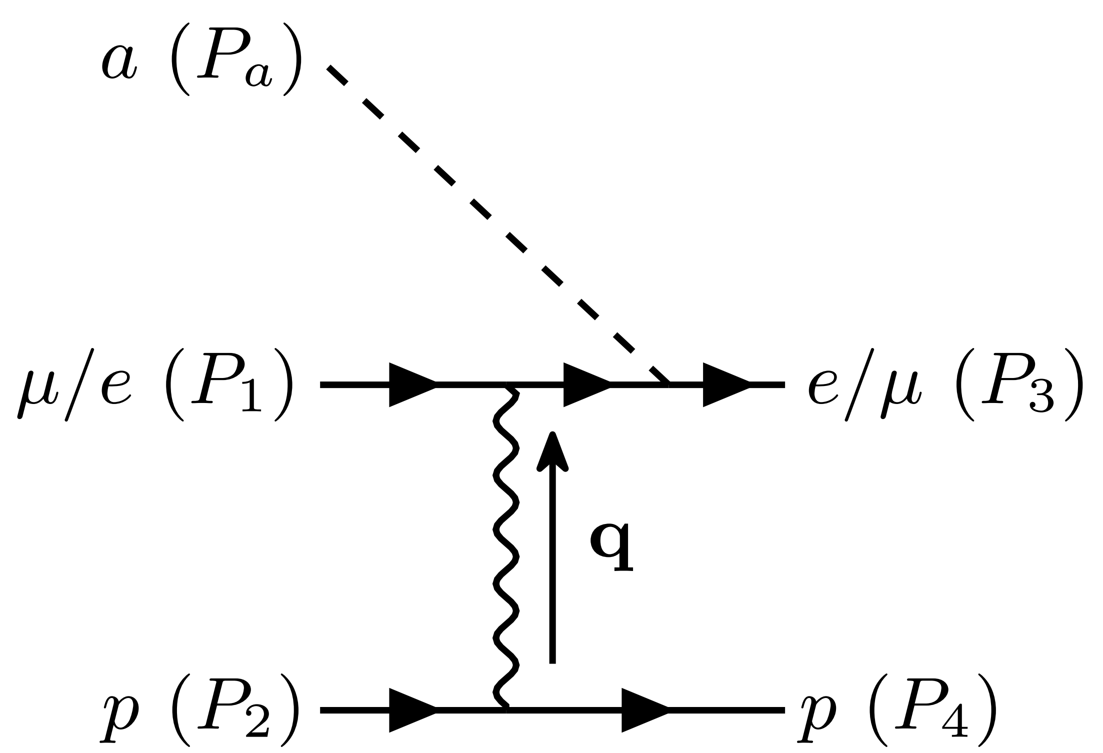

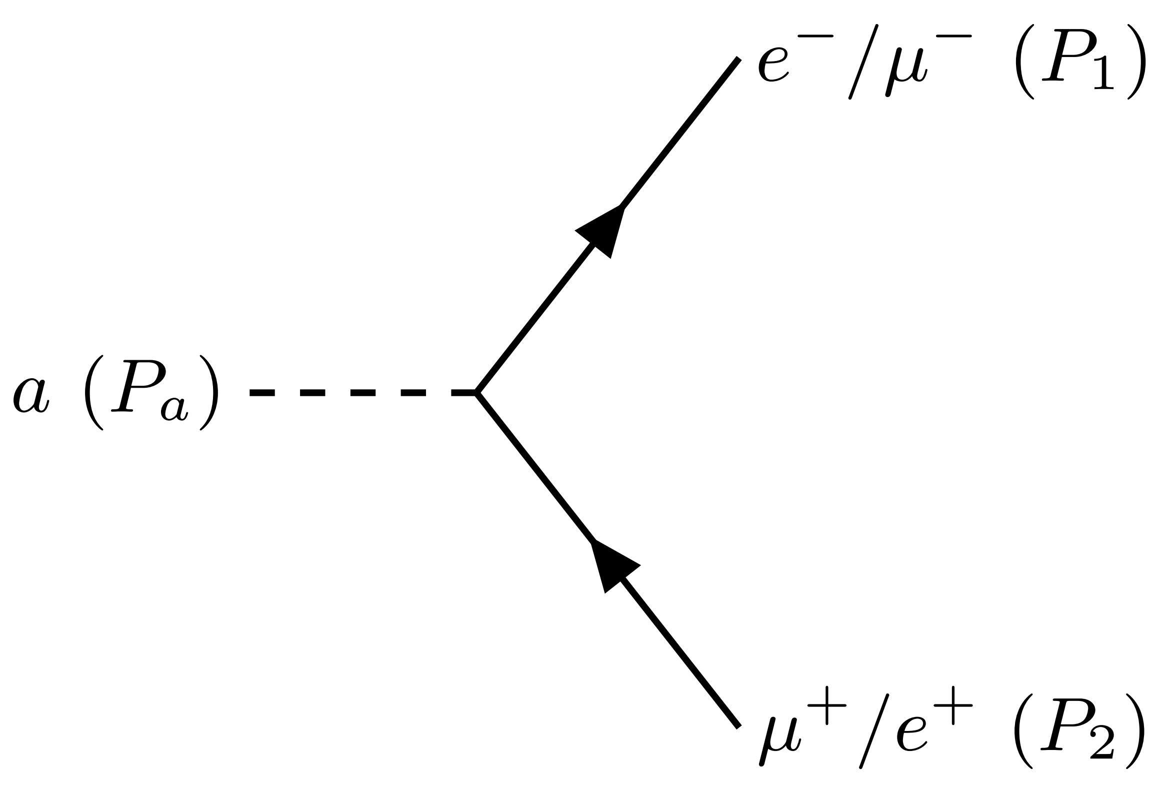

axion decay

inverse Compton

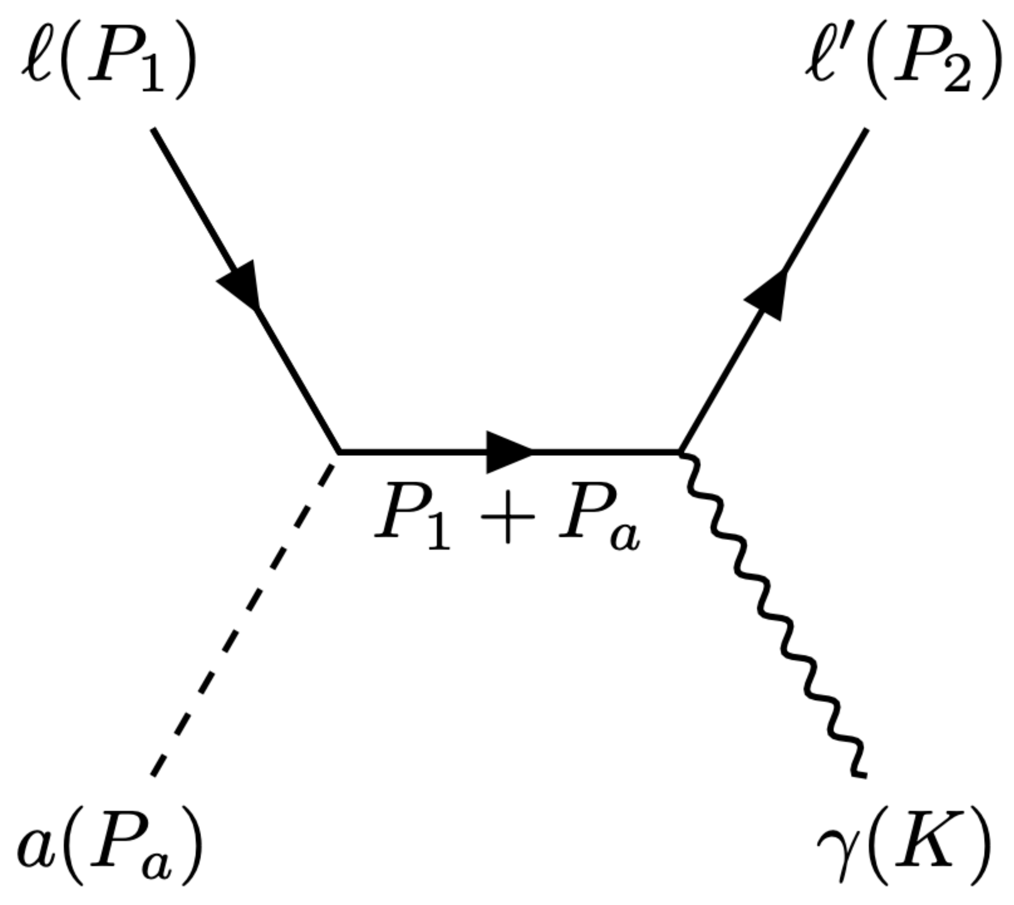

absorption rate in terms of production rate

$$\Gamma_A(E_a) = e^{(E_a - \mu_a^0)/T} \frac{2\pi^2}{|\mathbf{p}_a| E_a} \frac{d^2 n_a}{dt dE_a}$$

$$E_a = \sum_i E_i - \sum_{j \neq a} E_j$$

$$\mu_a^0 \equiv \sum_i \mu_i - \sum_{j \neq a} \mu_j$$

Energy transfers between core and mantle

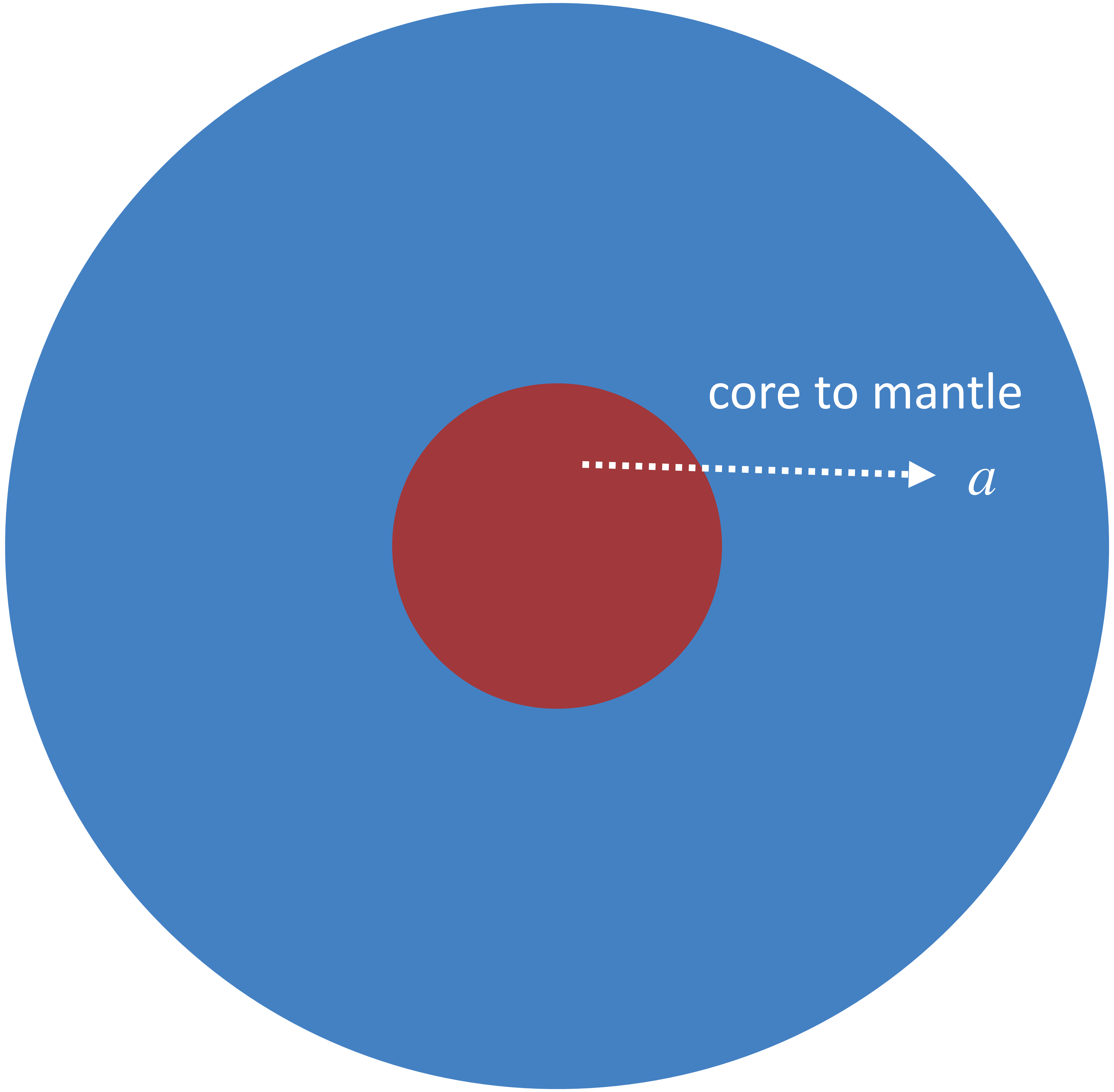

energy transfer from core to mantle

Energy transfers between core and mantle

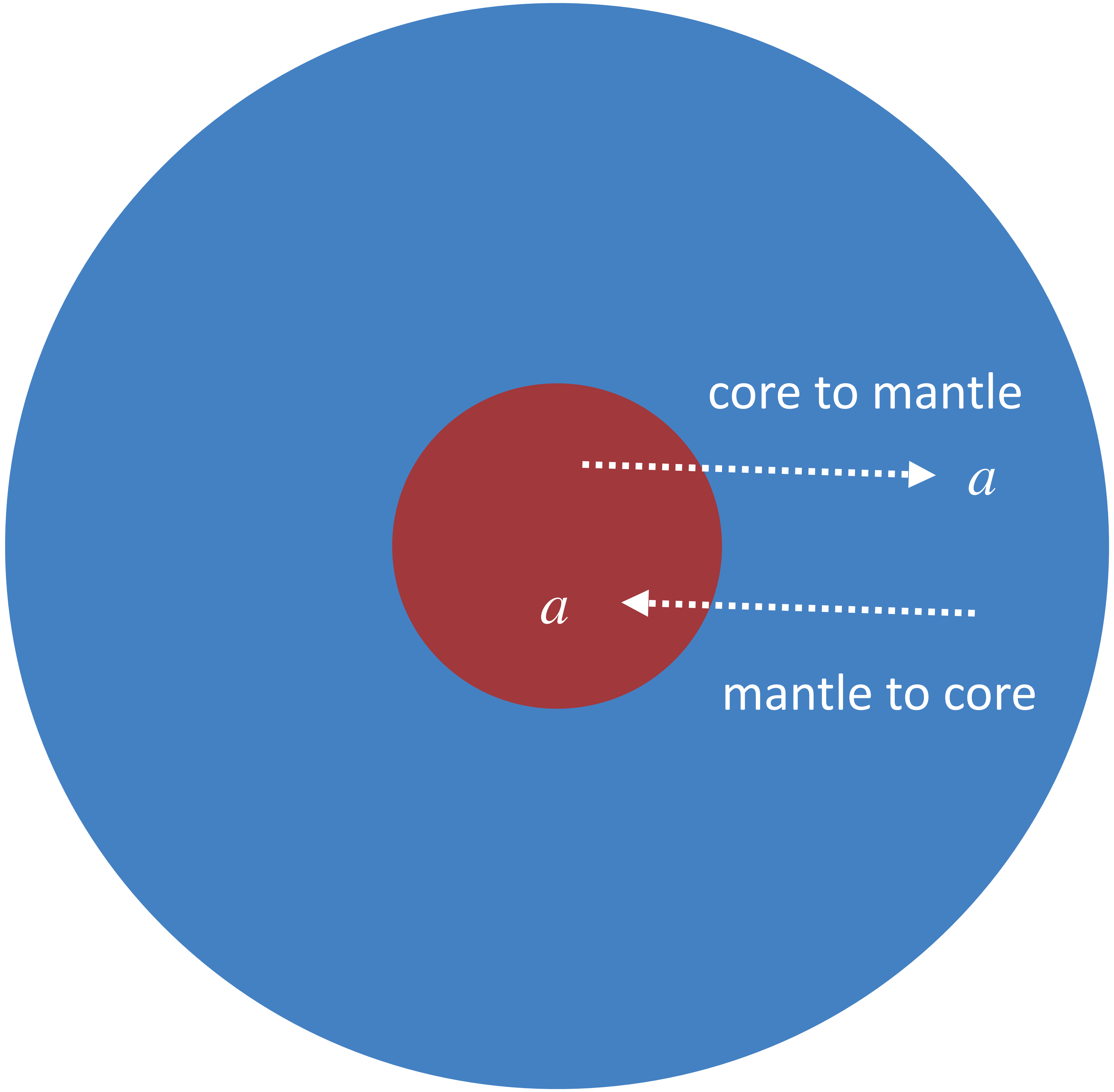

energy transfer from core to mantle

energy transfer from mantle to core

[Fiorillo, Pitik, Vitagliano, 2503.13653]

Energy transfers between core and mantle

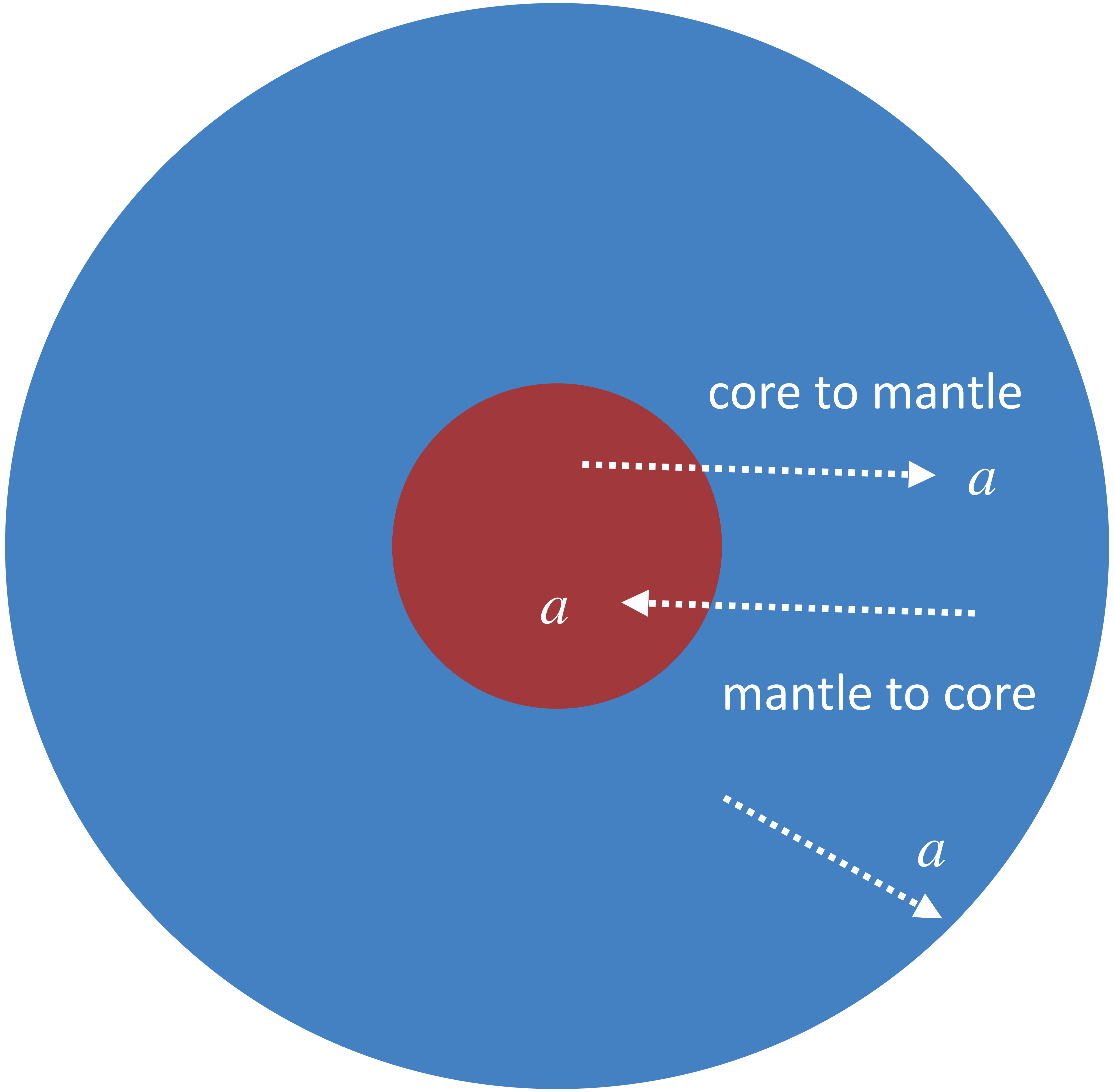

energy transfer from core to mantle

energy transfer from mantle to core

[Fiorillo, Pitik, Vitagliano, 2503.13653]

also energies escaping the progenitor

Energy loss due to ALPs production in the mantle

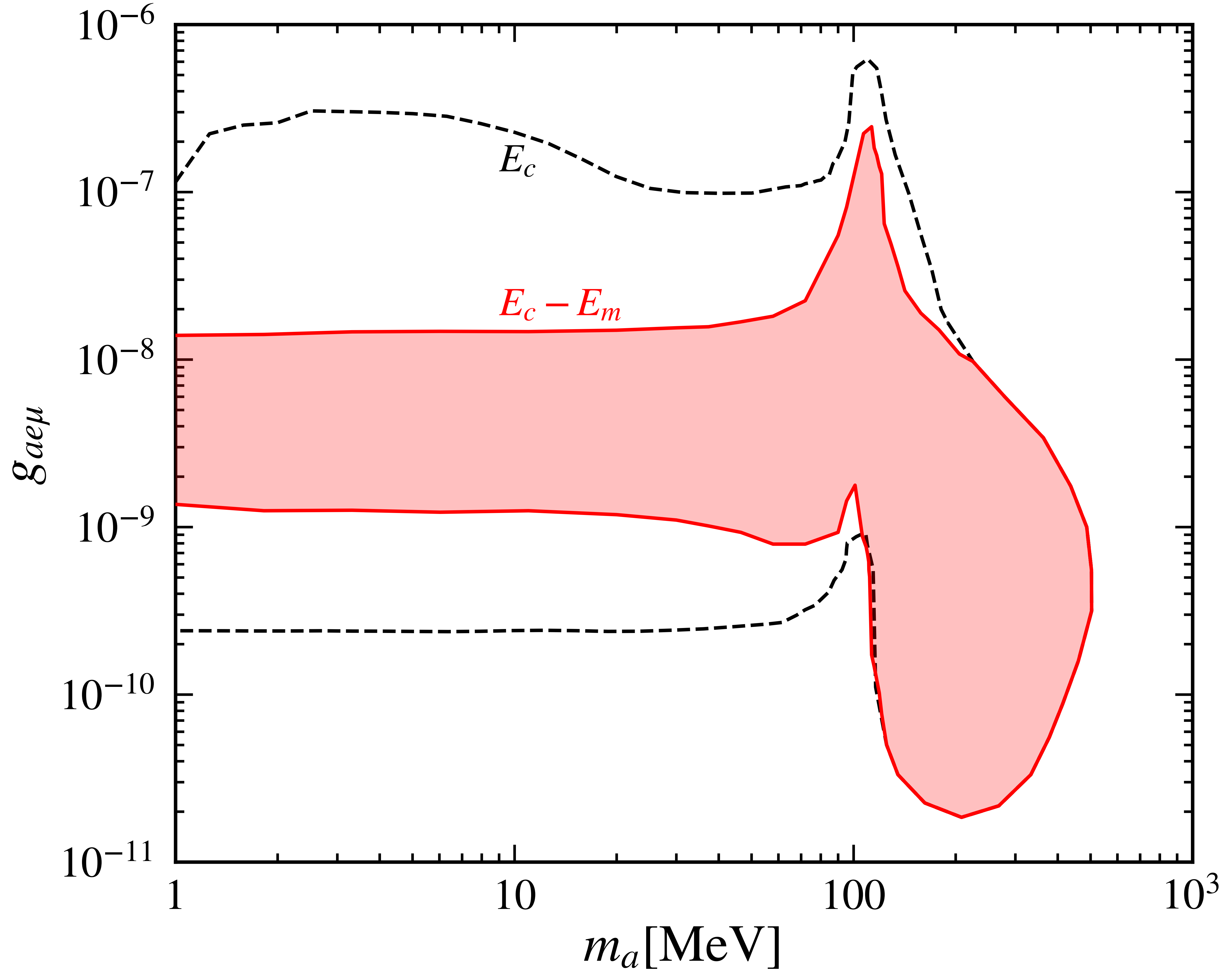

dashed: core

solid: core & mantle

energy drain from the mantle are significant for both strong & weak couplings

[Huang, Li, ZL, 2510.22523]

Refined LESN constraints on LFV axions

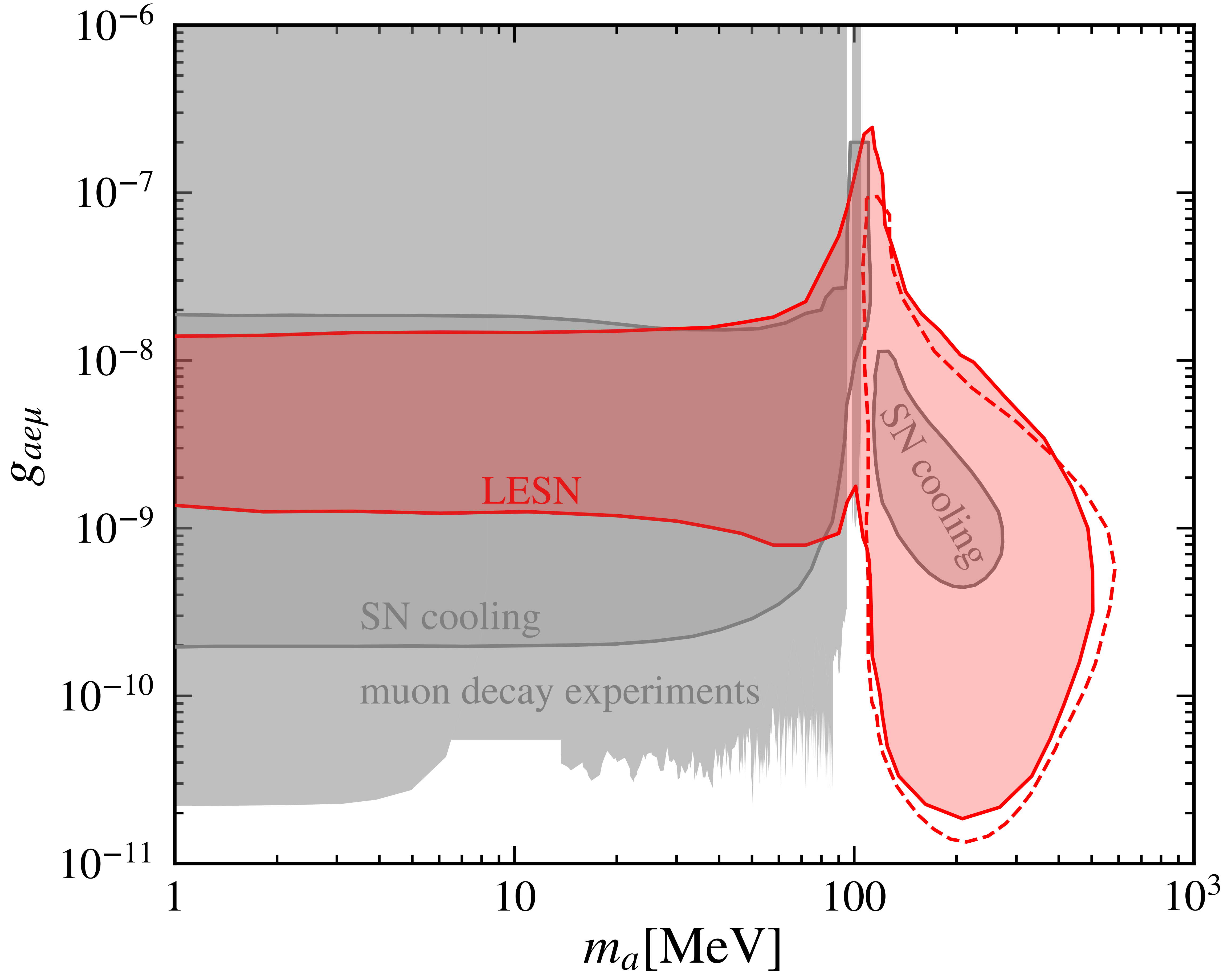

four production channels

- muon decay
- bremsstrahlung
- e-mu coalescence
- semi-Compton

energy drain from mantle considered

[Li, ZL, 2501.12075]

[Huang, Li, ZL, 2510.22523]

Summary

- We compute supernova cooling limits and low-energy supernova (LESN) constraints on millicharged particles (MCPs) and on lepton flavor violating (LFV) ALPs.

- For MCPs, besides plasmon decay and proton bremsstrahlung, we consider 2 new production channels: e^+e^- annihilation & pionic processes. We find that LESNe provide leading constraints for high massess, where e^+e^- annihilation dominates.

[Li, ZL, Lu, Ye, 2408.04953, JHEP]

- For LFV-ALPs, besides muon decay and bremsstrahlung, we consider 2 new production channels: e-mu coalescence & semi-Compton. We find that LESNe provide leading constraints for high masses, where e-mu coalescence dominates.

[Li, ZL, 2501.12075] [Huang, ZL, 2506.16922, JHEP] [Huang, Li, ZL, 2510.22523]

additional slides

Plasma effects

Photon properties are altered via scatterings w/ electrons

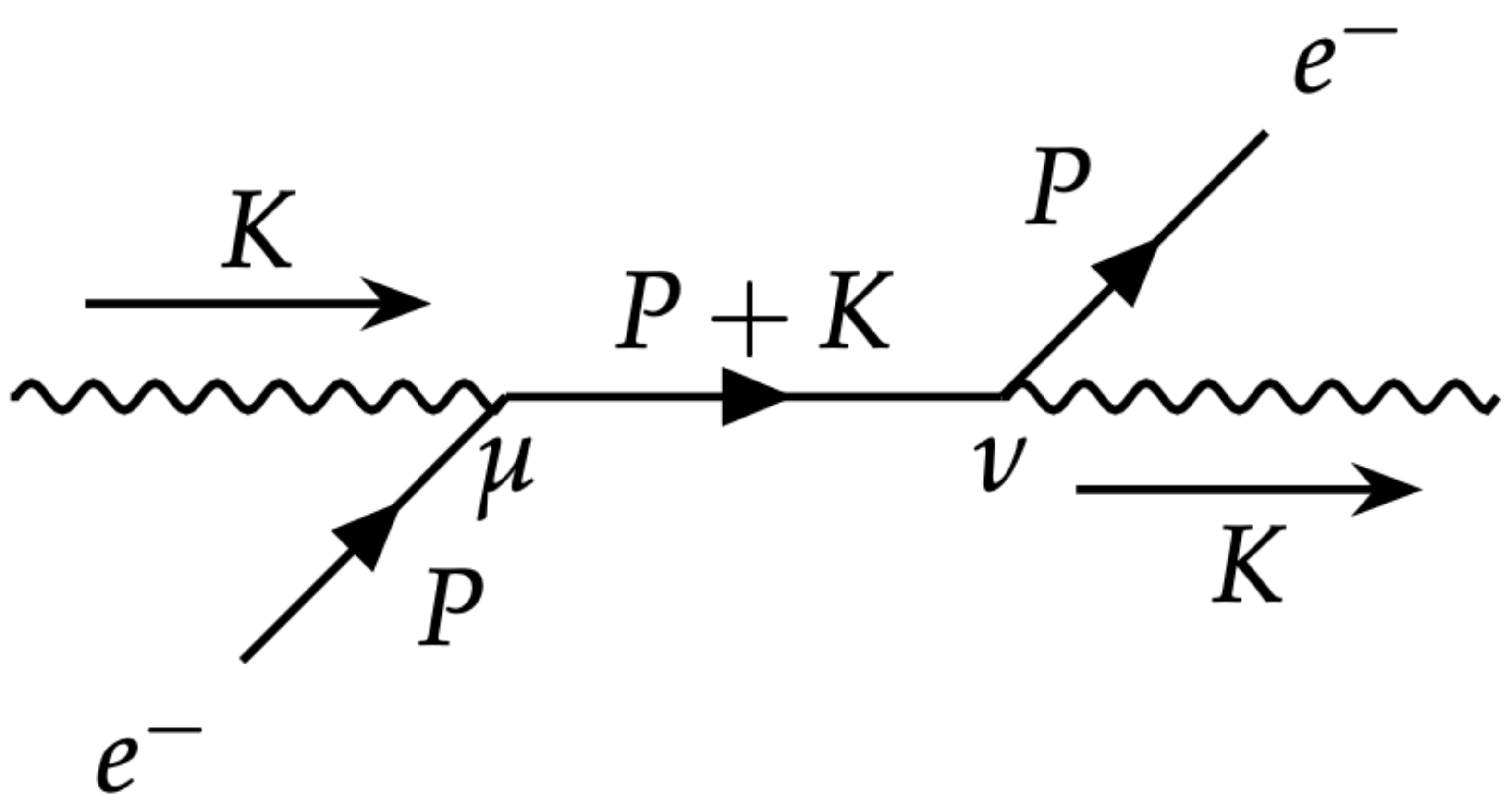

LO contributions to real part of the EM polarization tensor **[Braaten & Segel, 93]**

$$\mathrm{Re}\Pi^{\mu\nu} = 16\pi\alpha \int \frac{d^3p}{(2\pi)^3}\frac{1}{2E}[f_{e^-}(E) + f_{e^+}(E)]\frac{K\cdot P(P^\nu K^\mu + P^\mu K^\nu - P\cdot K g^{\mu\nu}) - K^2 P^\mu P^\nu}{(K\cdot P)^2 - (K^2)^2/4}$$

$\Longrightarrow$ dispersion relations & normalization

Plasma effects

Effective photon propagator in Lorenz gauge [Raffelt 96]

$$\tilde{D}^{\mu\nu}(\omega, k) = \sum_{a=\pm,L} \frac{i\epsilon_a^\mu \epsilon_a^{\nu *}}{K^2 - \mathrm{Re}\Pi_a(\omega, k) - i\mathrm{Im}\Pi_a(\omega, k)}$$

$$\epsilon_\pm^\mu = (0,1,\pm i,0)/\sqrt{2}$$

$$\epsilon_L^\mu = (k,0,0,\omega)/\sqrt{K^2}$$

The imaginary part of the EM polarization tensor is related to the photon absorption and production rates in the plasma [Weldon 82] [An+ 1302.3884]

In the equilibrium case $\mathrm{Im}\Pi = -\omega(1 - e^{-\omega/T})\Gamma_{\mathrm{abs}}$

In the SN core, the dominant contributions to $\mathrm{Im}\Pi$ (relevant for MCP production: photon is time-like with a positive energy):

- inverse-bremsstrahlung: $\gamma pn \to pn$
- decay process: $\gamma \to e^+e^-$

Plasmon decay

Plasmon decay

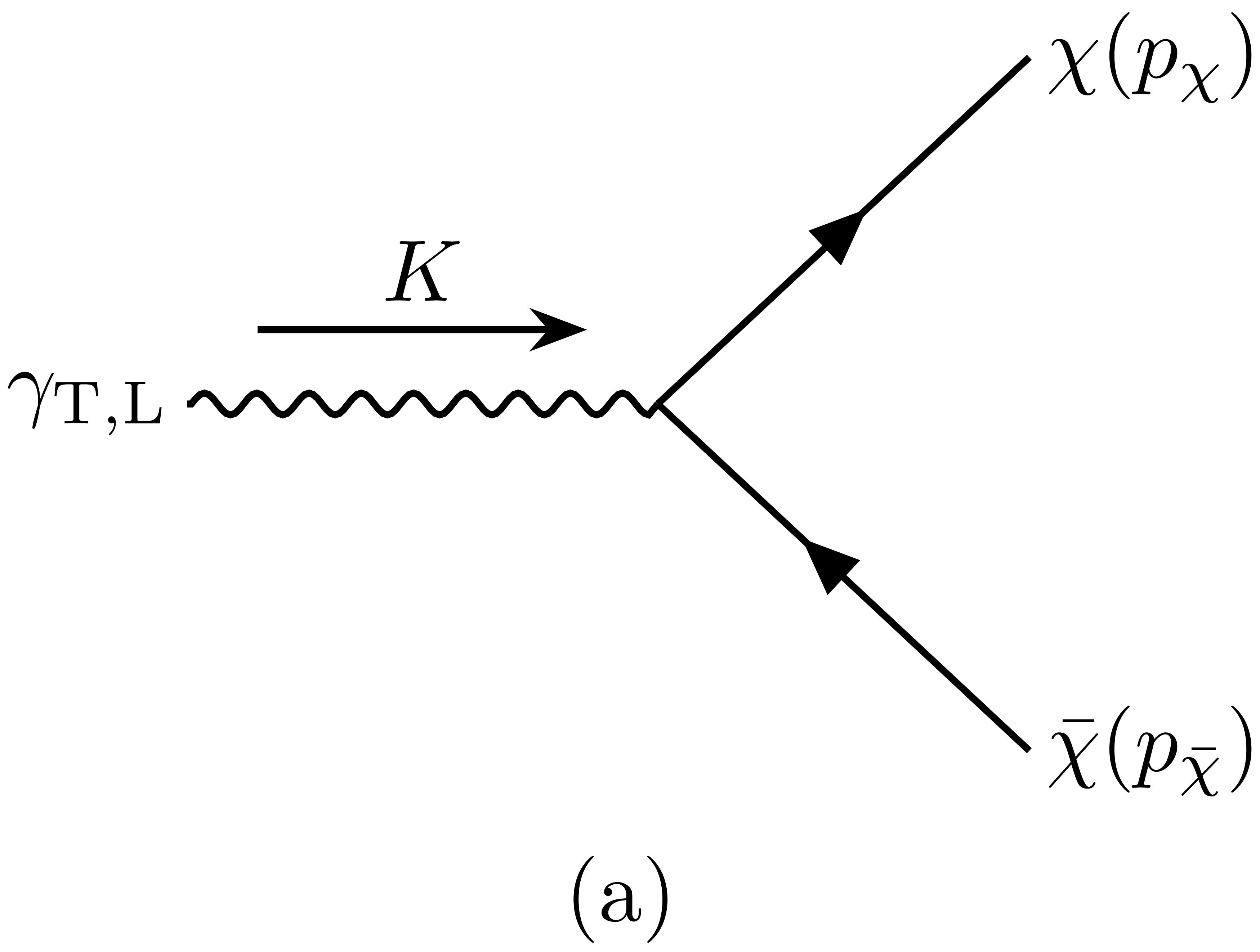

decay width (a = T, L) in the SN frame

$$\Gamma_a = Z_a \frac{\epsilon^2 \alpha K^2}{3\omega_a} f\left(\frac{m_\chi^2}{K^2}\right)$$

$$f(x) \equiv \sqrt{1-4x}\,(1+2x)$$

photon momentum $K^\mu = (\omega, \mathbf{k})$

Lorenz gauge

Z_a = normalization

millicharged particle flux from plasmon decay

MCP production rate per unit volume per unit energy (relativistic limit) $k \equiv |\mathbf{k}|$

$$\frac{d\Phi_a}{dE_\chi} = \frac{g_a}{2\pi^2}\int_0^\infty dk\, k^2 \frac{\Gamma_a}{e^{\omega_a/T_c}-1} g(E_\chi, m_\chi, K)$$

MCP energy spectrum per decay (plasma frame)

$$g(E_\chi, m_\chi, K) = 2\frac{\Theta(E_\chi - E_\chi^-)\Theta(E_\chi^+ - E_\chi)}{E_\chi^+ - E_\chi^-}$$

$$E_\chi^\pm = \frac{1}{2}\left(\omega \pm k\sqrt{1 - 4m_\chi^2/K^2}\right)$$

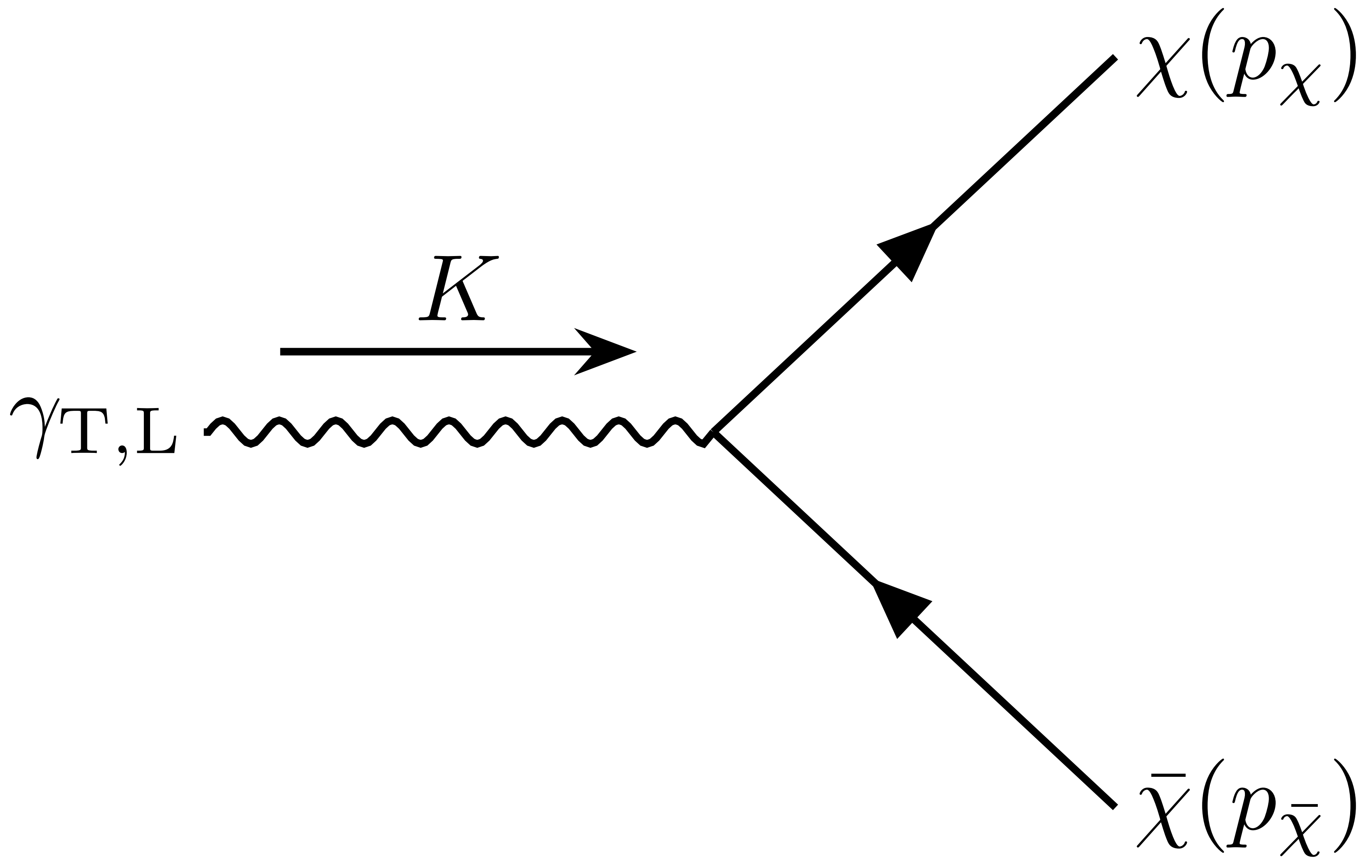

(a)

Proton bremsstrahlung

Proton bremsstrahlung

2-to-4 xsec in terms of 2-to-3 xsec (integrate out $\bar{\chi}\chi$ PS)

[Gninenko+, 1810.06856]

[Liang, ZL, Yang, 2111.15533]

[Du, Fang, ZL, 2211.11469]

$$\frac{d\sigma(np \to np\chi\bar{\chi})}{dK^2 d\omega} = \frac{\epsilon^2\alpha}{3\pi}\frac{1}{K^2}\frac{d\sigma(np \to np\gamma)}{d\omega} f\left(\frac{m_\chi^2}{K^2}\right)$$

$$\frac{d\sigma(np \to np\gamma)}{d\omega}$$ = 2-to-3 xsec

No plasmon corrections to the photon propagator to avoid double counting w/ plasmon decay

[Chu+, 1908.00553]

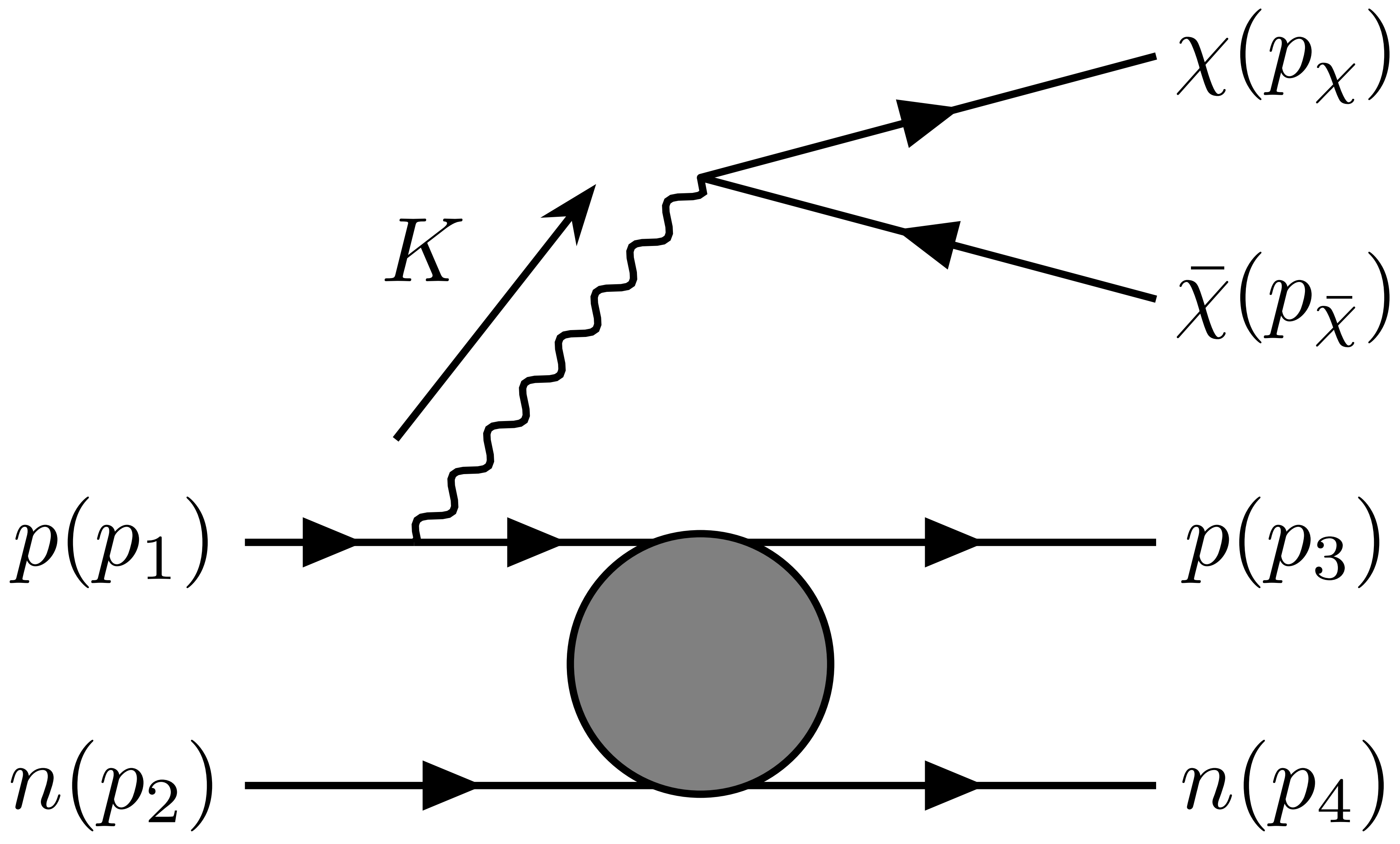

Proton bremsstrahlung

2-to-4 xsec in terms of 2-to-3 xsec (integrate out $\bar{\chi}\chi$ PS)

$$\frac{d\sigma(np \to np\chi\bar{\chi})}{dK^2 d\omega} = \frac{\epsilon^2\alpha}{3\pi}\frac{1}{K^2}\frac{d\sigma(np \to np\gamma)}{d\omega} f\left(\frac{m_\chi^2}{K^2}\right)$$

$$\frac{d\sigma(np \to np\gamma)}{d\omega}$$ = 2-to-3 xsec

No plasmon corrections to the photon propagator to avoid double counting w/ plasmon decay

[Chu+, 1908.00553]

[Gninenko+, 1810.06856]

[Liang, ZL, Yang, 2111.15533]

[Du, Fang, ZL, 2211.11469]

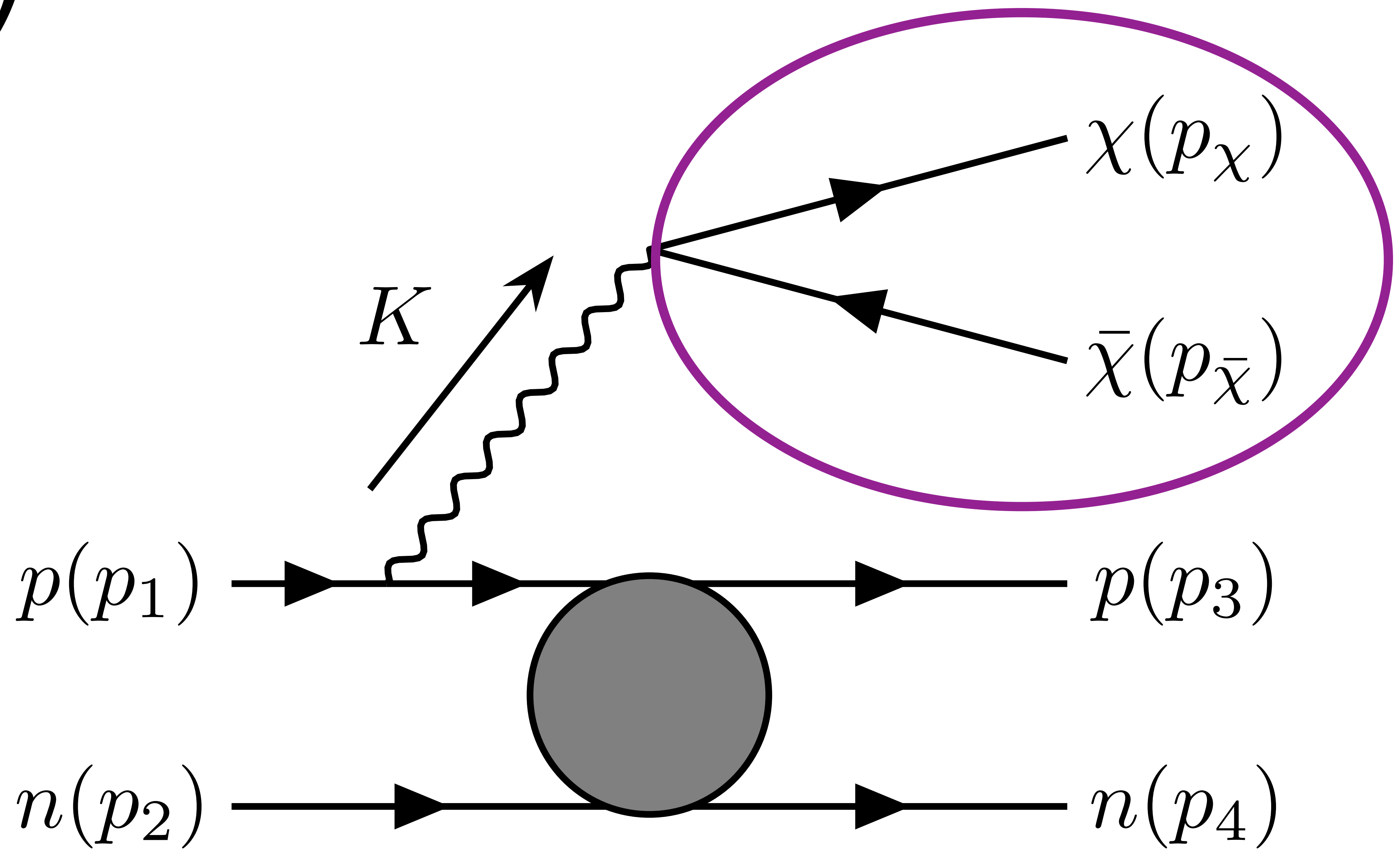

Photon emission in soft radiation approximation (SRA)

$$\frac{d\sigma(np \to np\gamma)}{d\omega} = \sigma_{np}^{T} \frac{d\mathscr{P}}{d\omega}$$

[Chu+, 1908.00553]

[Rrapaj & Reddy, 1511.09136]

σ_{np}^{T} = transport xsec of $(np \to np)$

$\frac{d\mathscr{P}}{d\omega}$ = photon splitting kernel

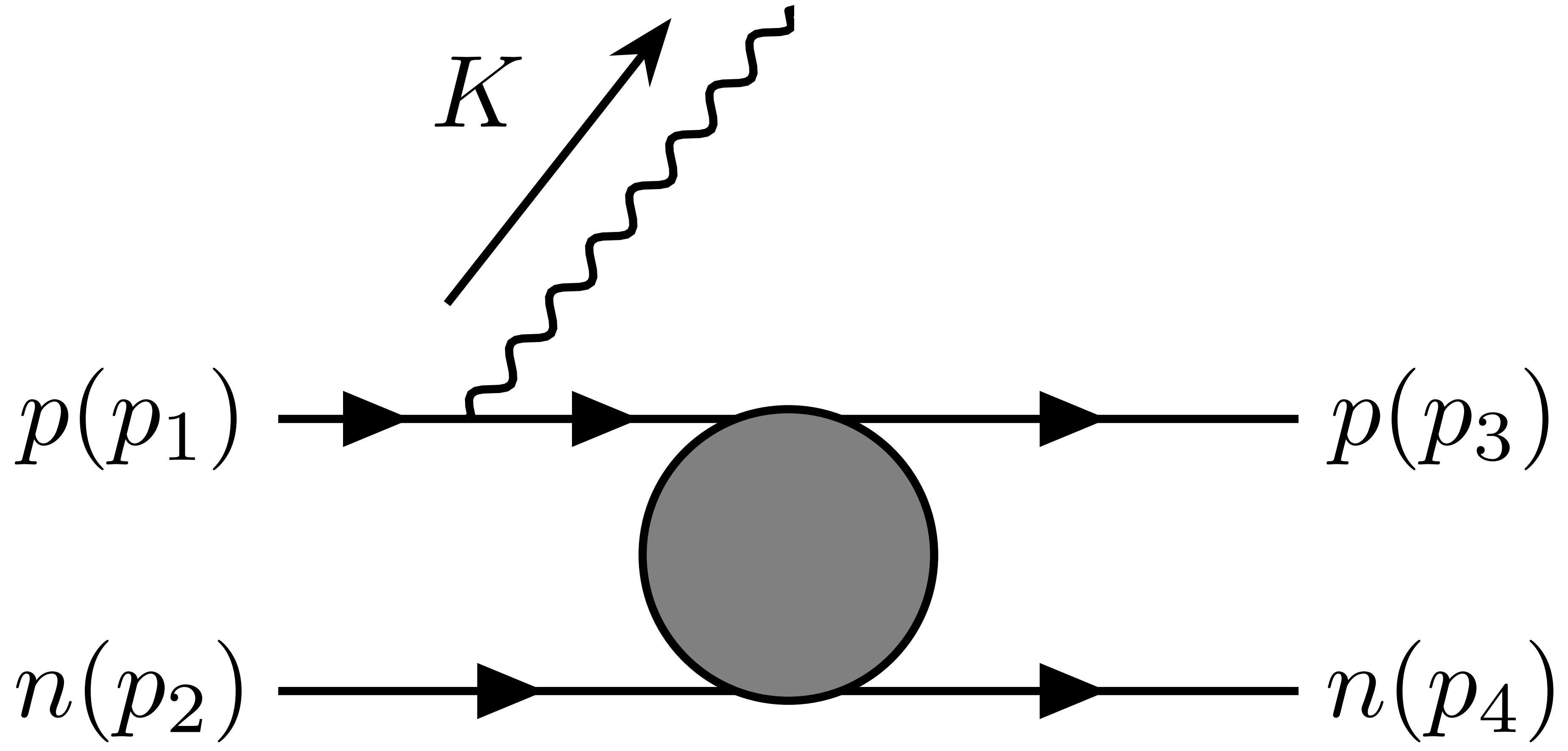

Photon emission in soft radiation approximation (SRA)

$$\frac{d\sigma(np \to np\gamma)}{d\omega} = \sigma^T_{np} \frac{d\mathscr{P}}{d\omega}$$

[Chu+, 1908.00553]

[Rrapaj & Reddy, 1511.09136]

σ^T_{np} = transport xsec of $(np \to np)$ ⇦ use data

$\frac{d\mathscr{P}}{d\omega}$ = photon splitting kernel

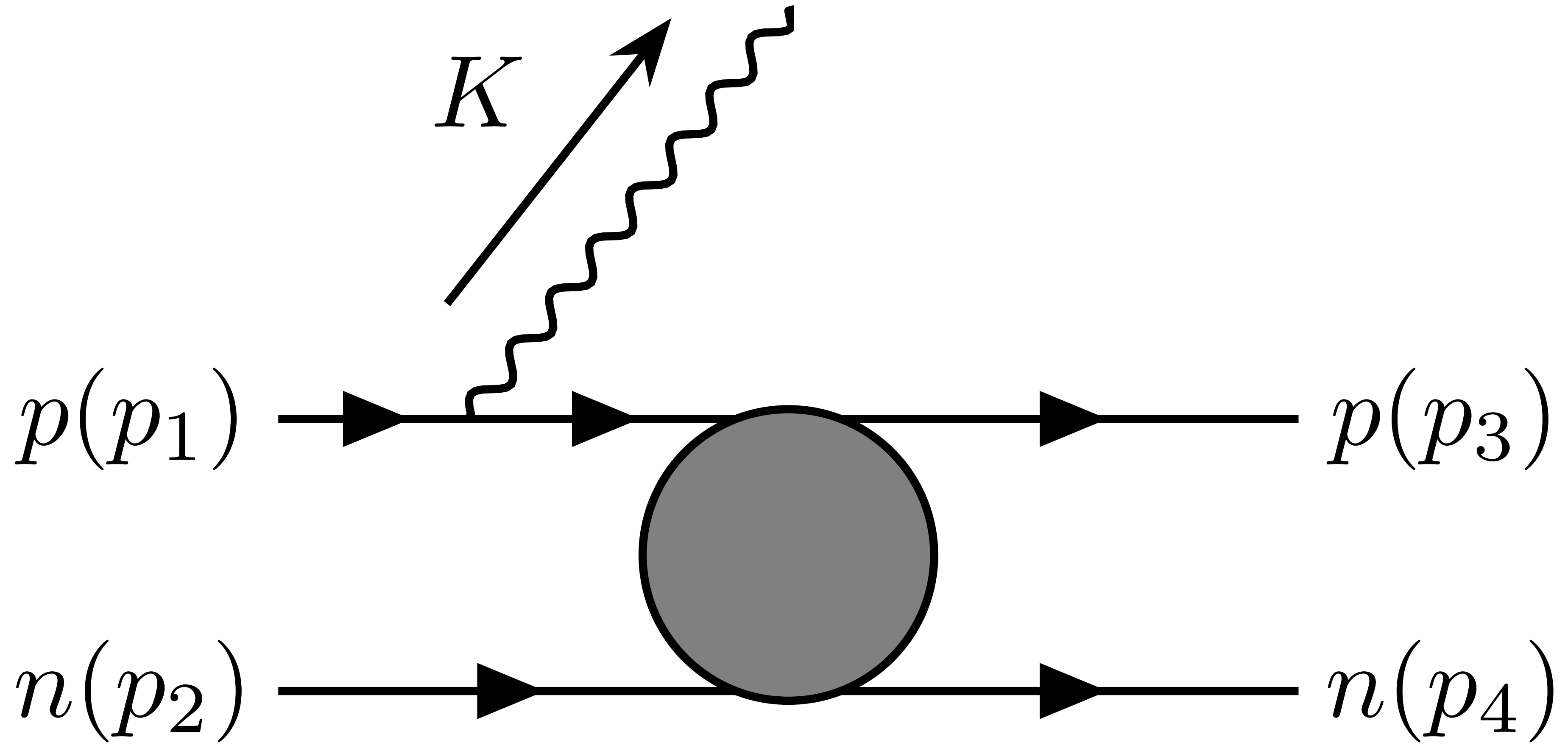

Photon emission in soft radiation approximation (SRA)

$$\frac{d\sigma(np \to np\gamma)}{d\omega} = \sigma^T_{np} \frac{d\mathscr{P}}{d\omega}$$

[Chu+, 1908.00553]

[Rrapaj & Reddy, 1511.09136]

σ^T_{np} = transport xsec of $(np \to np)$ ⇦ use data

$\frac{d\mathscr{P}}{d\omega}$ = photon splitting kernel ⇦

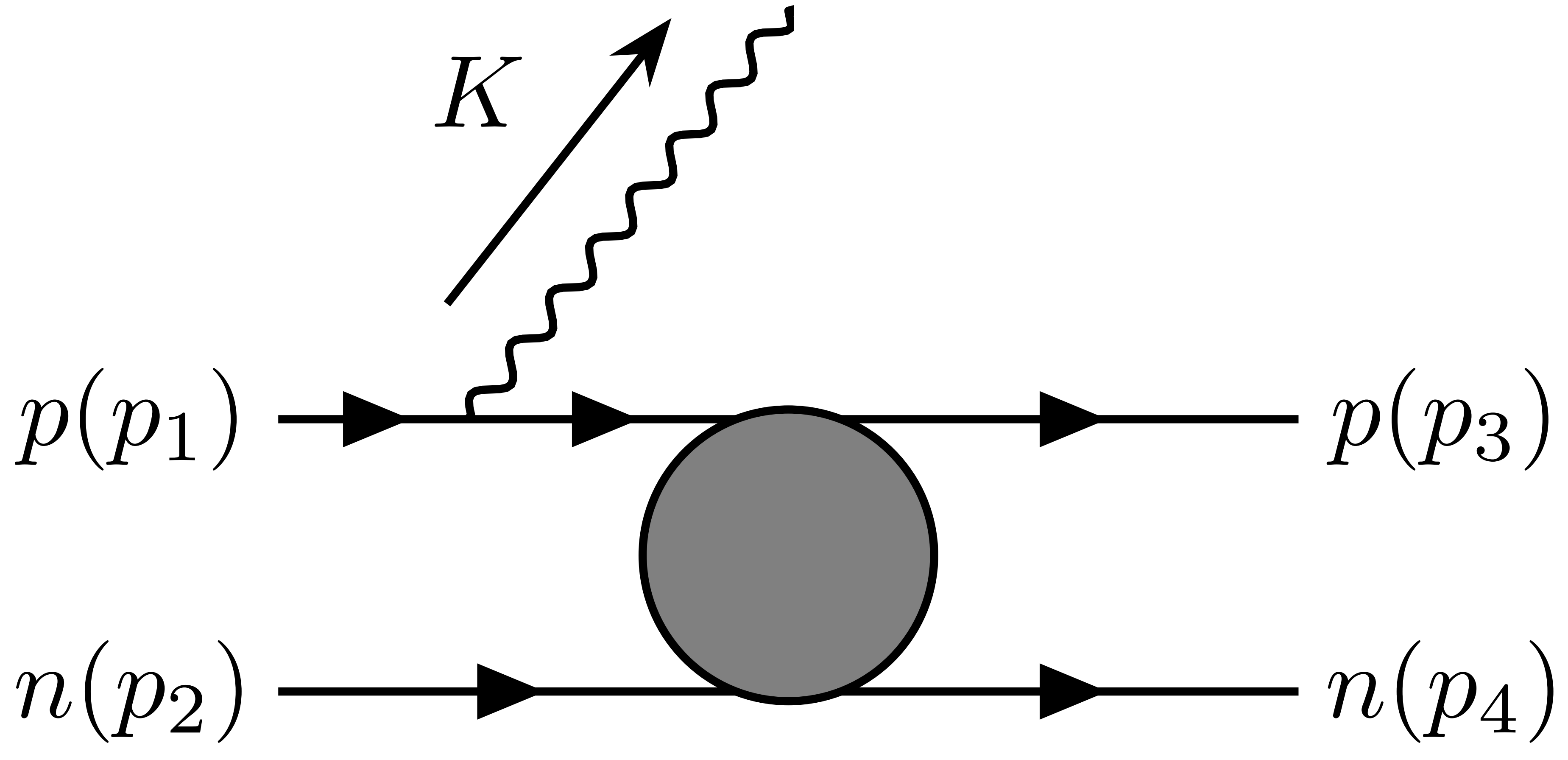

In SRA

$$\frac{d\mathscr{P}}{d\omega} = \frac{4\alpha}{3\pi\omega}\frac{E_{\rm cm}}{m_N} f\left(\frac{K^2}{4\omega^2}\right)$$

$$E_{\rm cm} = \frac{(\mathbf{p}_1 - \mathbf{p}_2)^2}{4m_N} \simeq 90\,\text{MeV}$$

millicharged particle flux in proton bremsstrahlung

MCP flux in the PB process

$$\frac{d\Phi_{\rm pb}}{dE_\chi} = \frac{4n_1 n_2 \epsilon^2 \alpha}{3\sqrt{m_N \pi^3 T_c^3}} \int_{2m_\chi}^{\infty} dE_{\rm cm} E_{\rm cm} e^{-E_{\rm cm}/T_c} \sigma_{np}^T(E_{\rm cm})$$

$$\times \int_{4m_\chi^2}^{E_{\rm cm}^2} \frac{dK^2}{K^2} f\left(\frac{m_\chi^2}{K^2}\right) \int_{\sqrt{K^2}}^{E_{\rm cm}} d\omega \frac{d\mathscr{P}}{d\omega} g(E_\chi, m_\chi, K)$$

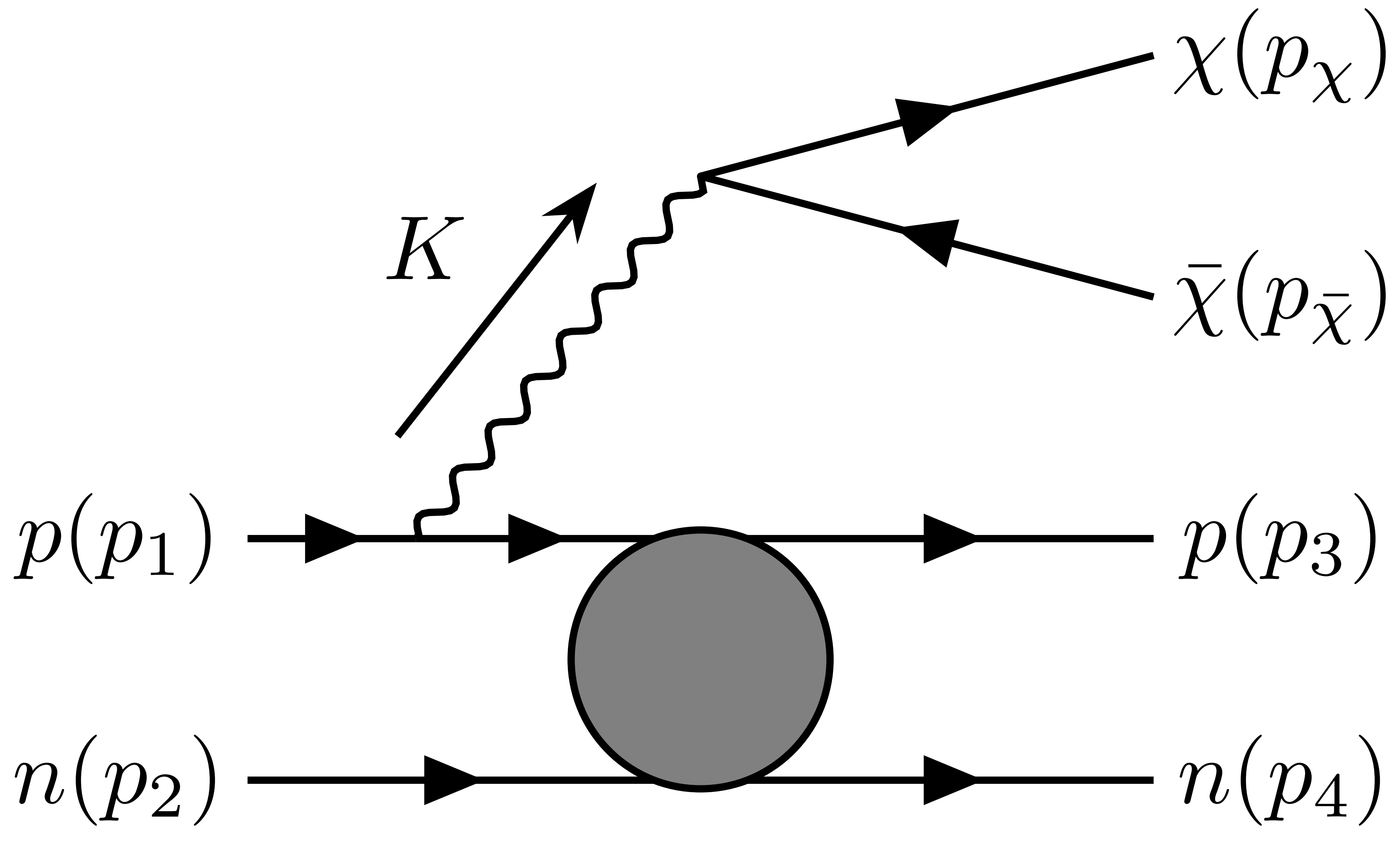

Electron-positron annihilation

Electron-positron annihilation

$$\sigma_{\text{ann}} = \sigma_T + \sigma_L$$

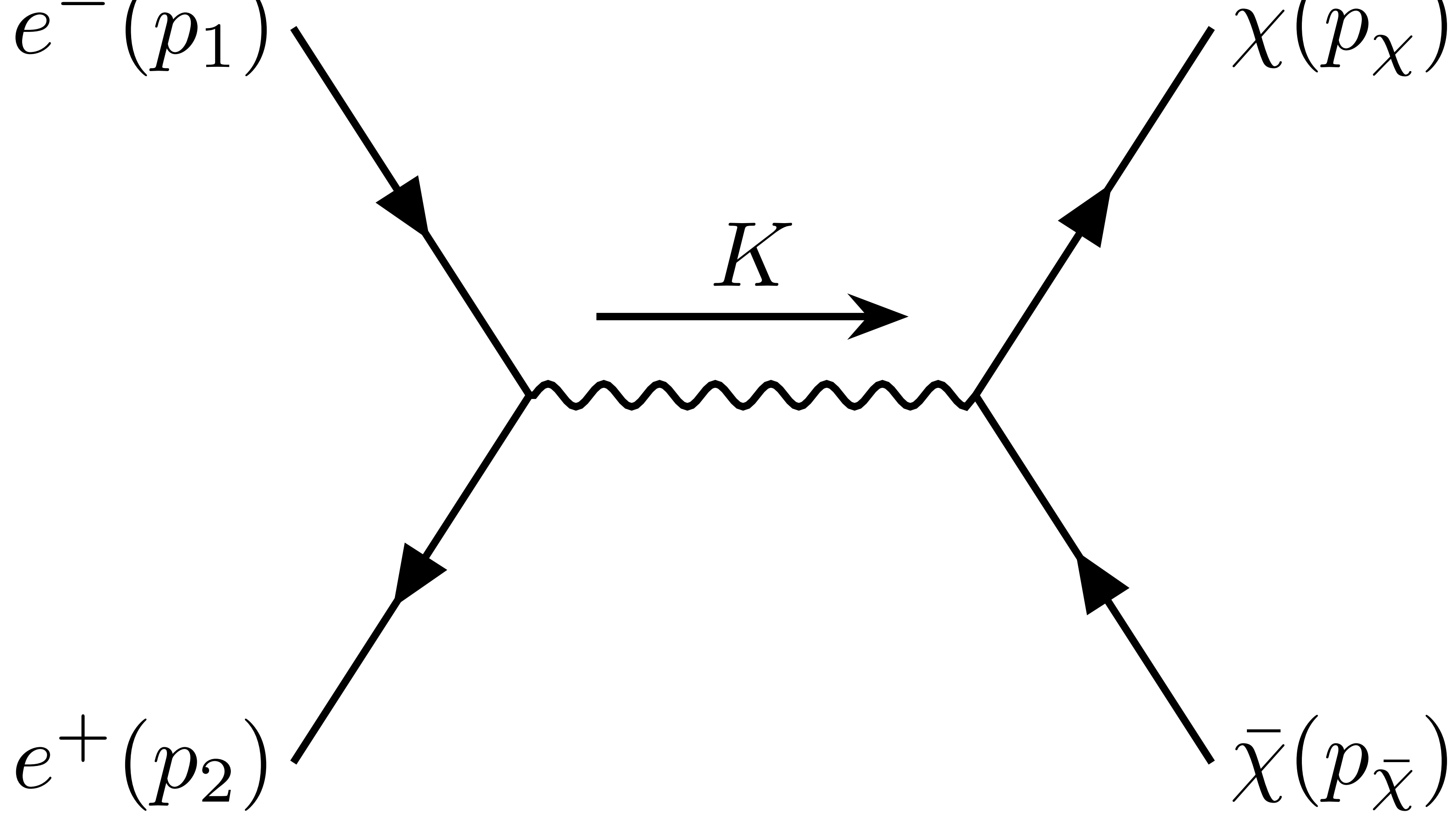

(c)

For transverse (T) and longitudinal (L) photons

$$\sigma_a = \frac{2\pi\epsilon^2\alpha^2}{3\beta_e} \frac{N_a K^2 f\left(m_\chi^2/K^2\right)}{(K^2 - \text{Re}\Pi_a)^2 + (\text{Im}\Pi_a)^2}$$

$$\beta_e = \sqrt{1 - 4m_e^2/K^2}$$

EM polarization tensor: $\Pi_a = \text{Re}\Pi_a + i\,\text{Im}\Pi_a$

$$N_L = 1 - E_-^2/(E_+^2 - K^2)$$

$$N_T = 1 + 4m_e^2/K^2 + E_-^2/(E_+^2 - K^2)$$

$$E_\pm \equiv E_1 \pm E_2$$

EM polarization tensor in the off-shell region

e^+e^- annihilates at $\sqrt{K^2}$ larger than the photon mass

One-zone model: $m_\gamma < 12$ MeV & $m_e \simeq 9$ MeV $\Longrightarrow m_\gamma < 2m_e$

In the relativistic limit, we use on-shell dispersion relations to compute $\mathrm{Re}\Pi$

[Braaten & Segel, 93]

[Scherer& Schutz, 2405.18466]

Dominant contributions to $\mathrm{Im}\Pi$: proton bremsstrahlung & its inverse $\Longrightarrow \lesssim 2\,\%$

millicharged particle flux in e^+e^- annihilation

$$\frac{d\Phi_{\rm ann}}{dE_\chi} = \frac{1}{16\pi^4}\int_{4m_{\rm th}^2}^{\infty} dK^2 K^2 \beta_e \int_{\sqrt{K^2}}^{\infty} dE_+ \int_{-E_-^m}^{E_-^m} dE_- f_1(E_1) f_2(E_2)\, \sigma_{\rm ann}\, g(E_\chi, m_\chi, K)$$

$$E_-^m \equiv \beta_e \sqrt{E_+^2 - K^2}$$

$$m_{\rm th} \equiv \max\{m_e, m_\chi\}$$

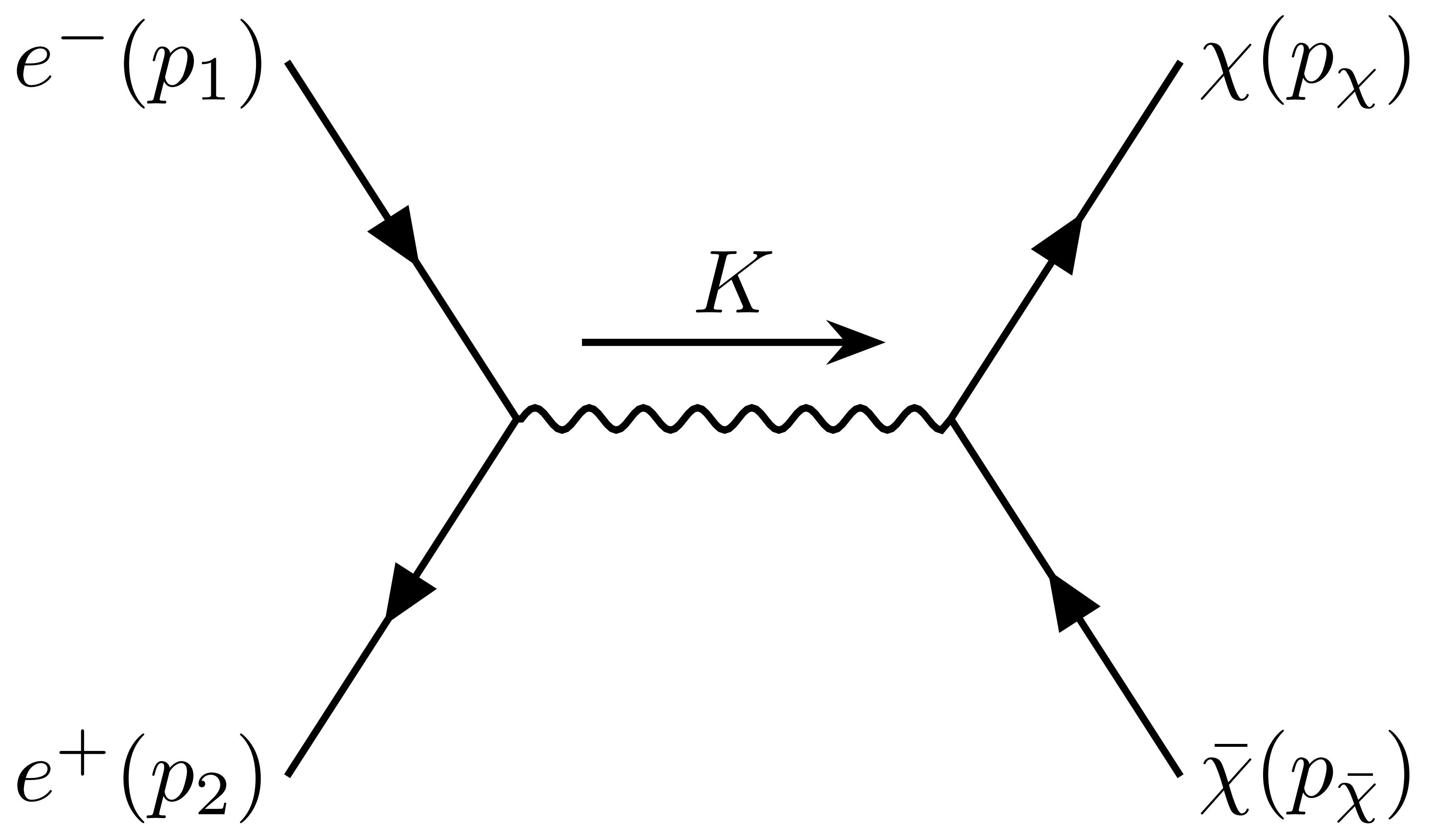

(c)

additional slides for MCPs

Plasmon decay for low-mass MCPs

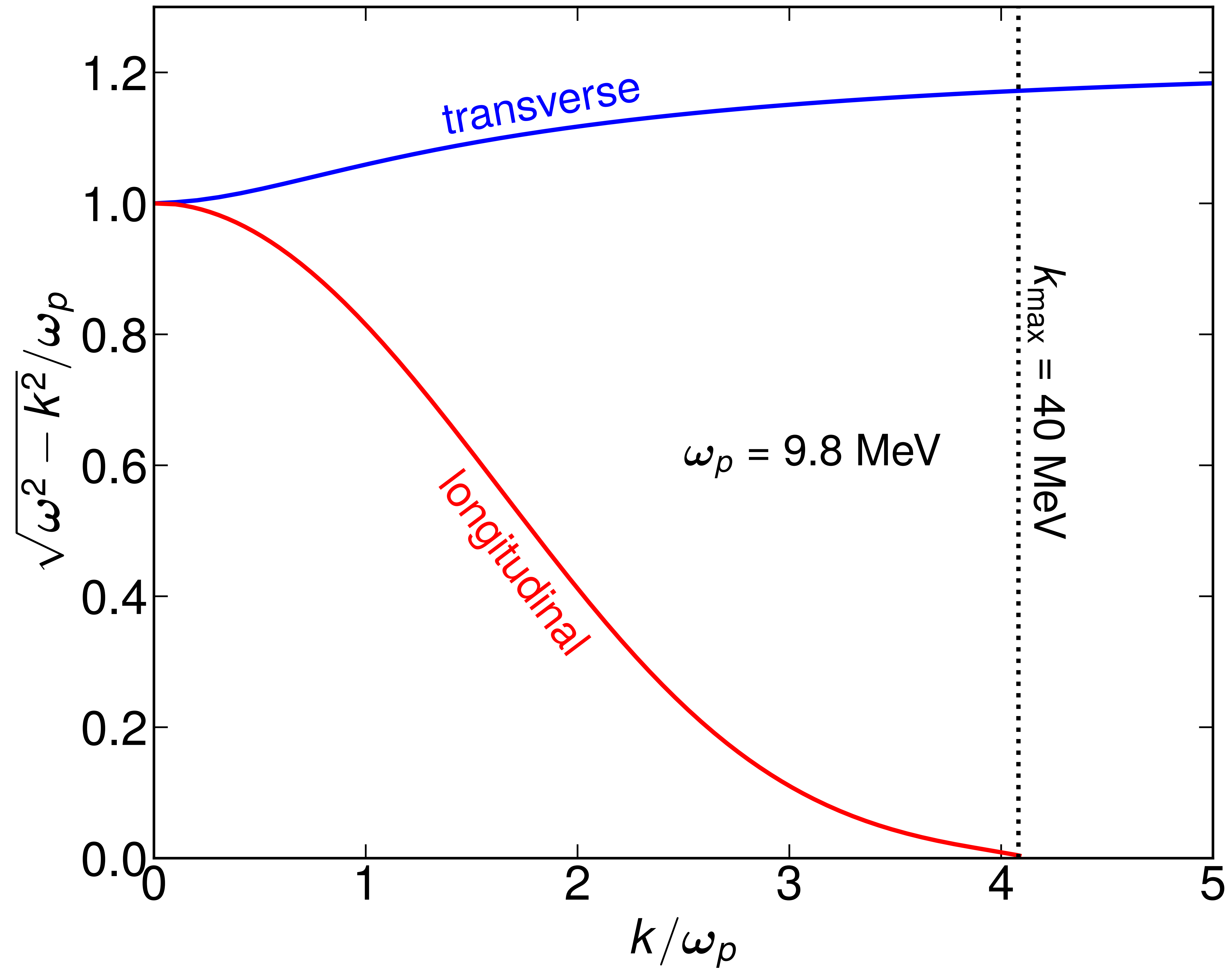

Photon mass < 12 MeV

Plasmon decay is the dominant production channel for MCPs w/ mass < 6 MeV

high-mass MCPs

- proton bremsstrahlung
- electron-positron annihilation

Supernova explosion energy

[Burrows & Vartanyan, 2009.14157]

Model [$M_\odot$]	Explosion Energy [B]	Run Time [s]	Baryonic Mass [$M_\odot$]	Gravitational Mass [$M_\odot$]
9	0.09	2.34	1.35	1.23
10	0.15	3.36	1.49	1.35
11	0.15	3.52	1.51	1.37
12	-0.03	2.75	1.82	1.62
13	0.78	4.60	1.89	1.68
14	0.28	4.51	1.81	1.62
15	-0.17	1.04	1.93	1.71
16	0.36	4.45	1.75	1.56
17	1.86	4.66	2.05	1.81
18	1.24	4.58	1.80	1.60
19	0.63	4.45	1.87	1.66
20	1.22	4.56	2.10	1.85
21	1.74	3.76	2.27	1.97
22	0.95	4.74	2.06	1.81
23	0.73	4.55	2.04	1.80
25	1.39	3.11	2.11	1.85
26	2.3	4.60	2.15	1.88
26.99	1.17	4.60	2.12	1.86

Supernova explosion energy

[Burrows & Vartanyan, 2009.14157]

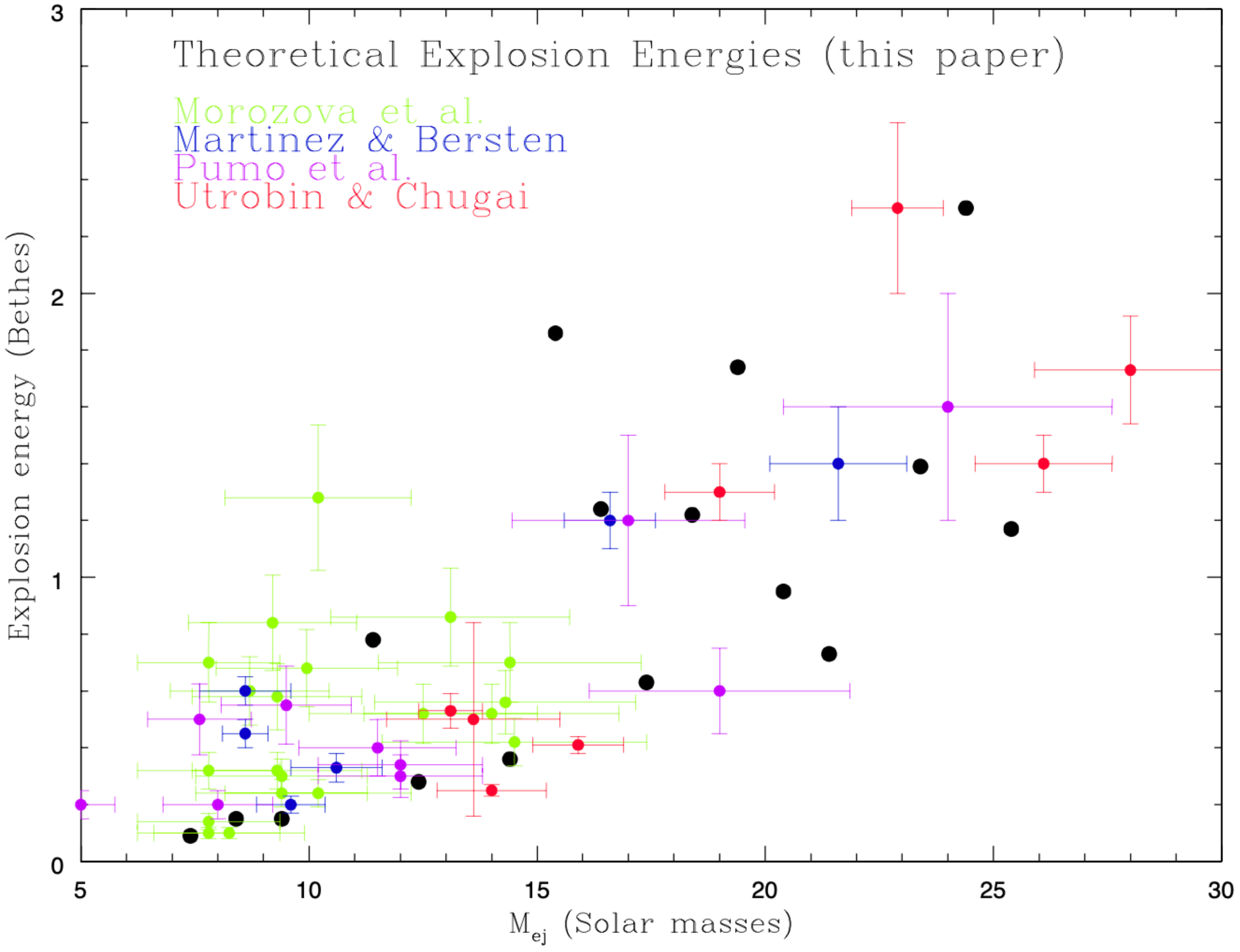

Empirically inferred explosion energies vs. the inferred ejecta masses, with error bars, for a collection of observed Type IIp (plateau) supernovae.

Black dots = theoretical explosion energies

On-shell approximation (OSA) for ReΠ_a in off-shell region

OSA: use on-shell dispersion relations to compute ReΠ_a in the off-shell region

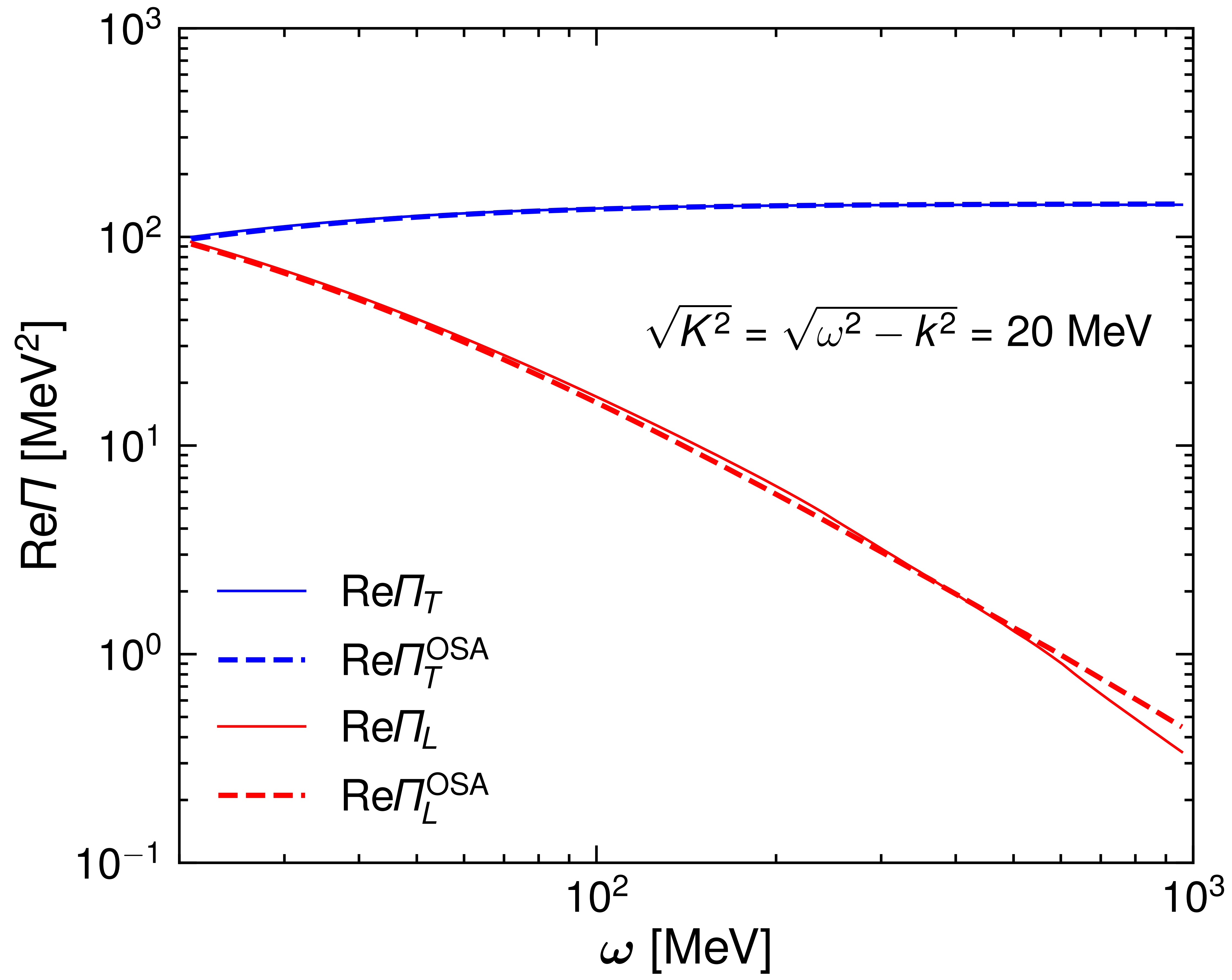

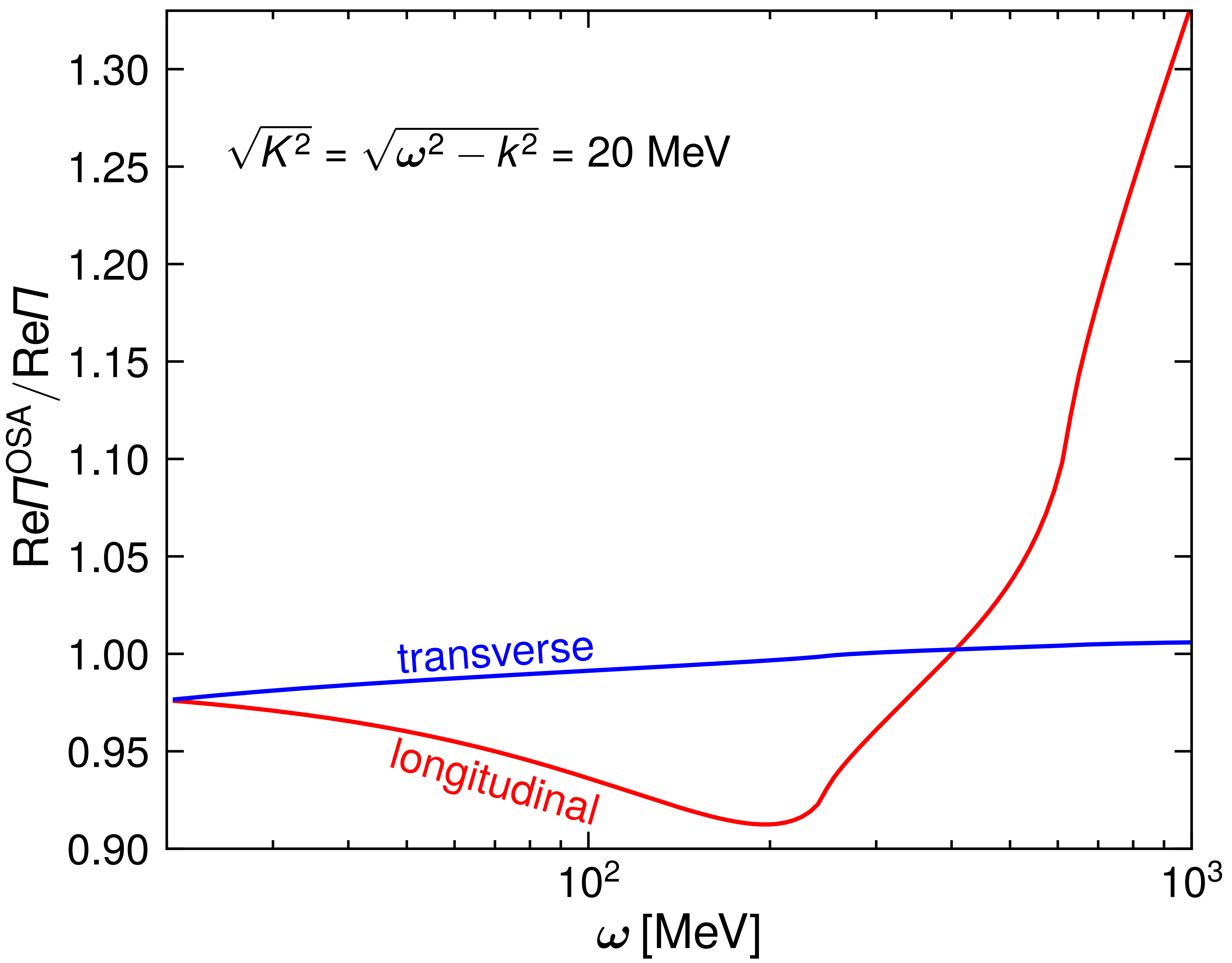

Imaginary part of Π_a in off-shell region

$\sqrt{K^2} = 20$ MeV

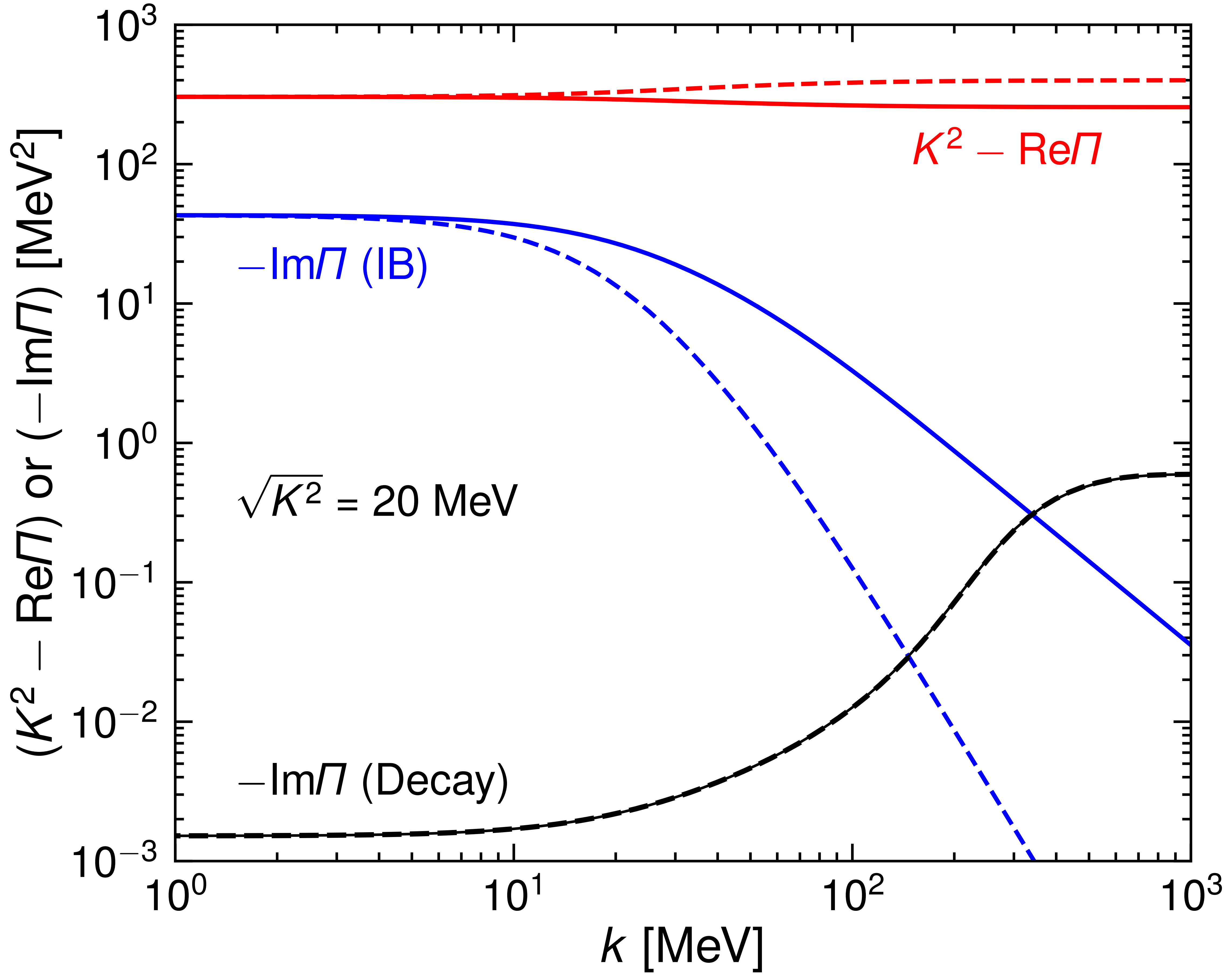

$\sqrt{K^2} = 30$ MeV